# DETECTION AND COMPENSATION OF

# VALVE STICTION IN CONTROL LOOPS

BY

## MUHAMMAD SABIH

A Thesis Presented to the
DEANSHIP OF GRADUATE STUDIES

### KING FAHD UNIVERSITY OF PETROLEUM & MINERALS

DHAHRAN, SAUDI ARABIA

In Partial Fulfillment of the
Requirements for the Degree of

# MASTER OF SCIENCE
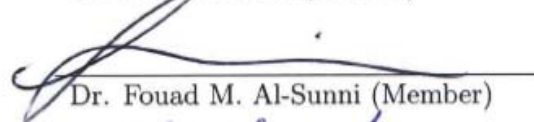
In

## Systems Engineering

**June 2009**

# KING FAHD UNIVERSITY OF PETROLEUM & MINERALS
## DHAHRAN 31261, SAUDI ARABIA
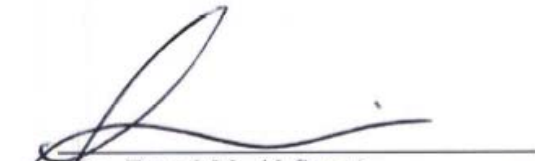
## DEANSHIP OF GRADUATE STUDIES

This thesis, written by **MUHAMMAD SABIH** under the direction of his thesis adviser and approved by his thesis committee, has been presented to and accepted by the Dean of Graduate Studies, in partial fulfillment of the requirements for the degree of **MASTER OF SCIENCE IN SYSTEMS ENGINEERING**.
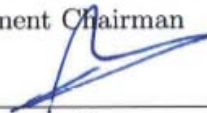
**Thesis Committee**

Dr. Sami El-Ferik (Adviser)

Dr. Fouad M. Al-Sunni (Member)

Dr. Moustafa El-Shafei (Member)

Dr. Fouad M. Al-Sunni
Department Chairman

Dr. Salam A. Zummo
Dean of Graduate Studies

9/12/09
Date

# ACKNOWLEDGMENTS

All praise is to Allah, the Almighty alone. May the Peace and Blessings of Allah be upon the Messenger of Allah (*salallahoalewasalam*), his family, and his companions (*radhiallahoanhum*).

I am grateful to the King Fahd University of Petroleum & Minerals for providing a great environment for research and academics.

I wish to extend my gratitude to my thesis adviser Dr. Sami El-Ferik for his continuous support, patience, and much needed encouragement. I am also thankful to my thesis committee Dr. Fouad M. Al-Sunni and Dr. Moustafa El-Shafei for their time, useful comments and extreme support in all matters.

I am very thankful to my friends Tahir, Shakil, Nadeem, Asif, Usama, Umair, and Atif for discussions, cooking, and the valuable tea hours. I am indebted to all the people I meet here at KFUPM.

My parents are always with me in my thoughts and I live with their encouragement and kindness. All good I do goes to my parents. For all my studies, credit goes to my eldest sister Tahira. I am also thankful to my brothers and sisters for their encouragement and support. I am thankful to my wife for her patience and help during long hours of studies and research, she equally shares this work. We are more than glad to dedicate this thesis to our beloved daughter Aaliyah.

# TABLE OF CONTENTS

**CHAPTER 6: SUMMARY, CONCLUSION AND FUTURE WORK   125**

# LIST OF TABLES

# LIST OF FIGURES

# THESIS ABSTRACT

**NAME:**  Muhammad Sabih

**TITLE OF STUDY:**  Detection and Compensation of Valve Stiction in Control Loops

**MAJOR FIELD:**  Systems Engineering

**DATE OF DEGREE:**  June 2009

A typical processing industry installs several hundreds of control loops to achieve desired process performance. Recent studies reveal that only about one-third of controllers provide acceptable performance, indicating significant commercial benefits exist in diagnosing and improving the remaining two thirds of the control loops. Performance degradation in control loops result in: ($i$) poor set point tracking, ($ii$) oscillations, ($iii$) poor disturbance rejection, and/or ($iv$) high excessive final control element variation. Recent surveys indicate that 20% to 30% of all control loops oscillate due to valve problems caused by static friction (also referred as stiction). In this thesis, loops that oscillate due to stiction are studied. Data driven techniques are discussed to model and to quantify valve stiction. Finally, proposed approaches to compensate valve stiction are presented.

# ملخص الرسالة

**الاسم** : محمد صبيح

**عنوان الرسالة**: كشف و تصحيح الصمام ذو احتكاك حالة السكون في دوائر التحكم

**القسم**: هندسة النظم

**التاريخ**: يونيو 2009

في عملية صناعية نموذجية من المعتاد تركيب المئات من حلقات التحكم للحصول على الاداء المطلوب من العملية. الدراسات الحديثة كشفت انه ثلث المتحكمات فقط تقوم بالاداء المطلوب، دالةً على وجود منفعة اقتصادية مقدرة في تشخيص و تحسين الثلثين الباقيين من حلقات التحكم.

التدهور في اداء حلقات التحكم يؤدي الى ا) تعقب ضعيف للقيمة المرادة ب) التذبذب ج) نبذ ضعيف للاضرابات و/او د) تغيرات كبيرة في العنصر النهائي للتحكم. الدراسات الحديثة كشفت ان 20% الى 30% من التذبذب في جميع دوائر التحكم الناتجة من مشاكل في الصمامت سببها احتكاك حالة السكون. في هذه الرسالة تمت دراسة الدوائر ذات التذبذب المسبب من احتكاك حالة السكون. تقنيات مبنية على البيانات تستخدم لنمذجة و تكمية احتكاك حالة السكون هذا. و قد تم تطوير طريقة لتصحيح وضعية احتكاك حالة السكون.

# CHAPTER 1

# INTRODUCTION

## 1.1   Overview

Research reports that 20 to 30% of all control loops perform poorly due to problems in control valves (see for example Desborough et al., [23]). Valve stiction is a form of friction-related problem very often encountered in process control plants. Valve stiction is a nonlinearity that leads to oscillations in process variables. Other nonlinearities that are common in practice are backlash, deadzone, and saturation. These are actuator hard nonlinearities and each has a specific nonlinear structure. Investigation and study of these nonlinearities may enable the design of improved control laws and better performance. As such, addressing valve stiction properly may result in better quality, economy, and safety.

  The general structure of a pneumatic control valve is shown in Fig.1.1. This valve is closed by elastic force and opened by air pressure. Flow rate is changes according to the plug position, which is determined by the balance between elastic force and air
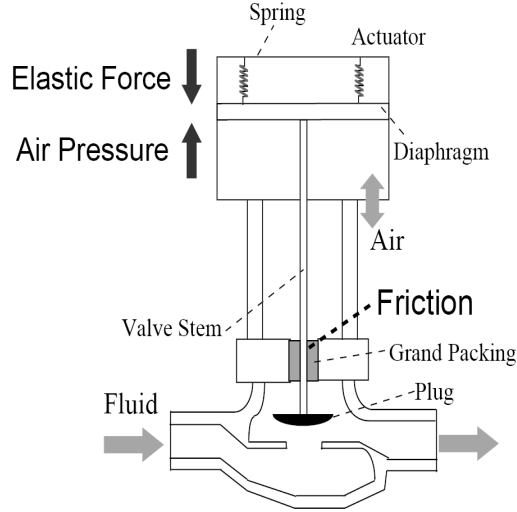
Figure 1.1: Structure of pneumatic control valve.

pressure. The plug is connected to the valve stem. The stem is moved against static or kinetic frictional force caused by packing, which is a sealing device to prevent leakage of process fluid. Tightening the packing also increases the static friction. Smooth movement of the stem is impeded by excessive static friction, and it is suddenly and considerably changed when the difference between elastic force and air pressure exceeds the maximum static frictional force.

In practice, valve maintenance is performed during production stops. Scheduled maintenance reduces the static friction force, which results in improved loop performance. However, normal periodical scheduled maintenance is typically between 6 months to 3 years. The loss of energy and product quality during maintenance period can be quite high. Identification, quantification and stiction compensation algorithms are crucial to ensure improved asset management and high quality product.

In this work, we will investigate the control loop suffering from valve stiction. A framework that can detect, quantify and improve the control loop performance is the

aim of this work. Control loop with a valve model is used in this work to generate the process data comprised of controller output, valve position and process variable (i.e., simulation data). This simulated data is used for the detection and quantification of stiction. We will explore the issues related to stiction itself and also highlight the pros and cons of the methods. Next we will propose a method for stiction compensation.

## 1.2 Problem Statement

The research problem for this thesis can be stated as: *"Given the process data (e.g., controller output, valve position, process variable) of a control loop, detect, quantify and compensate the control-valve stiction"*.

## 1.3 Objectives

The objectives of this thesis are the following:

- To investigate models for valve stiction specifically the data driven approaches. This investigation also includes the comparison of data driven models using International Society of Automation (ISA) bench tests for valves.

- Study and implementation of detection and quantification methods using the simulated data of a control loop.

- To propose compensation approach based on inverse modeling.

- Benchmark the proposed approach compared to an existing compensation ap-

proach.

## 1.4   Organization of the Thesis

The remainder of this thesis is organized as follows: First chapter opens the discussion of the thesis topic. A general literature review in the area of stiction modeling, detection and compensation is presented in chapter 2. In chapter 3, definition and modeling of valve-stiction are presented. Chapter 3 provides a comprehensive treatment of data driven models of valve stiction. These stiction models are tested using the International Society of Automation (ISA) recommended tests for control valves. In chapter 4, detection and quantification methods for valve stiction are discussed and applied on an example of a control loop for several cases of stiction and noise levels. Chapter 5 presents the proposed method for the compensation of valve stiction by using an approximated inverse for the stiction nonlinearity to reduce the stiction posed oscillations in the process control loop. The closing chapter 6, provides conclusions and recommendations for future research.

# CHAPTER 2

# LITERATURE SURVEY

Earlier work related to control loop diagnosis is contributed by Haris in 1989 [18]. Haris presented the idea of performance assessment of control loops. This work initiated research work in the area of control loop performance monitoring and assessment. This chapter will present the research work done in the area of modeling, detection, quantification and compensation of control valve stiction.

Many studies (Armstrong et al., [7]; Horch [19]; Gerry and Ruel [21]; Ruel [38]) have been carried out to define and detect static friction or stiction. However, there is lack of a unique definition and description of the mechanism of friction [31].

Earlier research work for friction related problems was mostly carried out for machines and servo positioning system (see for example, [7] and [34]). Valve stiction become active research area since last decade due to the considerable concerns from both academia and industry. Stenman et al., in [4], presented a detection method for stiction in control valves. This is a model-based method which exploits the ideas from the fields of change detection and multi-model model estimation. This is a fairly compli-

cated method which run in off-line mode. The authors in [4] recommend to integrate an alarm device to the detection of distinct peak which is found in the histogram when the valve jumps. Stenman et al. [4] with reference to private communication with Hägglund also reported a one parameter data-driven stiction model.

An early work on the stiction detection is done by Taha et al. in 1996 [33]. They presented an automatic procedure for diagnosis of oscillations in control loops. The procedure figures out one of the three possible causes of loop oscillations: high friction in valve, poorly tuned PID controller, presence of external perturbation.

Successive versions of a two parameter stiction model appeared in Choudhury et al. [30], [11] and [31]. They presented the model and proposed definition of stiction phenomena distinguishing stiction nonlinearity from other valve nonlinearities like hysteresis, backlash and deadband. Choudhury model in [30] has few disadvantages like the model assumed the input signal is deterministic and only sinusoidal input was investigated. Kano et al., in [25] improved and proposed an extended version of the model proposed by Choudhury et al. [30]. Kano model is also a two parameter data driven model which is further discussed in next chapter.

Srinivasan in his Ph.D. [41], utilized the Stenman stiction model for diagnosis and compensation approaches. Srinivasan investigated the deficiencies of the Stenman model and proposed a three parameter data driven model, but the model is quite complex for diagnosis and compensation of stiction. Therefore, Srinivasan carried out his work on the Stenman model even after discovering the problems with the Stenman model. The model is investigated in the next chapter.

Scali et al., in [10] presented an improved qualitative shape analysis technique to automatically detect valve stiction specially for flow control loops. It considers additional stiction patterns which were not observed in the original work by Yamashita [42]. Scali et al., in [10] simulates, compares and analyzes stiction patterns on the basis of valve type, loop dynamics and control system setup. [10] provides an extended technique for automatic stiction detection with improved efficiency over [42]. The observed stiction pattern in industrial data is explained on the basis of the measured delay between loop variables which can generate changes in the shape of PV-OP trends. This extended algorithm covers different possible stiction patterns. It is being suggested by authors to investigate external factors affecting negatively to the reliability of the method and to do a comprehensive comparison with other automatic detection techniques which will help to determine appropriate application area also. But this research mainly circulates around the MV-OP data while MV is not always available.

Mohieddine, in [22], used a combination of genetic algorithm (GA) and separable least squares to quantify valve stiction. It considers valve and process system as a Hammerstein system consisting of a two-parameter stiction model and a linear low-order process model. The Hammerstein system consists of a two-parameter stiction model and a linear low-order process model as shown in Fig. 2.1. The proposed method is based on a Hammerstein model for describing the global system and a separated identification of the linear part, i.e., the transfer function between the manipulated variable (MV) and the process output (PV), and the non-linear part, i.e.,

the function between the controller output (OP) and the manipulated variable (MV), using available industrial data for OP and PV. Nonlinear part, i.e., the sticky valve is represented by Hammerstein model. It assumes that the system part without stiction can be approximated by a linear model as shown by following ARMAX model.

$$A(q)y(k) = q^{-\tau}B(q)u_v(k) + C(q)\varepsilon(k) \tag{2.1}$$

where $q^{-i}$ is the backward shift operator, $\tau$ is the discrete time delay, i.e., the number of unit delays and $\varepsilon$ the unmeasured disturbance. $A(q)$, $B(q)$, and $C(q)$ are polynomials in $q^{-1}$ of specified order $n$, $m$, and $p$, respectively:

$A(q) = 1 + a_1 q^{-1} + a_2 q^{-2} + ......a_n q^{-n}$

$B(q) = b_0 + b_1 q^{-1} + ......b_m q^{-m}$

$C(q) = 1 + c_1 q^{-1} + c_2 q^{-2} + ......a_p q^{-p}$

It uses process output (PV) and controller output (OP) to estimate the parameters of the system. GA is used to estimate parameters of stiction model while separable least squares is used to identify the linear model parameters. This two-stage identification of the system parameters is illustrated in Fig. Since this is an offline quantification method, the relatively high computational time is not considered critical. The time delay estimation for the process plant requires a more efficient implementation of the algorithms, e.g., as C-code that can accelerate the computation of the overall algorithm.

Singhal et al., in [3] presented the idea of using the ratio of areas between and after the peak of the oscillating control error signal to distinguish the oscillations due to
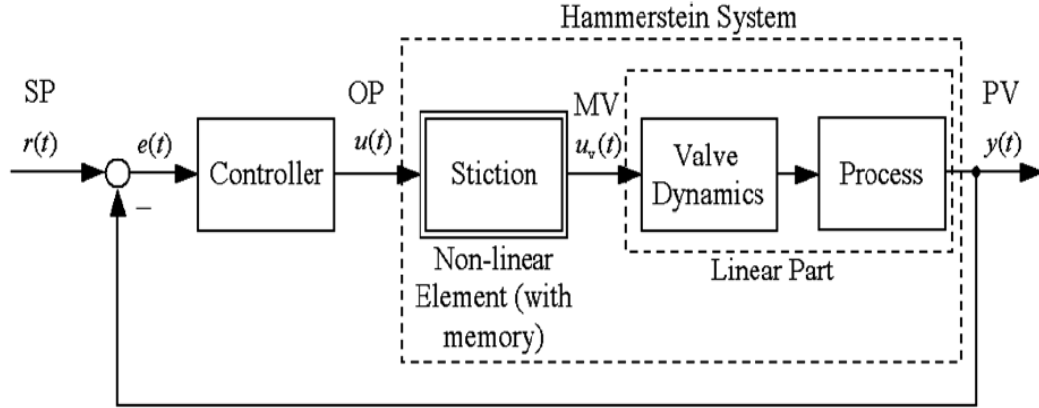
Figure 2.1: Process control loop with valve stiction within an identification framework [22].
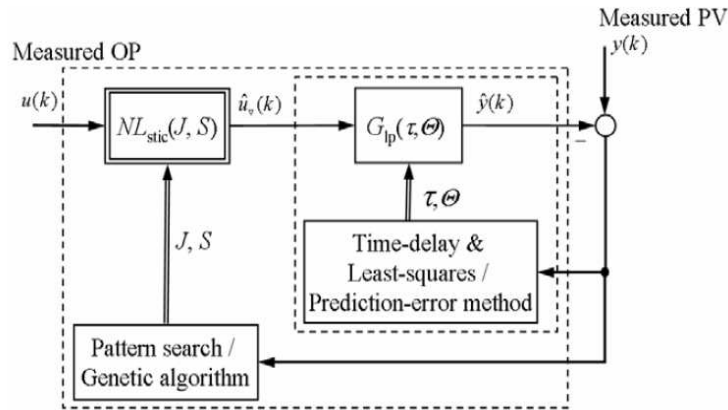


Figure 2.2: Two-stage identification of the system parameters [22].

aggressive controllers and sticky valves. For self-regulating plants (plant with all left-half plane poles) with a monotone step-response, aggressive control usually results in a sinusoidal control error signal, while for a sticking valve, the signal typically follows exponential decay and rise as shown in Fig. 2.3. This methodology distinguishes between the signals in Fig. 2.3 by calculating the ratio of the areas before and after the peaks. The quantity is called $R$ and is defined as $R = A1/A2$. The decision rule is summarized as $R > 1 => Stickyvalve$, $R \approx 1 => Aggressivecontrol$. The method

works with few assumptions which are: (1) the controller output is not cycling from one saturation limit to the other, and (2) the oscillations in the control loop are not caused by an external periodic disturbance. Violation of these assumptions can result in $R > 1$ even when stiction is absent. This method is designed for self-regulating
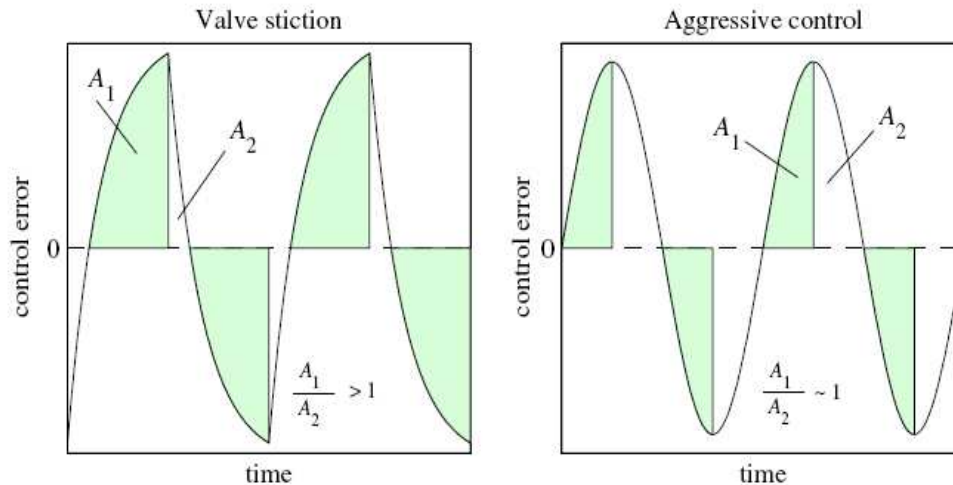


Figure 2.3: Control error signal shapes for valve stiction and aggressive control [3].

plants with monotone step-response. These plants can be represented by the $n$th-order transfer function,

$$G_p = \frac{K_p e^{-Ls}}{(T_1 s + 1)(T_2 s + 1)...(T_n s + 1)} \tag{2.2}$$

where $n$ is the plant order, $K_p$ is the plant gain, $L$ is the delay in the plant, and $T_i$ are time-constants of different dynamic components. It is common practice to approximate the $n$th-order transfer function in Eq. 2.2 to first-order for controller tuning. This approximation results in the popular first-order plus time-delay (FOPTD) transfer function,

$$G_p = \frac{K_p e^{-\theta s}}{(\tau s + 1)}, \tag{2.3}$$

10

where $\tau$ is an approximation of the plant dynamics, and $\theta$ represents a combination of the pure delay and an apparent delay caused by the higher order dynamics. Valve stiction model introduced by Choudhury et al. [31] is used in this work to analyze valve stiction in an oscillating control loop. This method only detects stiction in an oscillating control loop provided the assumptions for the method are true.

Ettaleb [13] invented a diagnostic procedure for analyzing control loops that are poorly performing. The method is comprised of:

- means for recording an error signal between a set-point value and a detected process value

- means for determining the power spectrum of the error signal

- means for determining a best fit analytical function describing the power spectrum associated with the error signal

- and means for calculating the difference between the best fit analytical function and the power spectrum, in order to output a diagnostic value.

The method by Ettaleb [13] determines whether or not the malfunctioning is caused principally by a poor adjustment of the controller tuning parameters, this method does not explicitly detect and quantify the valve stiction.

In Choudhury et al., [27], the main idea is to compute nonlinearity measures via Higher Order Statistics. Two measures are used, a nonlinearity index (NLI) and a non-Gaussianity index(NGI). Both indices are deduced from the signal bicoherence. Bicoherence is the same as the nomalized bi-spectrum of a signal. A Characteristic

of a non-liner time series is the presence of phase coupling such that the phase of one frequency component in the spectrum is determined by the phases of other frequency components. This characteristic does not exist for linear signals (i.e. signals that are generated by linear systems). The indices - the Non-Gaussianity Index (NGI) and the NonLinearity Index (NLI) - have been defined as

$$NGI = \overline{\hat{nic^2}} - \overline{bic^2}_{crit}, \tag{2.4}$$

$$NLI = \mid \hat{bic^2}_{max} - (\overline{\hat{bic^2}} + 2\sigma_{\hat{bic^2}}) \mid, \tag{2.5}$$

where $\overline{\hat{nic^2}}$ is the average squared bicoherence over the principal domain and $\hat{bic^2}_{max}$ is the maximum squared bicoherence, $\sigma_{\hat{bic^2}}$ is the standard deviation of the squared bicoherence and $\overline{bic^2}_{crit}$ is the statistical threshould/critical value obtained from the central chi-square distribution of the squared bicoherence. The nonlinearity test applied uses bicoherence to assess the nonlinearity. Bicoherence is defined as

$$bic^2(f_1, f_2) = \frac{|B(f_1, f_2)|^2}{E[|X(f_1 X(f_2))|^2] E[|X(f_1 + f_2)|^2]}, \tag{2.6}$$

where $B(f_1, f_2)$ is the bispectrum at frequencies $(f_1, f_2)$ and is given by

$$B(f_1, f_2) = E[X(f_1)X(f_2)X^*(f_1 + f_2)], \tag{2.7}$$

$X(f_1)$ is the discrete Fourier transform of the time series $x(k)$ at the frequency $f_1$, $X^*(f_1)$ is the complex conjugate and $E$ is the expectation operator. A key feature of

the bispectrum is that it has a non-zero value of there is significant phase coupling in the signal $x$ between frequency components $f_1$ and $f_2$. The bicoherence gives the same information as the bispectrum but it is normalized as a value between 0 and 1.

Ulaganathan et al., in [32], discusses possible approaches to detect stiction in nonlinear process control loops. The control loop that is being addressed is shown in Figure 2.4. Based on the figure, $y = y_p + y_d => y = N(u) + y_d =>$

$$y = N(V(v)) + y_d, \tag{2.8}$$

where $y$ is the $pv$, which is assumed to be comprised of a process component $y_p$ and a disturbance component $y_d$, which are additive. $N$ is the process transfer function and $u$ is the valve output, which might not be measured. The valve output $u$ is a function $(V)$ of the op $(v)$ dictated by the stiction phenomenon. In this paper, the identification and isolation of stiction from external disturbances for the system given in equation 2.8 is addressed. One parameter stiction model by Stenman et al., [4] is used in this paper. A nonlinear polymerization reactor process from [14] is used as a case study. The process is described by a second-order Volterra model in the frequency domain as given below

$P_1 = c_1{}^T(sI - A_{11})^{-1}b_1$

$P_2 = c^T[(s_1 + s_2)I - A]^{-1}N(s_1 - A)^{-1}b$, where details on the matrices $c, A, N, b$ can be found in [14]. Note that [32] used a simple one parameter stiction model for both generating the simulation data and to detect stiction.

A comparison of physical and data-driven friction models is presented in Garcia
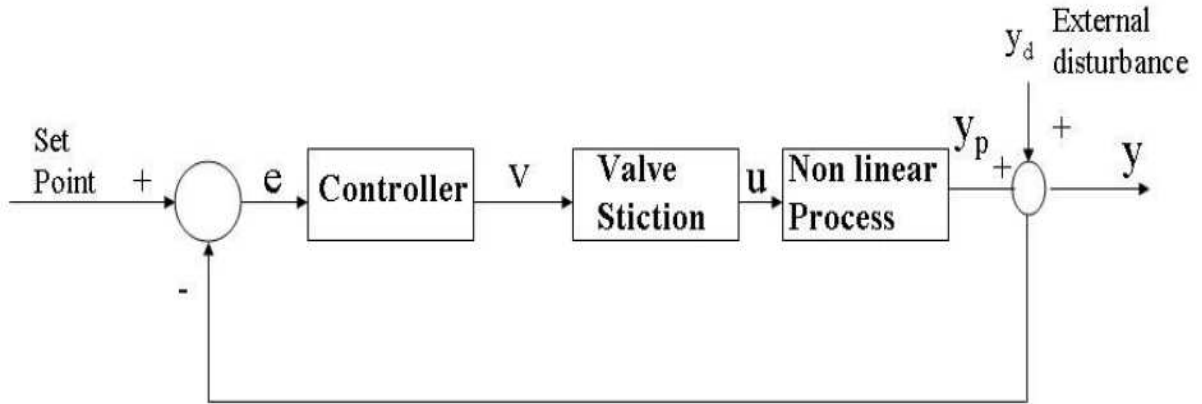
Figure 2.4: Nonlinear control loop with stiction [32].

[16]. The models are studied using different friction coefficients and input signals. Valve bench tests recommended by International Society of Automation (ISA) were performed in with the valve operating in open loop without considering any loop dynamics.

Gerry et al., in [21] presented a method to measure and combat stiction. This method requires controller in manual mode and then a sequence of steps with changing controller output and collecting process variable is suggested. This is an observation based method requires an expert operator. Repair the valve or positioner is recommended as first solution to improve a valve with stiction. If repair is not possible and replacing the valve is also too expensive, a PID tuning technique is recommended to keep the plant running. But, the tuning may raise other problems like tight tuning, windup etc.

Kayihan et al., in 2000 [2] and Hägglund in 2002 [17] have addressed stiction compensation algorithms for pneumatic control valves. Kayihan et al., in [2]

14

developed an actuator design which can work independently of the overall distributed control system (DCS). This actuator design is a nonlinear intelligent actuator local to the valve. In this work, a state space model of a pneumatic process valve is developed using force balances on valve components and friction effects. The valve model used is physical and requires all the design parameters of the valve. Although, this model-based, nonlinear local control strategy performs more proficiently than traditional linear control in presence of parametric disturbances, but not all the control valves have smart actuators to implement this control technique. The approach of Kayihan et al., [2] requires a valve model with valve parameters (e.g., stem mass, stem length, etc.) and also the process model to be known a priori. Obtaining such detailed valve and model information for several hundred valves is a practical limitation.

The approach by Hägglund proposed in 2002 [17] is a model-free method. Idea of this method is to add a special pulse called "knocker" to the controller output (OP) to compensate the valve stiction. The knocker pulse is characterized by an amplitude ($a$), a pulse width ($\tau$), and a time between each pulse ($h_k$). The choice of parameters is critical for the compensation of stiction, specifically the pulse amplitude is extremely important for the knocker technique to work [36]. The principal of this stiction compensation procedure is illustrated in Fig. 2.5. Control signal $u(t)$ consists of two terms: $u(t) = u_c(t) + u_k(t)$, where $u_c(t)$ is the output from a standard controller (normally a PID controller), and $u_k(t)$ is the output from the knocker. Output $u_k(t)$
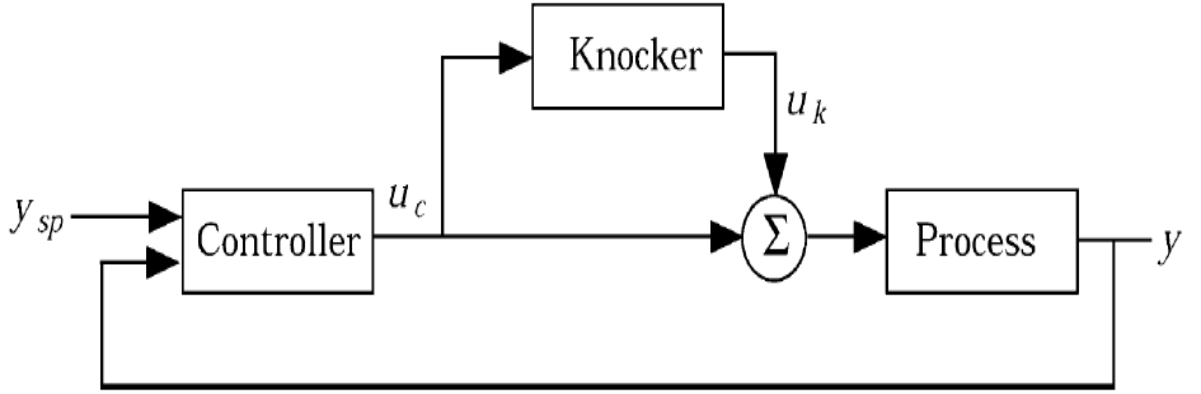
Figure 2.5: Block diagram illustrating the knocker used in a feedback loop [17].

from the knocker is a pulse sequence that is characterized by three parameters: The

time between each pulse $h_k$, the pulse amplitude $a$, and the pulse width $\tau$. During

each "pulse interval", $u_k$ is given by

$$u_k(t) = \begin{cases} asign(u_c(t) - u_c(t_p)) & t \le t_p + h_k + \tau \\ 0 & t > t_p + h_k + \tau \end{cases} \qquad (2.9)$$

where $t_p$ is the time of onset of the previous pulse. Hence, the sign of each pulse is

determined by the rate of change of control signal $u_c(t)$. The transfer function between

the knocker output $u_k(t)$ and the process output $y$ is $Y = (\frac{G_p}{1+G_pG_c})U_k$, where $G_p$ is the

process transfer function and $G_c$ is the controller transfer function. If $u_k(t)$ is a pulse

with amplitude $a$ and width $\tau$, the process output becomes $Y = \frac{G_p}{1+G_pG_c}(1 - e^{-s\tau})\frac{a}{s}$

$\approx \frac{G_p}{1+G_pG_c}a\tau$. This means that the disturbances are proportional to the product $a\tau$.

Hence, it is the product $a\tau$ that determines the energy of each pulse in the knocker.

The knocker was tested on a water-flow system with a 150mm ball-segment valve.

The valve was in bad shape, with damages on the valve ball, and shows practical

16

case of friction and hysteresis encountered in process control. The controller was a PI controller that could run with or without the knocker procedure connected. Decrease in the variations in the measurement signal due to knocker compensation is shown with the help of integrated absolute error (IAE) and the inegrated squared error (ISE), which are defined as

$$IAE = \frac{1}{T_2 - T_1} \int_{T_1}^{T_2} |e(t)| dt \qquad (2.10)$$

$$ISE = \frac{1}{T_2 - T_1} \int_{T_1}^{T_2} e(t)^2 dt \qquad (2.11)$$

This method is also tested in industrial field tests performed at the valve manufacturer Somas **AB**, Säffle, Sweden on two sets of data (see [17] for details). This friction compensator is patented and implemented in industrial controllers and distributed control systems manufactured by ABB (e.g., single-station controller ECA600 by ABB).

Horch in 2006 [20] examined few of the available oscillation detection methods and points out the need for reliable diagnosis of oscillation without human interaction. The assumptions and results for the detection and quantification methods need to be handled with care, especially when automatic diagnostics is targeted. All methods have special strengths and weaknesses and it is unavoidable to know these when applying them to real-world data [20].

# MODELING STICTION IN CONTROL VALVES

## 3.1 Introduction

This chapter discusses the different modeling approaches to illustrate stiction phenomena in control valves. The objective is to investigate these models for the purpose of both identification and compensation of stiction caused problems. Few definitions of stiction have been proposed in the literature. Neither the definition nor the models are fixed to be incorporated into a complete design task. During the investigation on modeling approaches, Hammerstein-wiener model structure appeared as a potential for modeling structure of the stiction phenomena. The problem with the Hammerstein-Wiener is the polynomial form of the identified model. Hammerstein-Wiener model only identifies the overall model in polynomial form and does not give stiction parameters. While other data-driven modeling approaches

use stiction parameters (e.g., S and J terms in Choudhury et al. [31]) to represent the valve stiction. Hence a unified approach based on Hammerstein-Wiener Model takes a different route. Therefore, at the end of this chapter, Hammerstein-Wiener modeling approach is investigated only. The rest of the work is carried out using the data driven models since they are able to express stiction value in terms of parameters.

Following sections covers stiction from definition to modeling. Important definitions and data driven models are discussed and evaluated on the basis of the International Society of Automation (ISA) recommended tests for control valves ([5], [6]). The ISA tests are conducted to assist the argument that data driven models can be used instead of physical model of valve for detection, quantification and compensation purposes, which are the subjects of coming chapters.

## 3.2   Definition

Stiction in control valves is defined by several people and organizations but a unified definition is missing. Stiction is taken as a phenomena in control valves which appears due to the increased static friction. Below is a few important definitions of stiction from literature:

According to the ISA (ISA Subcommittee SP 75.05, 1979 [40]), "*stiction is the resistance to the start of motion, usually measured as the difference between the driving values required to overcome stiction friction upscale and downscale*".

According to Entech (1998), "*stiction is a tendency to stick-slip due to high static*

*friction. The phenomenon causes a limited resolution of the resulting control valve motion. ISA terminology has not settled on a suitable term yet. Stick-slip is the tendency of a control valve to stick while at rest, and to suddenly slip after force has been applied".*

In a recent paper, Ruel(2000) reported "stiction as a combination of the words stick and friction, created to emphasize the difference between static and dynamic friction. Stiction exists when the static (starting) friction exceeds the dynamic (moving) friction inside the valve. Stiction describes the valves stem (or shaft) sticking when small changes are attempted. Friction of a moving object is less than when it is stationary. Stiction can keep the stem from moving for small control input changes, and then the stem moves when there is enough force to free it. The result of stiction is that the force required to get the stem to move is more than is required to go to the desired stem position. In presence of stiction, the movement is jumpy". This definition resembles stiction as measured online in process industries - putting the control loop in manual and then increasing the valve input in small increments until there is a noticeable change in the process variable.

All of the above definitions agree that stiction is the static friction that keeps the valve stem from moving and when external force overcomes the static friction that valve starts moving. However, these definitions disagree in the way stiction is **measured** and how it can be **modeled**. This lack of stiction measure and modeling approach motivated data-driven approaches to model and define the stiction

phenomenon in terms of input-output behavior of the valve ([4], [30]).

Stenman et al., [4] proposed a data driven model for stiction. This model defines a valve stiction band $d$, which is used as the stiction parameter to represent the stiction phenomenon in a control valve. Using Stenman model, stiction can be defined as "*valve position (i.e., valve stem) can follow the input signal to the valve only if the difference between the current input and the previous valve position is greater than the valve stiction band d, otherwise the valve will not follow the input and will keep the old position*".

Choudhury et al., [31] proposed a definition of stiction and a two-parameter data driven model for valve stiction. Therefore, "*stiction is a property of an element such that its smooth movement in response to a varying input is preceded by a sudden abrupt jump called the slip-jump. Slip-jump is expressed as a percentage of the output span. Its origin in a mechanical system is static friction which exceeds the friction during smooth movement*".

Figure 3.1 shows a typical input-output behavior of a sticky valve. Stiction is illustrated with the help of two parameters S and J [30]. S is comprised of deadband plus stickband while J represents the slip jump.

## 3.3 Physical Model of Stiction

The purpose of this section is to understand the physics of valve friction and reproduce the behavior seen in real plant data.
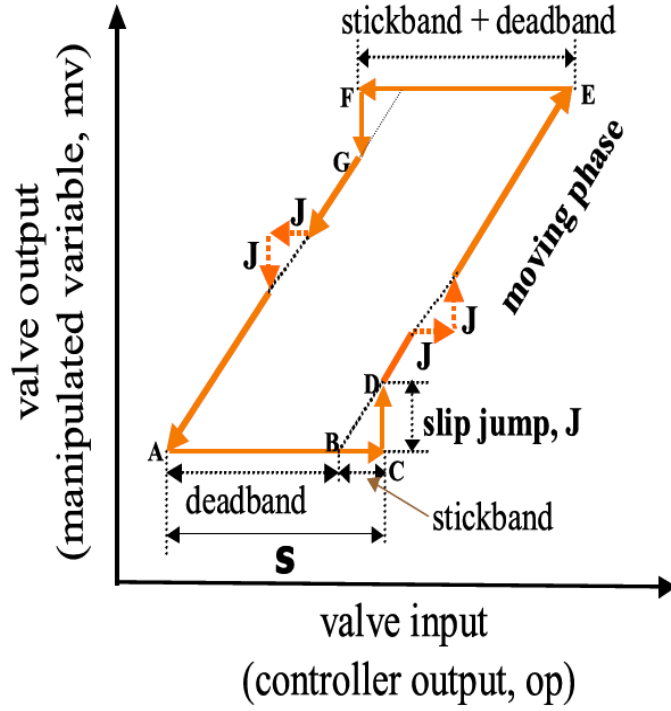
Figure 3.1: Input-Output characteristic of a sticky valve [29].

## Model formulation

For a pneumatic sliding stem valve, the force balance equation based on Newton's second law can be written as

$$M\frac{d^2x}{dt^2} = \sum Forces = F_a + F_r + F_f + F_p + Fi \qquad (3.1)$$

where M is the mass of the moving parts, $x$ is the relative stem position, $F_a = Au$ is the force applied by pneumatic actuator where $A$ is the area of the diaphragm and $u$ is the actuator air pressure or the valve input signal, $F_r = -kx$ is the spring force where k is the spring constant, $F_p = -\alpha\Delta P$ is the force due to fluid pressure drop where $\alpha$ is the plug unbalance area and $\Delta P$ is the fluid pressure drop across the valve, $F_i$ is

22

the extra force required to force the valve to be into the seat and $F_f$ is the friction force [2].

Following [2], $F_i$ and $F_p$ are assumed to be zero because of their negligible contribution in the model. The friction model includes static and dynamic friction [34]. The expression for the dynamic friction is in the first line of Eq. 3.2 and comprises a velocity-independent term $F_c$ known as Coulomb friction and a viscous friction term $vF_v$ that depends linearly upon velocity. Both act in opposition to the velocity, as shown by the negative signs.

$$F_f = \begin{cases} -F_c sgn(v) - vF_v, & if\ v \neq 0, \\ -(F_a + F_r), & if\ v = 0\ and\ |F_a + F_r| \leq F_s, \\ -F_s sgn(F_a + F_r), & if\ v = 0\ and\ |F_a + F_r| > F_s \end{cases} \tag{3.2}$$

Where $F_s$ is the maximum static friction. The second line in Eq. 3.2 is the case when the valve is stuck. When the valve get stuck, its velocity becomes zero, and therefore the acceleration is zero also. Thus, the right-hand side of Newton's law is zero, so $F_f = -(F_a + F_r)$. The third line of the model represents the situation at the instant of breakaway. At that instant, the sum of forces is $(F_a + F_r) - F_s sgn(F_a + F_r)$, which is not zero if $|F_a + F_r| > F_s$ . Therefore, the acceleration becomes non-zero and the valve starts to move. The physical model requires several parameters to be known. For instance, mass (M) of the moving parts, spring constant, diaphragm area and typical friction forces which depend upon the design of the valve.

# Types of Stiction

Types of stiction in control valves can be described as follows [31]:

**Deadband:** If $J = 0$, it represents pure deadband case without any slip jump. Valve deadband is due to the presence of Coulomb friction $F_c$; a constant friction which acts in the opposite direction to the velocity. In the deadband simulation case the static friction is the same as the Coulomb friction, $F_s = F_c$. The deadband arises because, on changing direction, the valve remains stationary until the net applied force is large enough to overcome $F_c$. The deadband becomes larger if $F_c$ is larger. Fig. 3.2 shows the friction force with respect to valve-stem velocity in case of pure deadband.
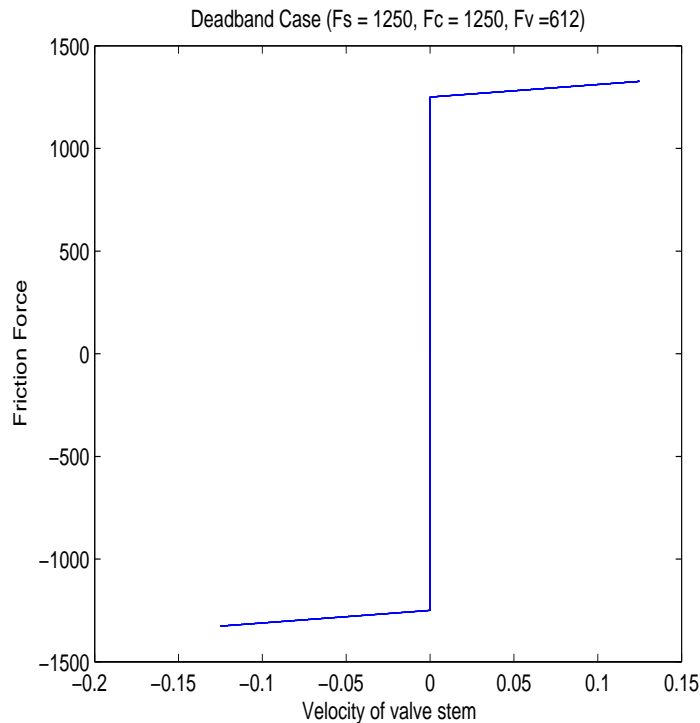


Figure 3.2: Deadband: Friction force vs. stem velocity.

**Stiction (undershoot):** If $0 < J < S$, the valve output can never reach the

24

valve input. There is always some offset. This represents the undershoot case of stiction. A valve with high initial static friction such that $F_s > F_c$ exhibits a jumping behavior that is different from a deadband, although both behaviors may be present simultaneously. When the valve starts to move, the friction force reduces abruptly from $F_s$ to $F_c$. There is therefore a discontinuity in the model on the righthand side of Newtons second law and a large increase in acceleration of the valve moving parts. The initial velocity is therefore faster than in the $Fs = Fc$ case, leading to the jump behavior. Fig. 3.3 shows the friction force with respect to valve-stem velocity in case of stiction undershoot.

**Stiction (no offset):** If $J = S$, the pure stick-slip behavior. There is no offset
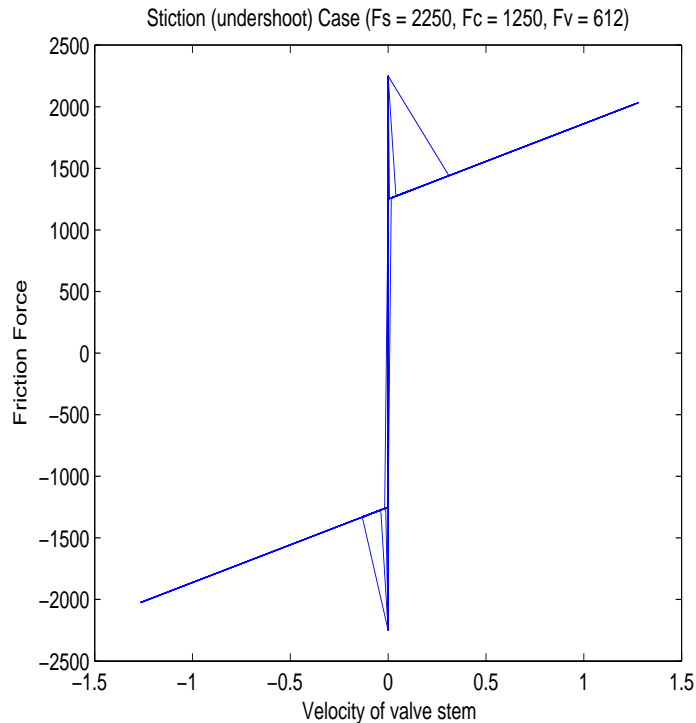


Figure 3.3: Stiction (undershoot): Friction force vs. stem velocity.

between the input and output. Once the valve overcomes stiction, valve output tracks

the valve input exactly. This is the well-known "stick-slip case". If the Coulomb friction $F_c$ is absent, then the deadband is absent and the slip jump allows the MV to catch up with the OP. Fig. 3.4 shows the friction force with respect to valve-stem velocity in case of stiction no-offset.

**Stiction (overshoot):** If $J > S$, the valve output overshoots the valve input due
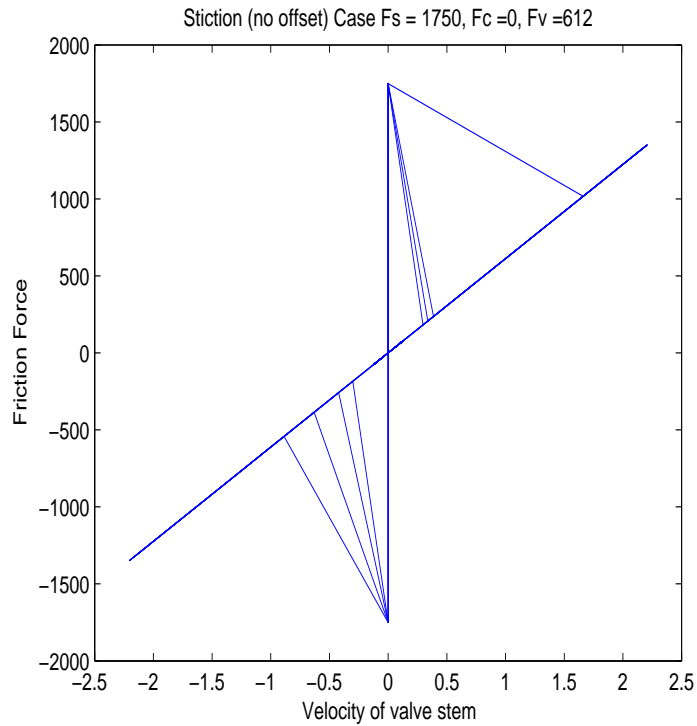


Figure 3.4: Stiction (no offset): Friction force vs. stem velocity.

to excessive stiction. This is termed as overshoot case of stiction. If the valve is miscalibrated, then swings in the valve position (MV) are larger than swings in the demanded position (OP). In that case, the gradient of the OP-MV plot is greater than unity during the moving phase. Fig. 3.5 shows the friction force with respect to valve-stem velocity in case of stiction no-offset.
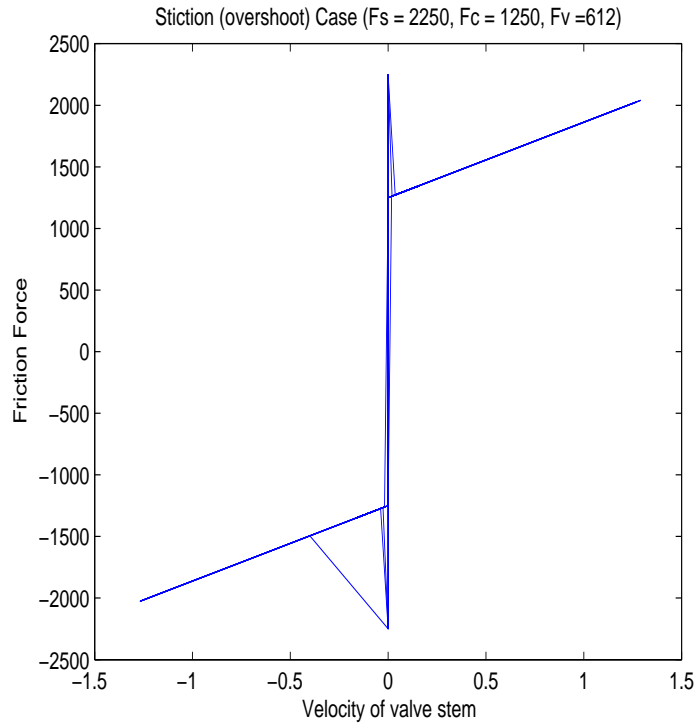
Figure 3.5: Stiction (overshoot): Friction force vs. stem velocity.
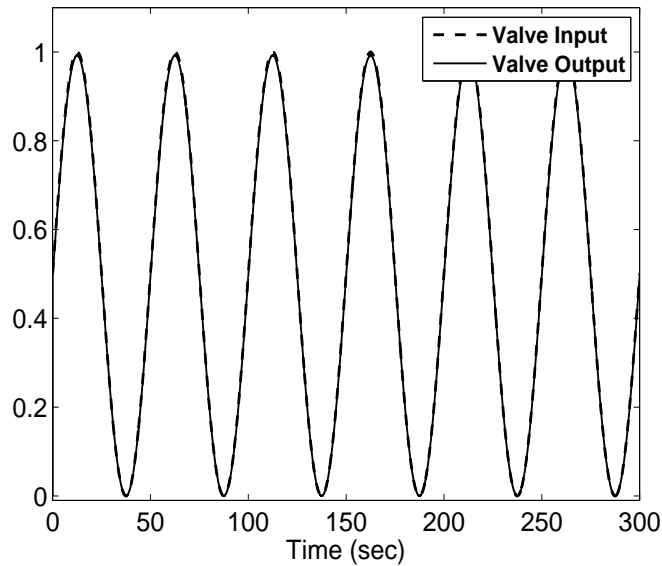


Figure 3.6: Time trends for OP and MV in case of linear friction (open-loop).

## Input-Output Valve Behavior - Simulation

The purpose of simulation of physical model of the valve is to determine the influence

of the friction terms on the process variables. Extensive simulations are conducted

| Parameters | Nominal case |
|---|---|
| $M$ | 1.36 $Kg$ |
| $F_s$ | 1750 $N$ |
| $F_c$ | 1250 $N$ |
| $F_v$ | 612 $Nsm^{-1}$ |
| Spring constant, $k$ | 52500 $N/m$ |
| Diaphragm area, $A$ | 0.0645 $m^2$ |
| Calibration factor, $k/A$ | 807692 $Pa/m$ |
| Air pressure | 68950 $Pa$ |

Table 3.1: Nominal values used for physical valve simulation [11].

for several cases of stiction. It is found that the nonlinearity in the model is able to induce limit cycle oscillations in a feedback loop. Input-output behavior of a control valve for different cases of valve stiction is shown in the following paragraphs.

undershoot case - physical

Figure 3.6 and 3.7 show the time trends and phase plot of OP and MV in case of no valve stiction. The input signal to the valve is sinusoidal to imitate the opening and closing of the valve.
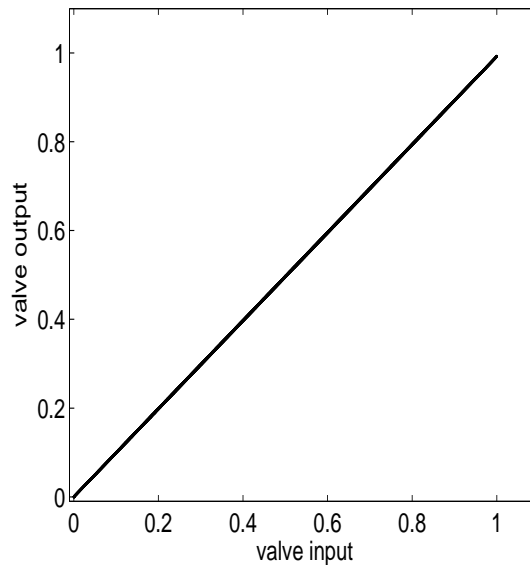


Figure 3.7: Phase plot of OP and MV in case of linear friction (open-loop).
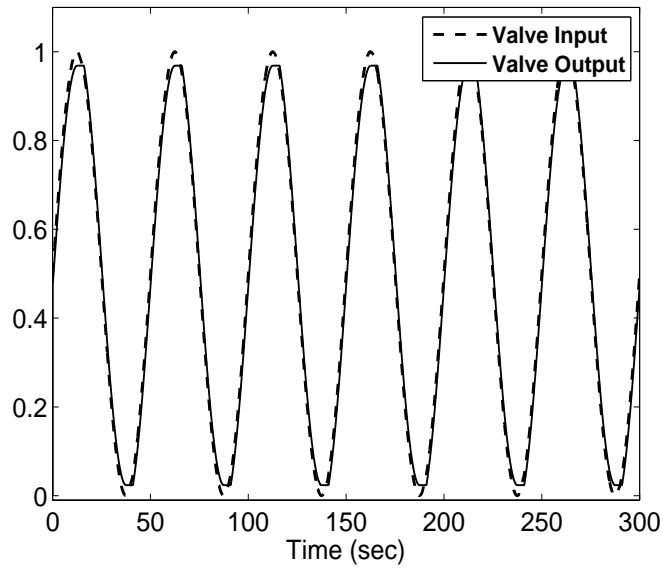
Figure 3.8: Time trends of OP and MV in case of pure deadband (open-loop).

Figure 3.8 and 3.9 show the time trends and phase plot of OP and MV in case of deadband only. Figure 3.10 and 3.11 show the time trends and phase plot of OP and MV in case of undershoot type of valve stiction. Figure 3.12 and 3.13 show the
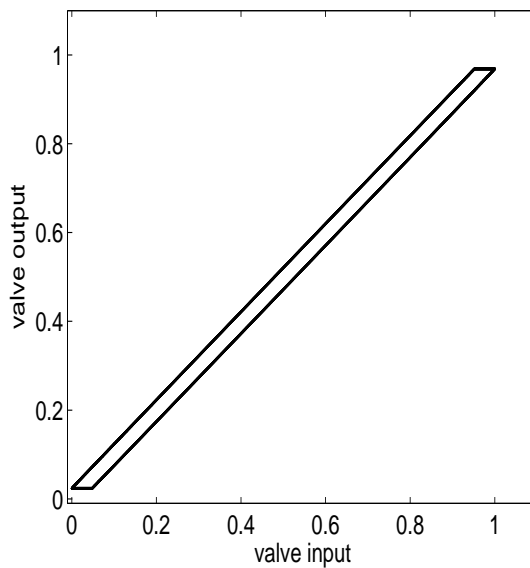


Figure 3.9: Phase plot of OP and MV in case of pure deadband (open-loop).
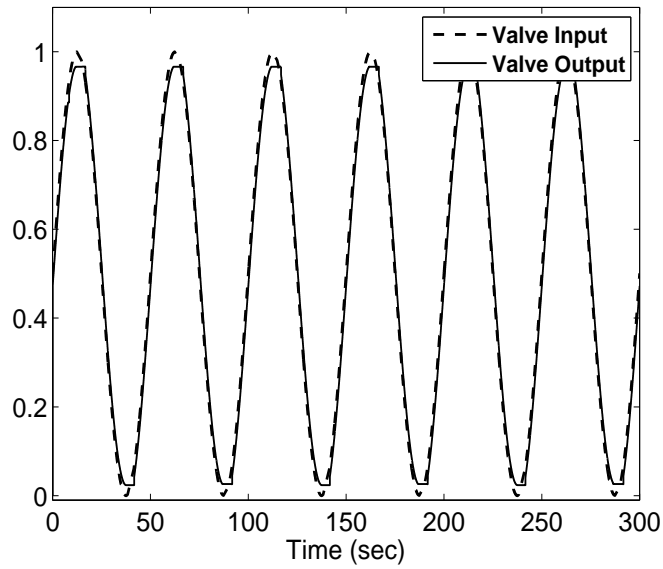
Figure 3.10: Time trends for in case of stiction undershoot (open-loop).

time trends and phase plot of OP and MV in case of no-offset type of valve stiction. Figure 3.14 and 3.15 show the time trends and phase plot of OP and MV in case of overshoot type of valve stiction.
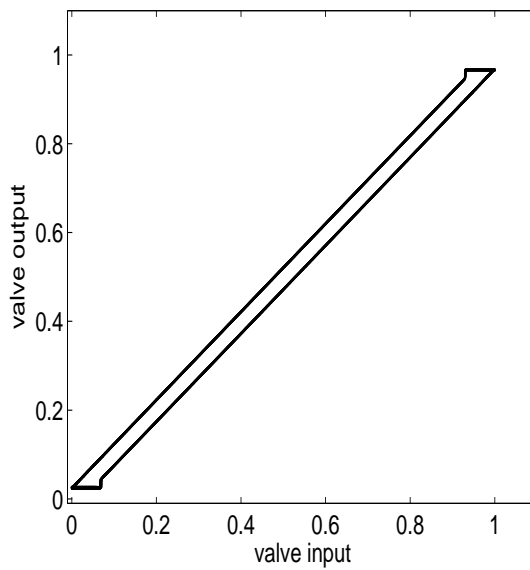


Figure 3.11: Phase plot of OP and MV in case of stiction undershoot(open-loop).
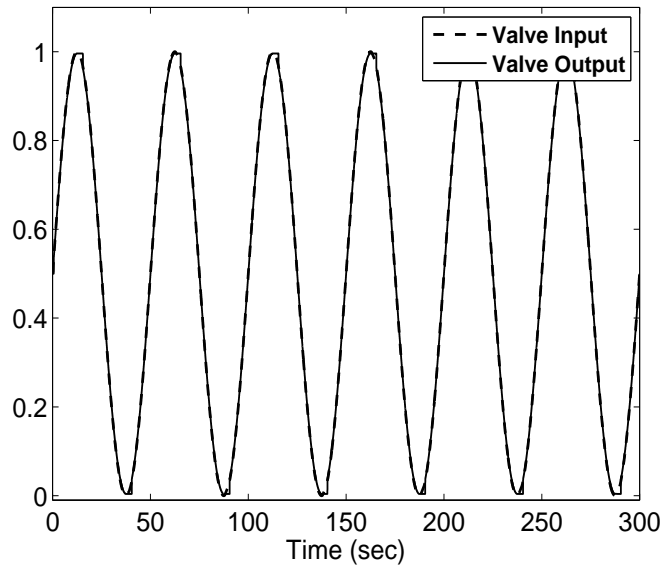
Figure 3.12: Time trends for OP and MV in case of stiction with no offset (open-loop).

The simulations for physical valve are conducted on MATLAB-SIMULINK environment. The shape of the time trends and phase plot show minor difference for different cases of valve stiction. Stuck-Slip-Jump behavior of the valve in case of stic-
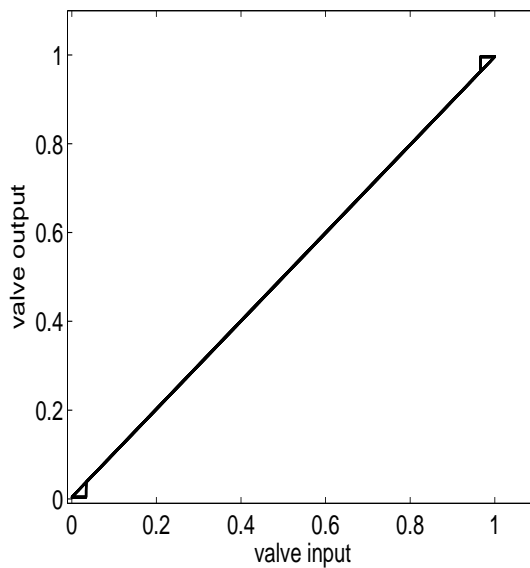


Figure 3.13: Phase plot of OP and MV in case of stiction with no offset (open-loop).
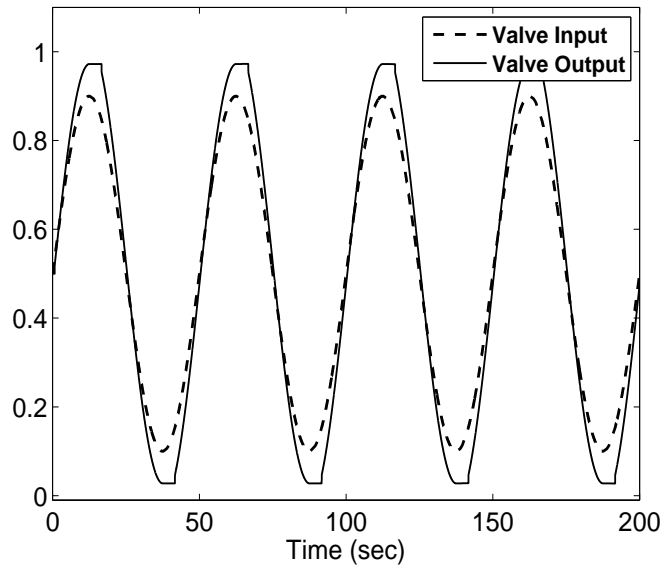
Figure 3.14: Time trends for OP and MV in case of stiction overshoot (open-loop).

tion causes process variables to oscillate around the set point in a control loop. Such

oscillations are referred as limit cycles which are internally generated due to valve stic-

tion and are sustained by the loop in the absence of any external set-point excitation
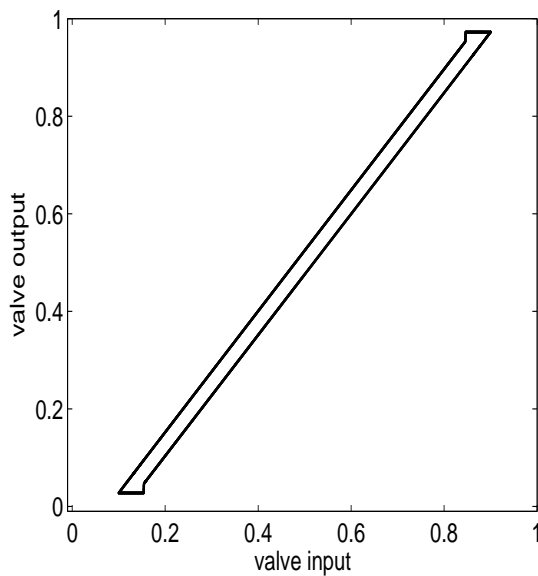


Figure 3.15: Phase plot of OP and MV in case of stiction overshoot (open-loop).

and compensation.

## 3.4 Data-Driven Models of Stiction

Complete description of a valve using a physical model needs many parameters which are difficult to obtain for all the control valves installed in a plant. Moreover, the physical models are quite complex and run slower during computations. The difficulties to deal with physical models redirected research towards data driven stiction models. A data-driven model is useful because it has only a few parameters to identify, and can run faster. In recent years, the models presented in technical literature are all data-driven, for example Stenman model [4], Choudhury model [31], He model [35], Kano model [25], and Two Layer Binary Tree model [39].

### 3.4.1 Stenman Model

**Model formulation**

The basic concept behind this model is to try to imitate the jump that occurs in the stem position, when stiction is overcome. The Stenman stiction model is parameterized by a single parameter "$d$" and is expressed by the following equation:

$$x(t) = \begin{cases} x(t-1) & if\,|u(t) - x(t-1)| \leq d, \\ u(t) & otherwise, \end{cases} \tag{3.3}$$

where $x(t-1)$ and $x(t)$ correspond to past and present stem positions, respectively, $u(t)$ is the present controller output and $d$ is defined as the valve stiction band.

## 3.4.2 Choudhury Model

Successive versions of the Choudhury model were presented in [30] [31] [11] [27]. It requires two parameters ($J$ and $S$) as shown in Figure 3.1. $S$ represents the amplitude of the input signal (pressure) during the time in which the stem is stuck (stickband+deadband). $J$ represents the size of the stem slip (slip jump). This model is described in the flowchart presented in Fig. 3.16.

**Model formulation:**

The valve sticks only when it is at rest or it is changing its direction. When the valve changes its direction, it comes to rest momentarily. Once the valve overcomes stiction, it starts moving and may keep on moving for sometime depending on how much stiction is present in the valve. In this moving phase, it suffers only dynamic friction, which may be smaller than the static friction. It continues to do so until its velocity is again very close to zero or it changes its direction.

In the process industry, stiction is generally measured as a % of the valve travel or the span of the control signal [21]. For example, a 2% stiction means that when the valve gets stuck it will start moving only after the cumulative change of its control signal is greater than or equal to 2%. If the range of the control signal is $4 - 20mA$, then a 2% stiction means that a change of the control signal less than $0.32mA$ in magnitude will not be able to move the valve. $[(20 - 4) * (2/100) = 0.32]$.

The model consists of two parameters-namely the size of deadband plus stickband

34
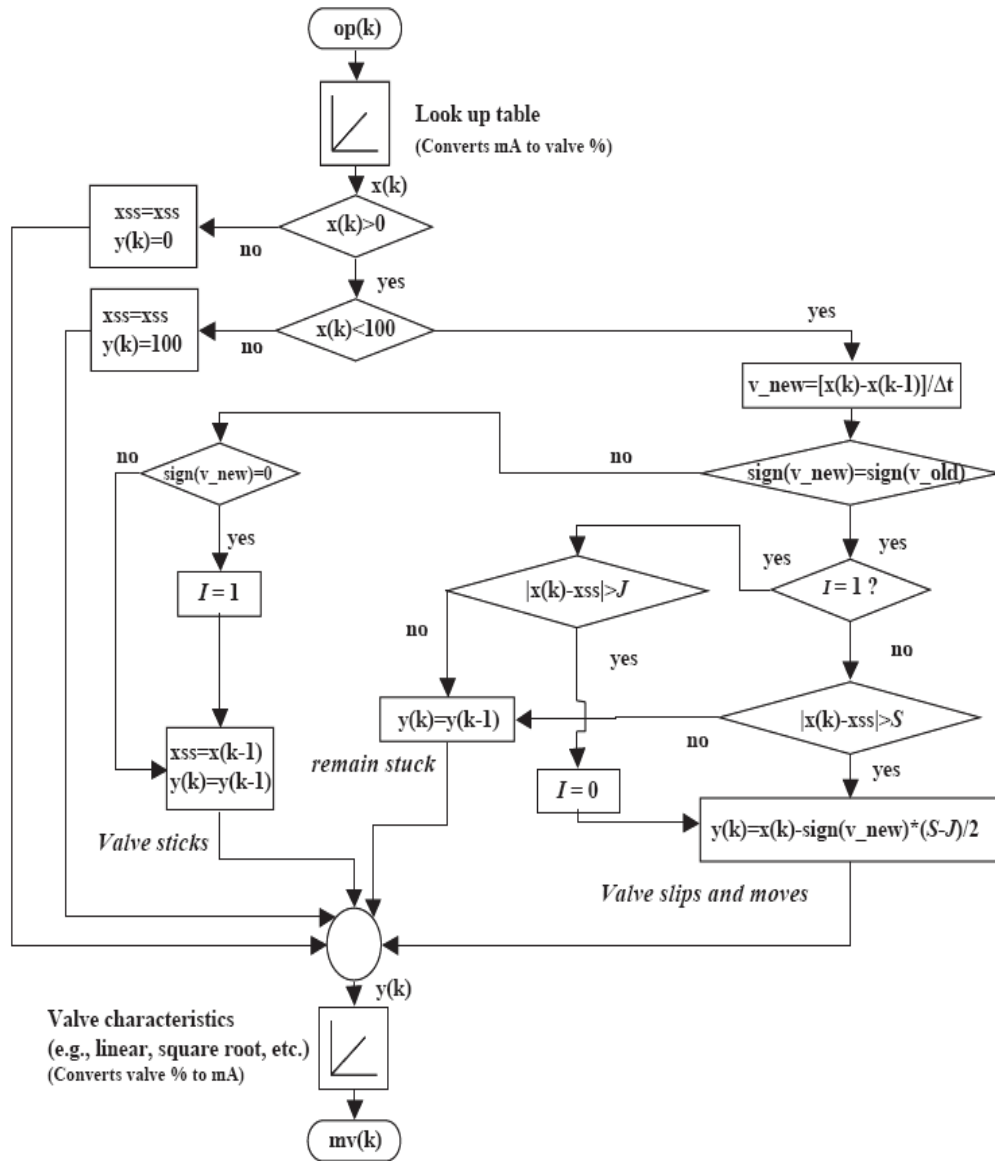
Figure 3.16: Flowchart for the Choudhury model [11]

S (specified in the input axis) and slip jump J (specified on the output axis). Note that the term 'S' contains both the deadband and stickband.

The model algorithm can be described as:

- First, the controller output ($mA$) is provided to the look-up table where it is converted to valve travel %.

- If this is less than 0 or more than 100, the valve is saturated (i.e., fully closed or fully open).

- If the signal is within 0-100% range, the algorithm calculates the slope of the controller output signal.

- Then the change of the direction of the slope of the input signal is taken into consideration. If the 'sign' of the slope changes or remains zero for two consecutive instants, the valve is assumed to be stuck and does not move. The 'sign' function of the slope gives the following:

  - If the slope of input signal is positive, the sign (slope) returns '+1'

  - If the slope of input signal is negative, the sign (slope) returns '-1'

  - If the slope of input signal is zero, the sign (slope) returns '0'.

Therefore, when sign (slope) changes from '+1' to '-1' or vice versa, it means the direction of the input signal has been changed and the valve is in the beginning of its stick position (points A and E in the Fig 3.1). The algorithm detects stick position of the valve at this point. Now, the valve may stick again while traveling in the same

direction (opening or closing direction) only if the input-signal to the valve does not change or remains constant for two consecutive instants, which is usually uncommon in practice. For this situation, the sign (- slope) changes to '0' from '+1' or '-1' and vice versa.

The algorithm again detects here the stick position of the valve in the moving phase and this stuck condition is denoted with the indicator variable $I = 1$. The value of the input signal when the valve gets stuck is denoted as $x_{ss}$. This value of $x_{ss}$ is kept in memory and does not change until the valve gets stuck again. The cumulative change of input signal to the model is calculated from the deviation of the input signal from $x_{ss}$.

- For the case when the input signal changes its direction (i.e., the sign(slope) changes from '+1' to '-1' or vice versa), if the cumulative change of the input signal is more than the amount of the deadband plus stickband (S), the valve slips and starts moving.

- For the case when the input signal does not change direction (i.e., the sign(slope) changes from '+1' or '-1' to zero, or vice versa), if the cumulative changes of the input signal is more than the amount of the stickband (J), the valve slips and starts moving. Note that this takes care of the case when the valve sticks again while traveling in the same direction ([12], [25]).

- The output is calculated using the equation:

$$output = input - sign(slope)(S - J)/2 \qquad (3.4)$$

and depends on the type of stiction present in the valve. It can be described as follows:

  - Deadband: If J = 0, it represents pure deadband case without any slip jump.

  - Stiction (undershoot): If $J < S$, the valve output can never reach the valve input. There is always some offset. This represents the undershoot case of stiction.

  - Stiction (no offset): If $J = S$, the algorithm produces pure stick-slip behavior. There is no offset between the input and output. Once the valve overcomes stiction, valve output tracks the valve input exactly. This is the well-known "stick slip case".

  - Stiction (overshoot): If $J > S$, the valve output overshoots the valve input due to excessive stiction. This is termed as overshoot case of stiction.

  Recall that J is an output (y-axis) quantity. Also, the magnitude of the slope between input and output is 1.

- The parameter J signifies the slip jump start of the control valve immediately after it overcomes the deadband plus stickband. It accounts for the offset between the valve input and output signals.

38

- Finally, the output is again converted back to a mA signal using a look-up table based on the valve characteristics such as linear, equal percentage or square root, and the new valve position is reported.

### 3.4.3 Kano Model

The Choudhury model is not able to deal with both deterministic and stochastic signals [25]. The Kano model is an extension that requires the same two parameters used in the Choudhury model. The algorithm for Kano model is presented in a flowchart ([25]) shown in Fig.3.17

**Model formulation** To model the relationship between the controller output and the valve position of a pneumatic control valve, the balance among elastic force, air pressure, and frictional force needs to be taken into account. The relationship can be described as shown in following Fig. 3.18

The dashed line denotes the states where elastic force and air pressure are balanced. The controller output and the valve position change along this line in an ideal situation without any friction. The ideal relationship is disturbed when friction arises. For example, the valve is resting at (a) where elastic force and air pressure are balanced. The valve position cannot be changed due to static friction even if the controller output, i.e., air pressure, is increased. The valve begins to open at (b) where the difference between air pressure and elastic force exceeds the maximum static frictional force. Since the frictional force changes from static $f_S$ to kinetic $f_D$ when the valve starts to move at (b), a slip-jump of the size $J = f_S - f_D$ happens and the valve state
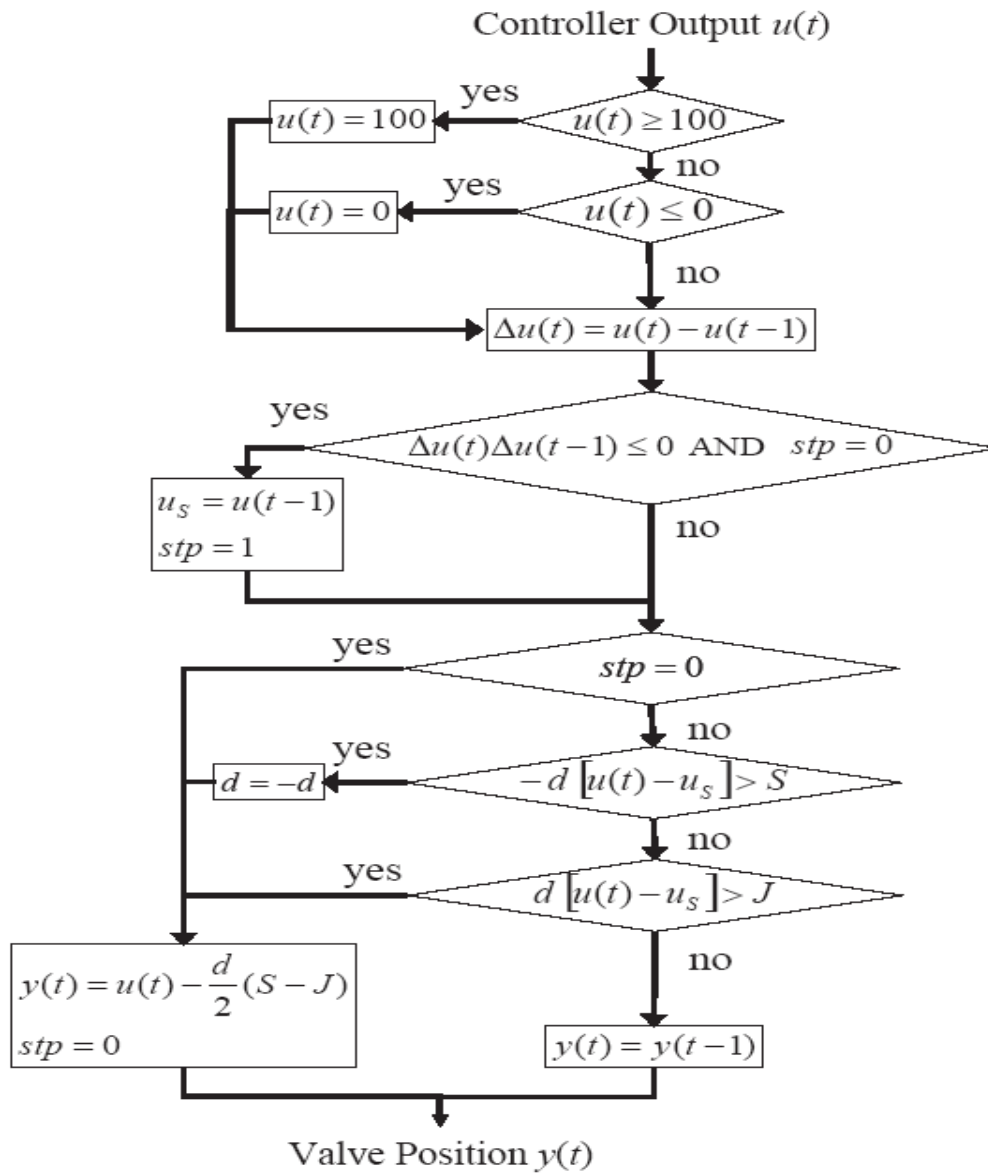
Figure 3.17: Flowchart for the Kano model [25]
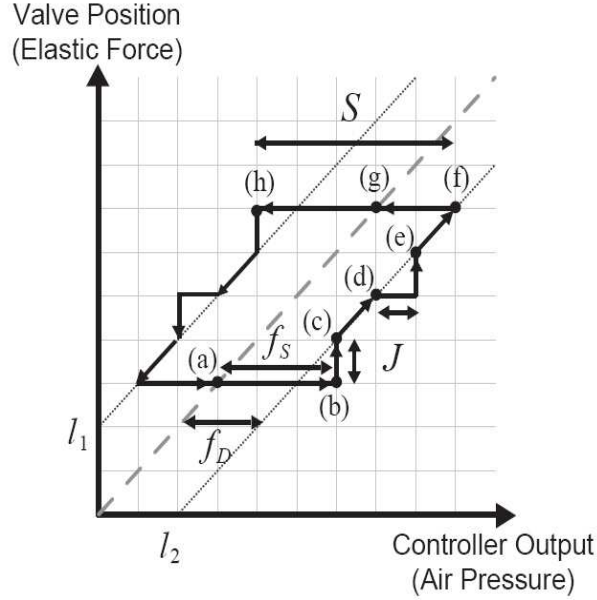
Figure 3.18: Relation between controller output and valve position under valve stiction [25].

changes from (b) to (c). Thereafter, the valve state changes along the line l2 which deviates from the ideal line by $f_D$ because the difference between air pressure and elastic force is equal to $f_D$. When the valve stops at (d), the difference between air pressure and elastic force needs to exceed $f_S$ again for the valve to open further. Since the difference between them is $f_D$ at (d), air pressure must increase by J to open the valve. Once air pressure exceeds elastic force by $f_D$, the valve state changes to (e) and then follows l2. Air pressure begins to decrease when the controller orders the valve to close at (f). At this moment, the valve changes its direction and comes to rest momentarily. The valve position does not change until the difference between elastic force and air pressure exceeds the maximum static frictional force $f_S$. The valve state (h) is just point-symmetric to (b). The difference of air pressure between (f) and (h) is given by $S = f_S + f_D$.

The valve state follows the line $l_1$ while the valve position decreases. The above-

41

mentioned phenomena can be modeled as a flowchart shown in Fig. 3. The input and output of this valve stiction model are the controller output u and the valve position y, respectively. Here, the controller output is transformed to the range corresponding to the valve position in advance. The first two branches check if the upper and the lower bounds of the controller output are satisfied. In this model, two states of the valve are explicitly distinguished: 1) a moving state $(stp = 0)$, and 2) a resting state $(stp = 1)$. In addition, the controller output at the moment the valve state changes from moving to resting is defined as $u_S$. $u_S$ is updated and the state is changed to the resting state $(stp = 1)$ only when the valve stops or changes its direction $(\Delta u(t)\Delta u(t - 1) \leq 0)$ while its state is moving $(stp = 0)$. Then, the following two conditions concerning the difference between u(t) and $u_S$ are checked unless the valve is in a moving state. The first condition judges whether the valve changes its direction and overcomes the maximum static friction (corresponding to (b) and (h) in Fig. 3.18). Here, $d = \pm 1$ denotes the direction of frictional force. The second condition judges whether the valve moves in the same direction and overcomes friction. If one of these two conditions is satisfied or the valve is in a moving state, the valve position is updated via the following equation.

$$y(t) = u(t) - df_D = u(t) - \frac{d(S - J)}{2} \tag{3.5}$$

On the other hand, the valve position is unchanged if the valve remains in a resting state.

**Claimed:** The Kano's valve stiction model has several advantages compared with the model proposed by Choudhury [30]. First, it can cope with stochastic input as

well as deterministic input. Second, $u_S$ can be updated at appropriate timings by introducing the valve state *stp*. Third, it can change the degree of stiction according to the direction of the valve movement.

### 3.4.4  Two-Layer Binary Tree Model

This is the improved version of He model [35]. The Two-Layer Binary Tree model addresses all possible state transitions, as well as different stiction patterns which were missing in [35].

**Model formulation:**

The model proposed in this paper is as shown in Fig. 3.19. According to Fig. 3.19, the model first updates the value of $cum_u(k)$, and, in addition, the direction of movement $d(k)$ is obtained via $sgn - (cum_u(k))$; then, if the valve status flag (Stop) is equal to 1, the logic flows to the left branch, which determines the position of the valve if it is stuck in the previous interval. The algorithm does not mention the initial values for d and Stop falgs. During the investigation of this model, it is found necessary to initialize these flags properly, otherwise the model does not work properly. The algorithm contained in the left branch is identical to the He et al. [35] model. If $cum_u(k)$ is large enough to overcome the static friction $f_S$, the valve position $u_v(k)$ will be the controller output $u(k)$ minus the dynamic friction $f_D$. The term $cum_u(k)$ is updated to be equal to $\pm f_D$, because, when the valve starts slipping, the force being counteracted by friction is equal to $\pm f_D$ (the sign is dependent on the direction of movement $d(k)$). In addition, the valve status flag Stop is updated to be zero, to
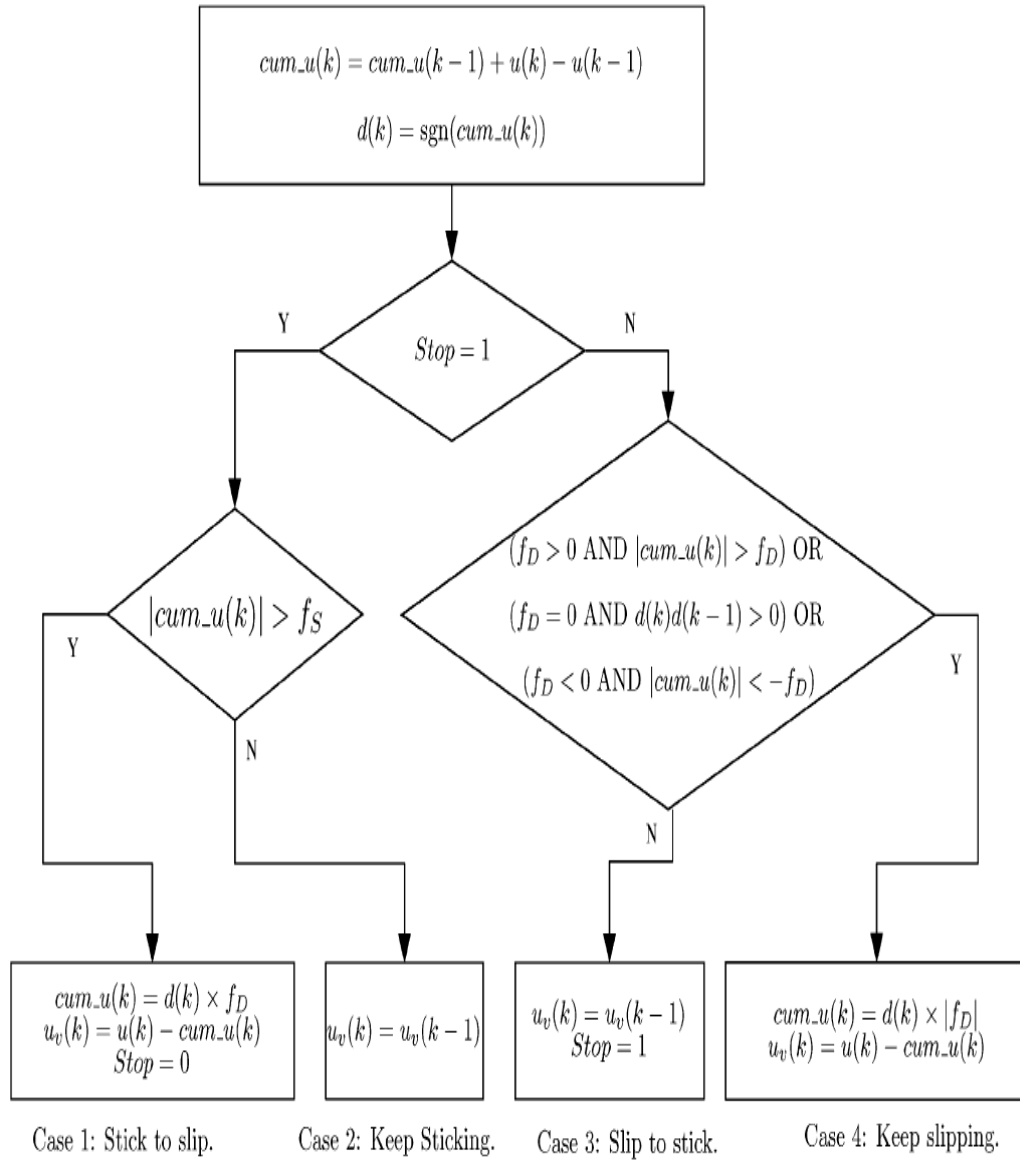
Figure 3.19: Relation between controller output and valve position under valve stiction [39].

indicate that the valve switches to a slipping mode. Otherwise, the valve remains in the previous position. When the valve is in a slipping state, the condition to determine the status in the next instant is dependent on the sign of $f_D$, because the two pairs $f_S, f_D$ and $S, J$ have the following relationships [25]:

$$f_S = \frac{S + J}{2} \tag{3.6}$$

$$f_D = \frac{S - J}{2} \tag{3.7}$$

Note that $f_S > 0$, because $S > 0$ and $J > 0$. The MV-OP pattern that corresponds to $f_D$ can be summarized as follows:

- $f_D > 0 (or S > J)$, which indicates stiction with undershoot or pure deadzone.

- $f_D = 0 (or S = J)$, which indicates stiction with no offset or linear.

- $f_D < 0 (or S < J)$, which indicates stiction with overshoot.

Pure deadzone and linear patterns can be seen as special cases of a stiction pattern with $f_S = f_D > 0$ and $f_S = f_D = 0$ accordingly. In what follows, the major three patterns - stiction with undershoot, no offset, and overshoot - are discussed separately. The MV-OP plot of stiction with an undershoot pattern is shown in Fig. 3.20. The shaded area in the MV-OP plane shows the region where $|cum_u| > f_D$. From this figure, it can be observed that, if the valve is currently slipping, it will keep slipping as long as $|cum_u| > f_D$. Otherwise, it will change to stick mode. When the valve keeps slipping, $cum_u$ is updated to be $d(k) x f_D$, whereas the actual valve displacement is the
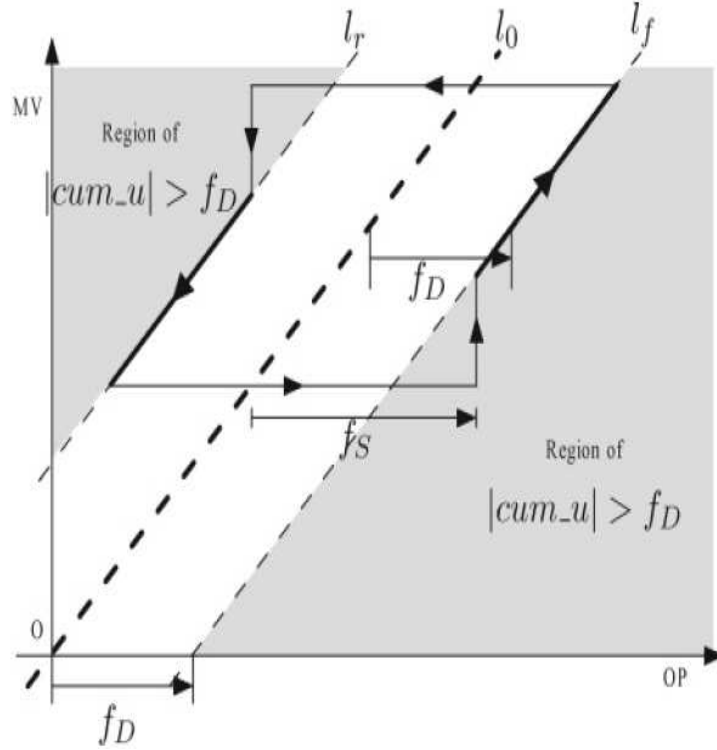
Figure 3.20: MV-OP plot of stiction with an undershoot pattern [39].

offset between input u and the updated $cum_u$ parameter. When the valve changes to a stick mode, the valve remains in the previous position and the status parameter Stop is set to be 1. Fig. 3.21 gives the MV-OP plot of stiction with an overshoot pattern. Similar to the undershoot case, the slipping valve will keep slipping as long as $cum_u$ falls into the shading region, i.e., $|cum_u| < -f_D$. In this case, the parameter $cum_u$ is updated by $d(k)x(-f_D)$. The valve position is determined by the same equation as that in the undershoot pattern, in both cases of keeping slipping and starting sticking. The stiction without an offset pattern is somewhat special. Fig. 3.22 shows the MV-OP plot in this case. The slipping valve will keep slipping when the direction flag d has the same sign over two consecutive sampling intervals. Because, in the slipping mode, there is no dynamic friction or $f_D = 0$, the parameter $cum_u$ is reset
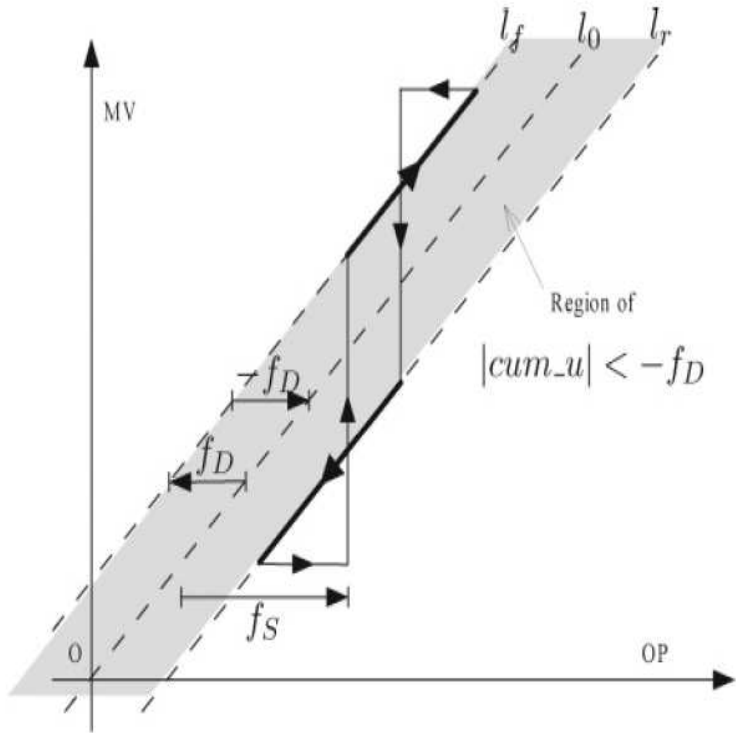
Figure 3.21: MV-OP plot of stiction with an overshoot pattern [39].
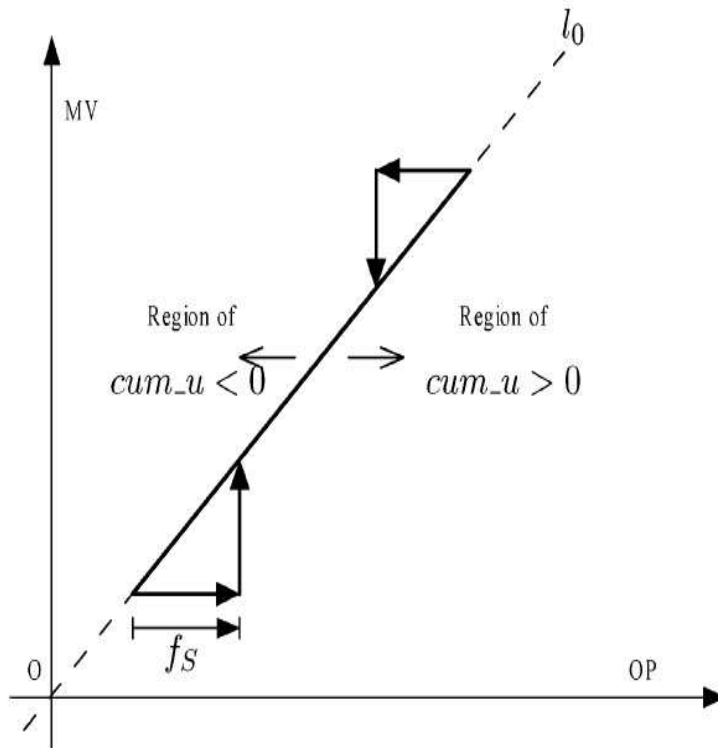


Figure 3.22: MV-OP plot of stiction with no offset pattern [39].

to be zero and the actual valve position is uv = u. The condition for determining the valve position when it changes from slip to stick is identical to the previous two cases. Combining the aforementioned three cases, the position of the valve when it is currently in a slipping mode can be summarized in the right branch of Fig. 3.19. A complete, two layer binary tree logic stiction model has been configured.

## 3.5 ISA tests

### 3.5.1 Dynamic test method

Starting with the user defined minimum signal specified, ramp the input signal (control signal to a positioner or pressure signal to an actuator) to the maximum signal specified, wait for the pause time and ramp down to the minimum signal. Then wait for the pause time again. The format of the input signals corresponds to a trapezoidal wave. During the travel, record the input signal and valve position. This test generates what are known as signature curves of the valve, which are produced by operating a valve through its signal range which, according to ISA (2006), are plotted with stem travel in the vertical axis and actuator pressure in the horizontal axis, with both scales ranging from 0% to 100%. Thus, the signature curves are derived by plotting the valve position versus the input signal in both directions, over the minimum to the maximum input signal specified for the application. This test signal is a trapezoidal wave with ramp time of 4 seconds, pause time of 1 second and contains 2 test cycles. The response of data driven stiction models to the dynamic test are shown in Figures
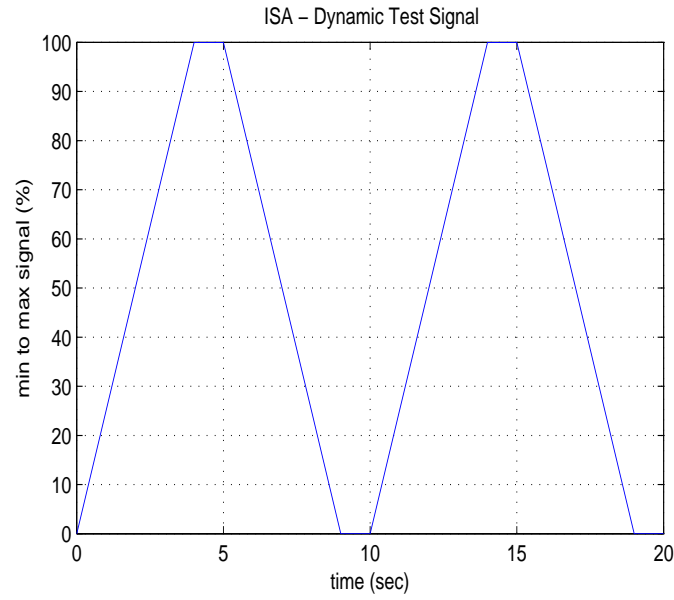
Figure 3.23: Dynamic Test Signal.

3.24, 3.25, 3.26 and 3.27.

## 3.5.2  Ramp and pause test method

Starting at the user defined minimum input signal specified, ramp the input signal at a slow rate. Wait for the ramp and pause time specified. Repeat the procedure up to the maximum input signal specified. Record the input signal and valve position. Repeat the preceding process in the opposite direction. This is also a trapezoidal wave with ramp and pause times of 1 second each. The pauses are given at 20%, 40%, 60%, 80%, and 100%. This signal contains 2 test cycles. The response of data driven stiction models to the Ramp and Pause test are shown in Figures 3.29, 3.30, 3.31 and 3.32.

49
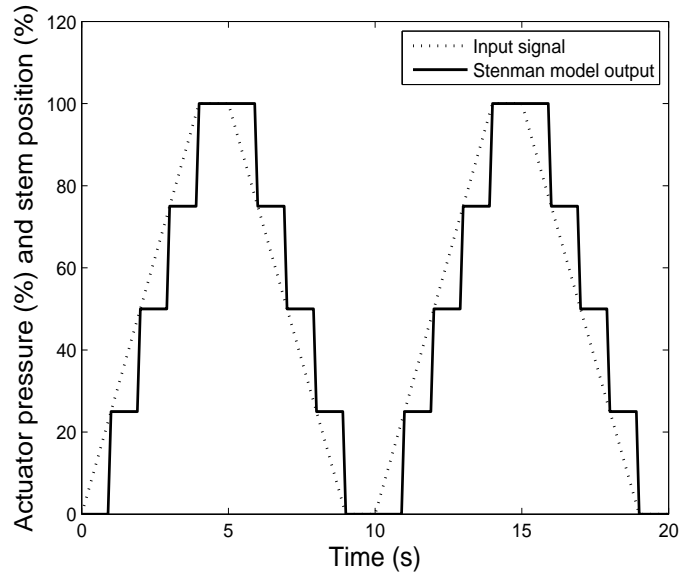
Figure 3.24: Dynamic Test on Stenman Model (No Stiction).
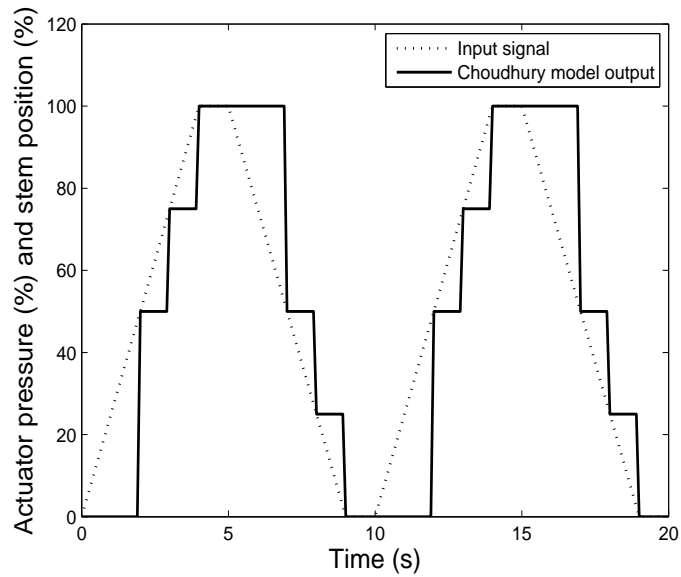


Figure 3.25: Dynamic Test on Choudhury Model (No Stiction).
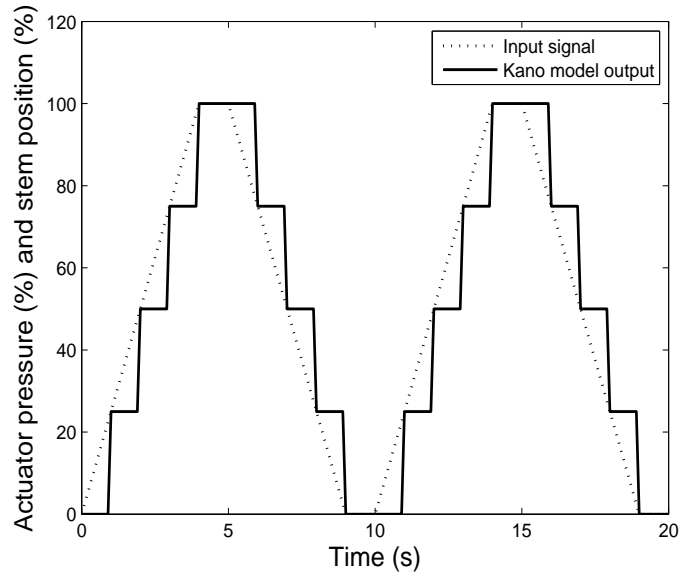
Figure 3.26: Dynamic Test on Kano Model (No Stiction).
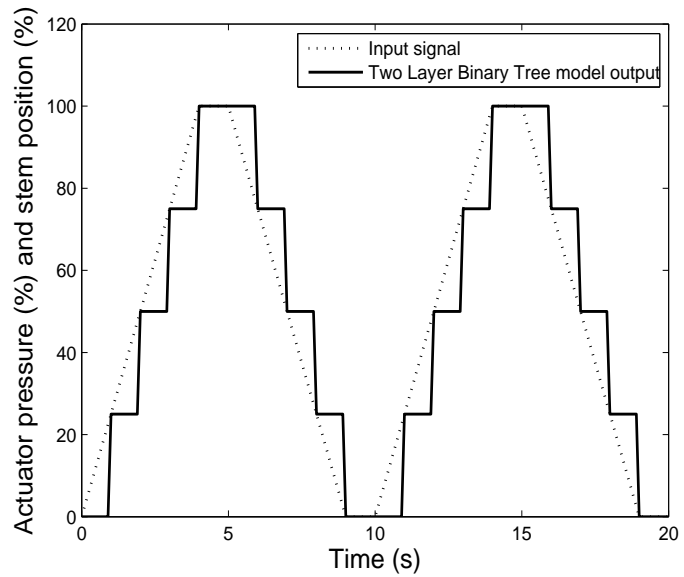


Figure 3.27: Dynamic Test on Two Layer Binary Tree Model (No Stiction).

Figure 3.28: Ramp and Pause Test Signal.
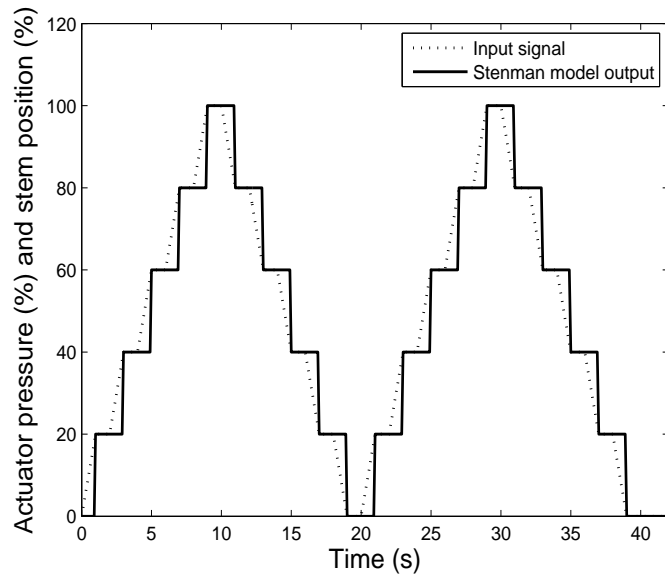


Figure 3.29: Ramp and Pause Test on Stenman Model (No Stiction).
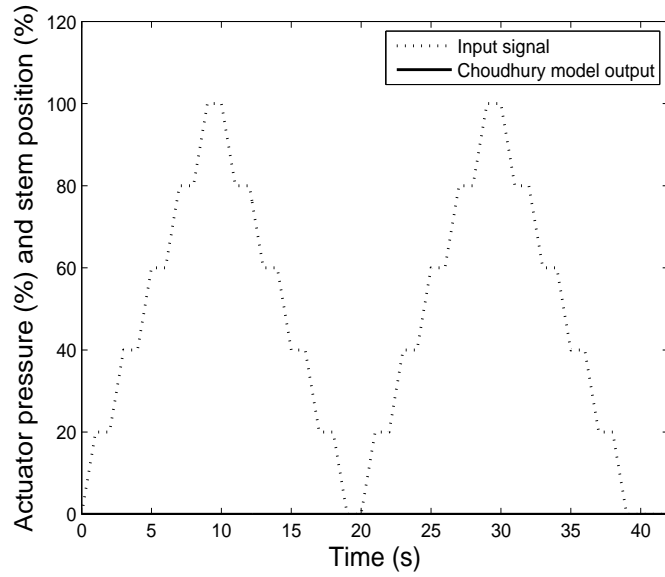
Figure 3.30: Ramp and Pause Test on Choudhury Model (No Stiction).
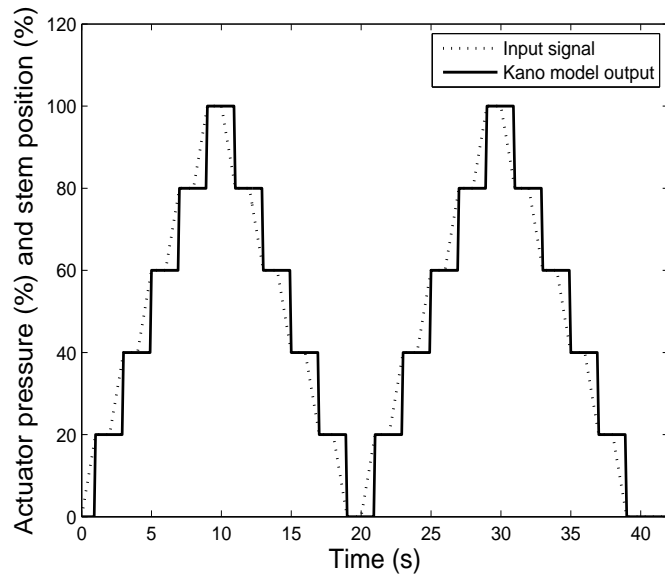


Figure 3.31: Ramp and Pause Test on Kano Model (No Stiction).
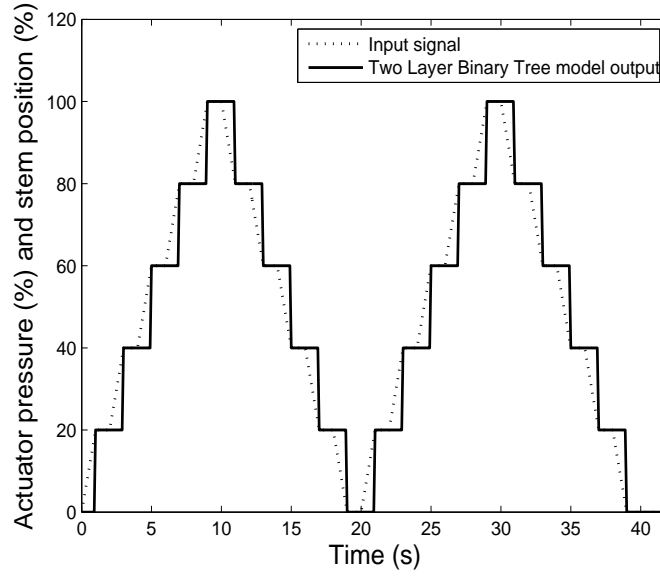
Figure 3.32: Ramp and Pause Test on Two Layer Binary Tree Model (No Stiction).

### 3.5.3 Baseline test method

Used to evaluate measurement noise, the presence of limit cycles, and the baseline response time $T_{86}$, that corresponds to the interval of time between initiation of an input signal step change and the moment at which the response reaches 86.5% of its full steady state value. In the example given in ISA (2000) [5], two steps up are applied in the input signal, from 50% to 52% and from 52% to 54%; and two steps down, from 54% to 52% and from 52% to 50%. This test signal is a staircase wave. The step time is every 1 second with step amplitude of 2% (starting step ups from 50% to 100% and step down to 50%). This test signal is applied for 1 cycle.

The response of data driven stiction models to the Ramp and Pause test are shown in Figures 3.34, 3.35, 3.36 and 3.37.
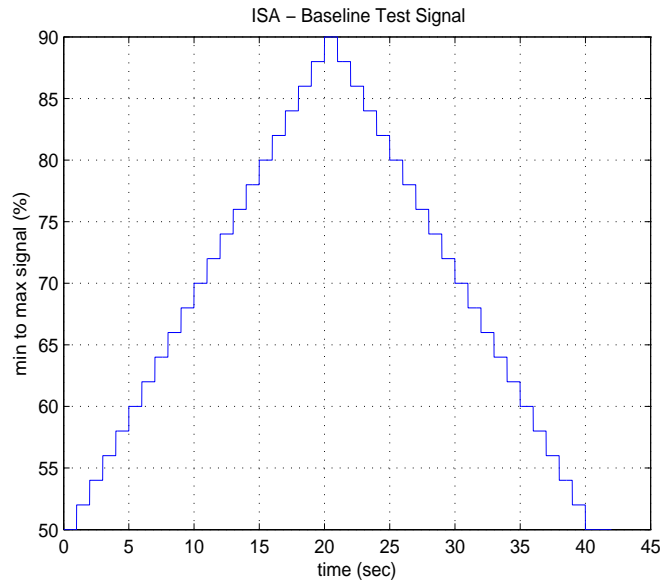
Figure 3.33: Baseline Test Signal.
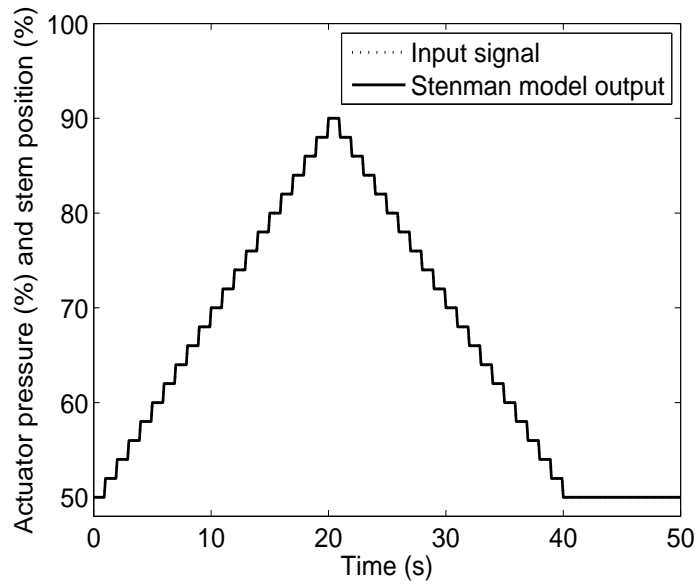


Figure 3.34: Baseline Test on Stenman Model (No Stiction).
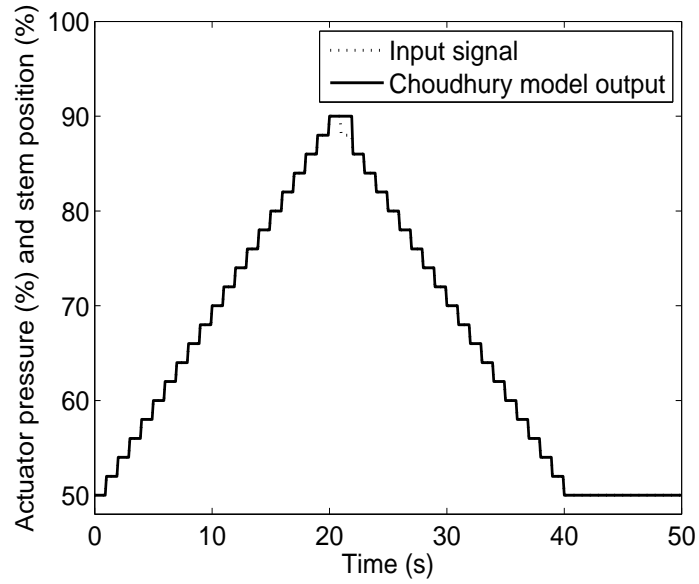
Figure 3.35: Baseline Test on Choudhury Model (No Stiction).
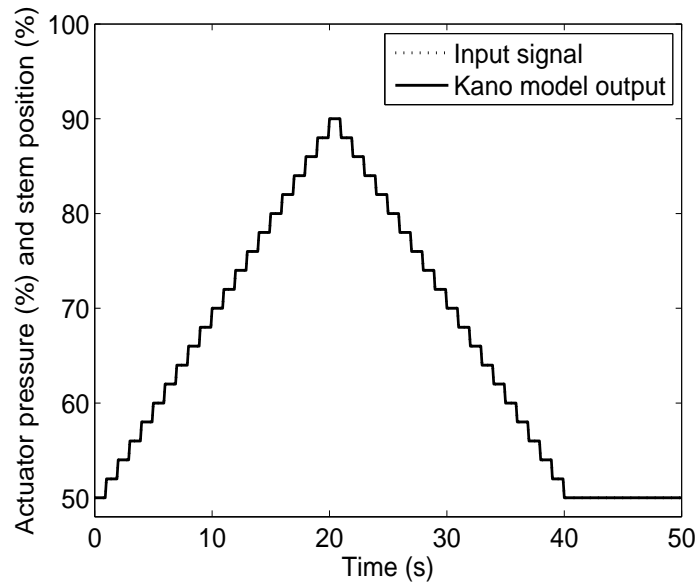


Figure 3.36: Baseline Test on Kano Model (No Stiction).
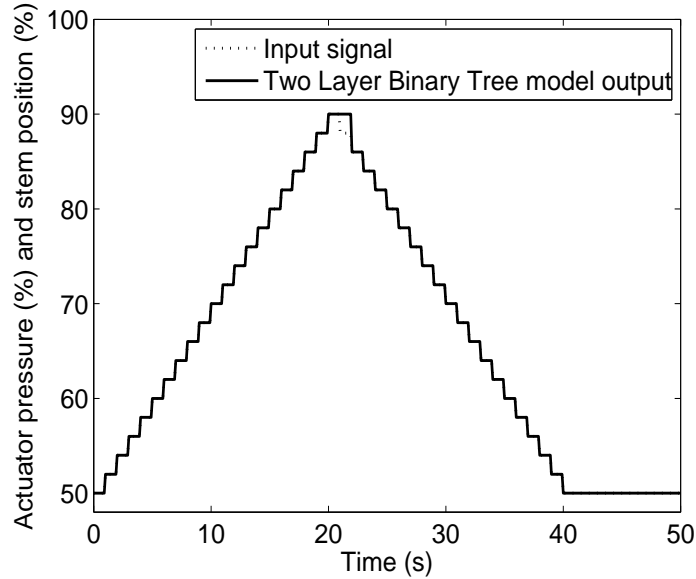
Figure 3.37: Baseline Test on Two Layer Binary Tree Model (No Stiction).

## 3.5.4 Small step test method

Used to determine dead band and resolution. The dead band is the range through which an input signal may be varied, with reversal of direction, without initiating an observable change in output signal. In ISA (2000) [5] it is defined as a percentage of input span. The resolution is the smallest step increment of input signal in one direction for which movement of the output is observed, expressed as percentage of input span. In ISA (2000) [5] the test given as example was performed with incremental steps of 0.1%, starting at 50% of the input signal and reaching 50.6% and coming back to 50%, each step lasting 30 s. The whole cycle must be repeated twice. It is necessary to assure that there is at least one step in addition to the step causing initial movement. This is a staircase wave with step time at every 1 second and step amplitude of 0.1% (starting at 50% to 51.7% and step down to 50%). It is applied for two test cycles and the pause time between each step is 1 second.
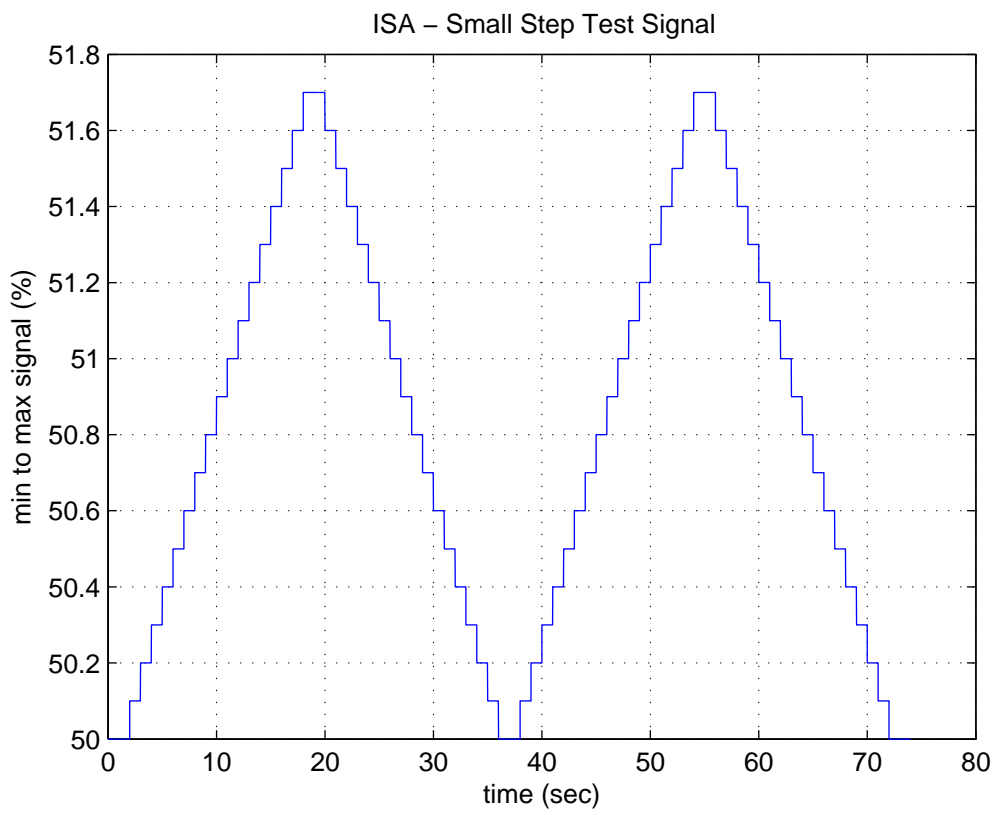
Figure 3.38: Small Step Test Signal.
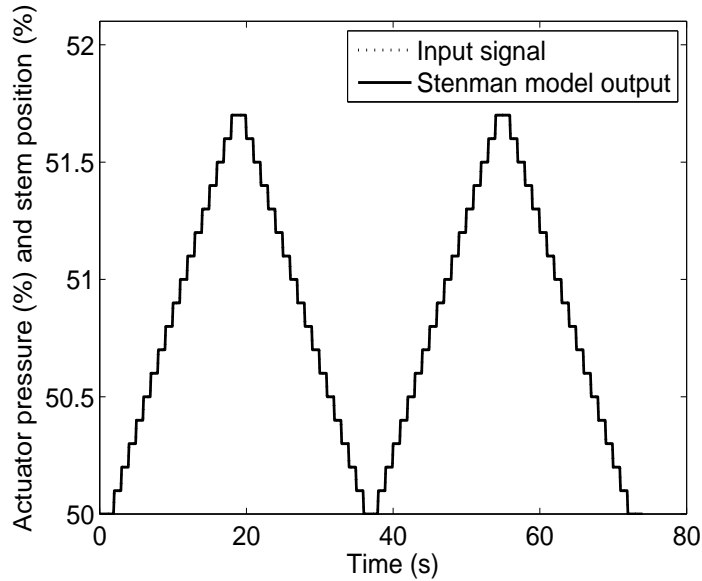
Figure 3.39: Small Step Test on Stenman Model (No Stiction).

The response of data driven stiction models to the Ramp and Pause test are shown in Figures 3.39, 3.40, 3.41 and 3.42.

### 3.5.5 Response time test method

Consists of an increasing sequence of step sizes. Start the test with a step size of 0.1% and end with 10%, assuming the following values: 0.1%, 0.2%, 0.5%, 1%, 2%, 5% and 10% of input signal span. Larger steps sizes such as 20% and 50% may be used if desired. In the example given in ISA (2000) [5], each step lasts 1 min. This test signal is shown in Fig. 3.43.

This is like a staircase wave (consisting of increasing sequence of step sizes) with step time at every 1 second. The step sizes are 0.1%, 0.2%, 0.5%, 1%, 2%, 5%, 10% (Both up and down of 50% of input signal). Each step has a pause time of 1 second and the test has 2 cycles.
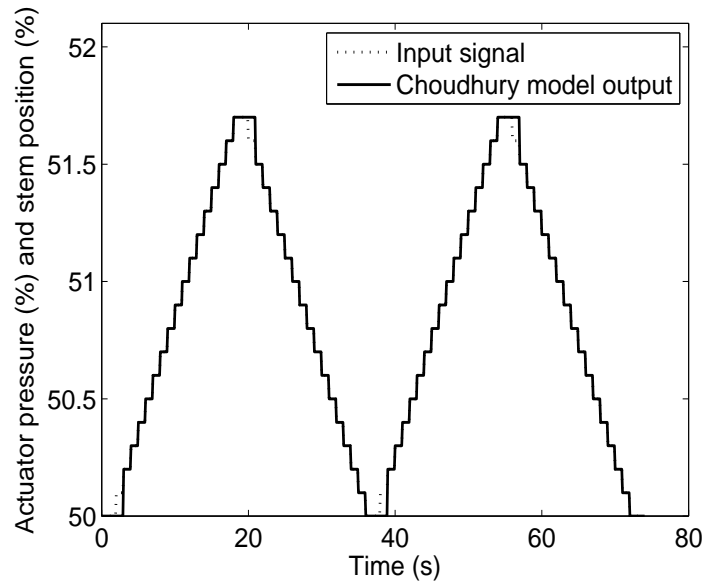
Figure 3.40: Small Step Test on Choudhury Model (No Stiction).
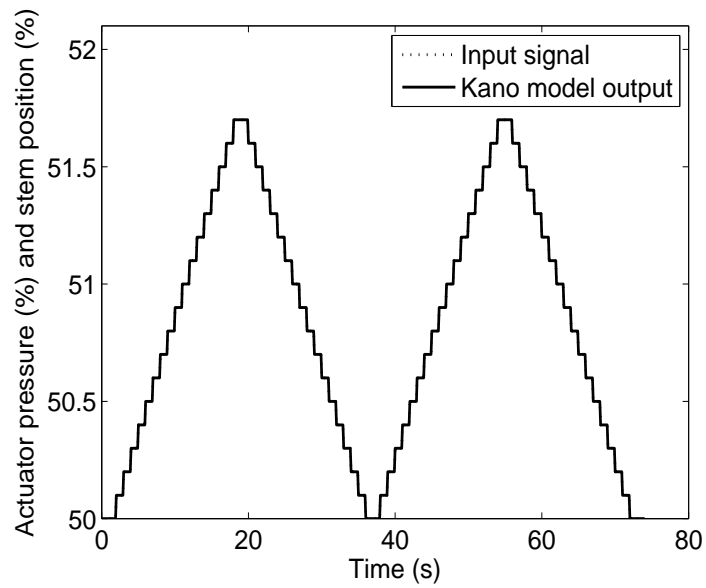


Figure 3.41: Small Step Test on Kano Model (No Stiction).
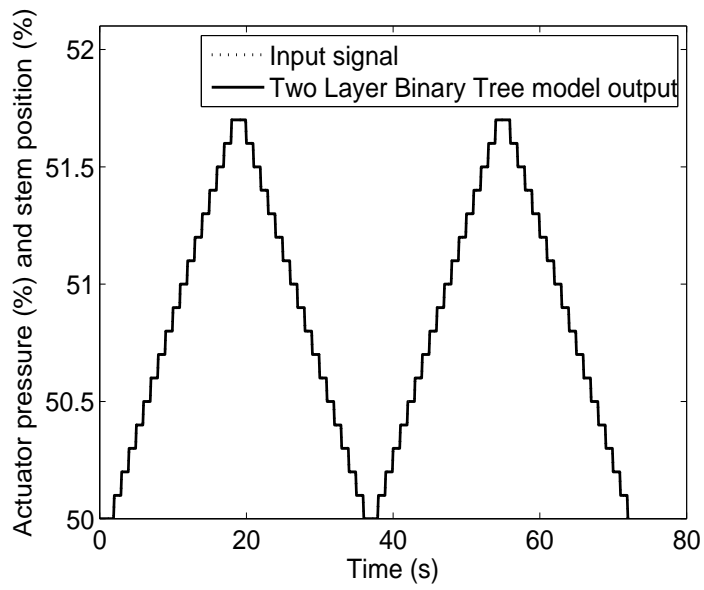
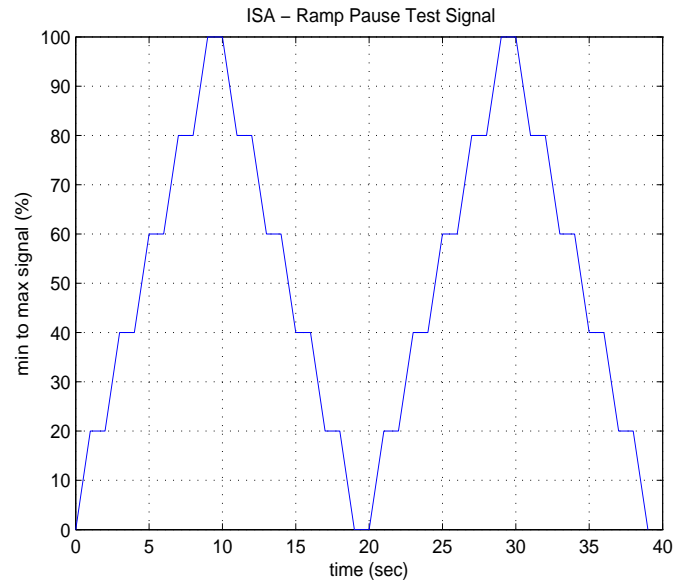Figure 3.42: Small Step Test on Two Layer Binary Tree Model (No Stiction).
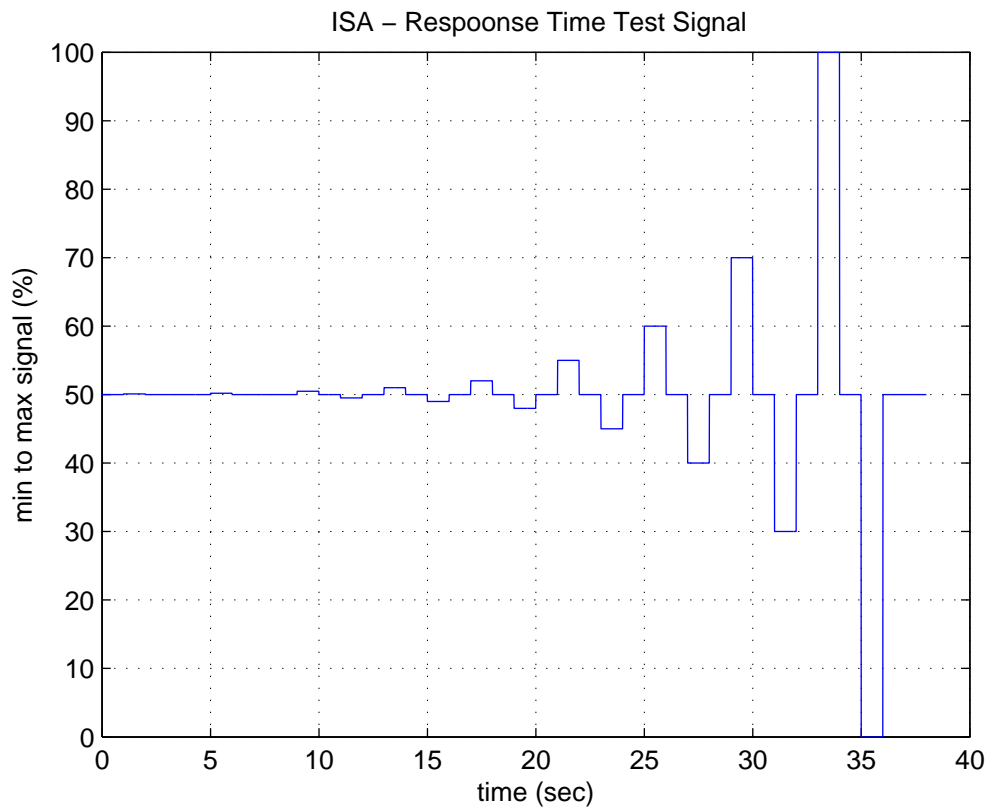


Figure 3.43: Response Time Test Signal.
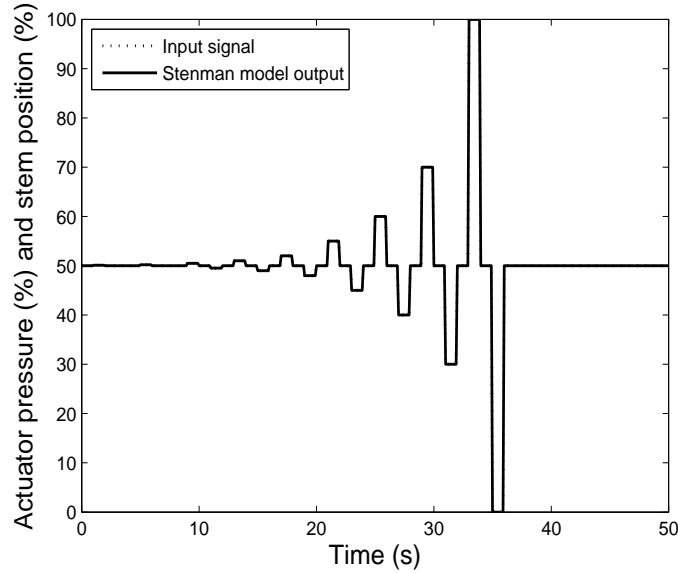
Figure 3.44: Response Time Test on Stenman Model (No Stiction).

The response of data driven stiction models to the Ramp and Pause test are shown in Figures 3.44, 3.45, 3.46 and 3.47.

## 3.6 Applications of the control valve friction models

At this point, we would like to highlight the key requirements and uses of the stiction models. Modeling of stiction was initiated to better understand and to quantify the valve friction coefficients to help reduce the control loop variability [16]. It is part of what is known as control performance monitoring/assessment, an important asset-management technology to maintain highly efficient operation performance of automation systems in production plants (Jelali, 2006; Thornhill & Horch, 2006, 2007). Some of the control valve friction models investigated here have been applied
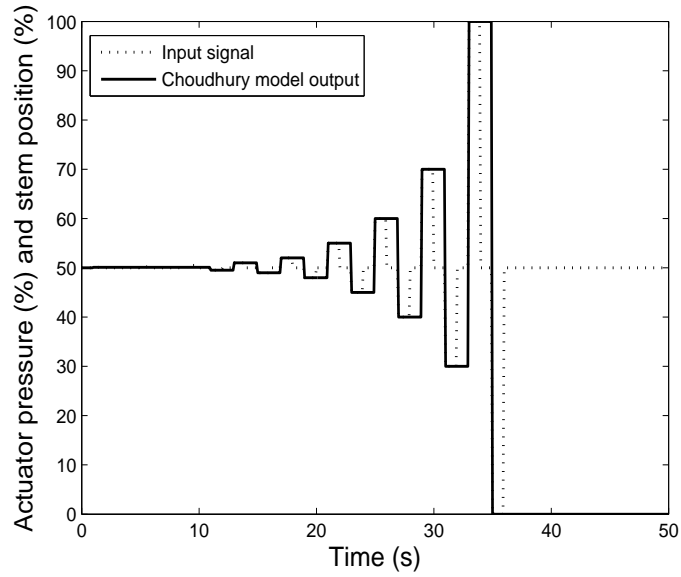
Figure 3.45: Response Time Test on Choudhury Model (No Stiction).
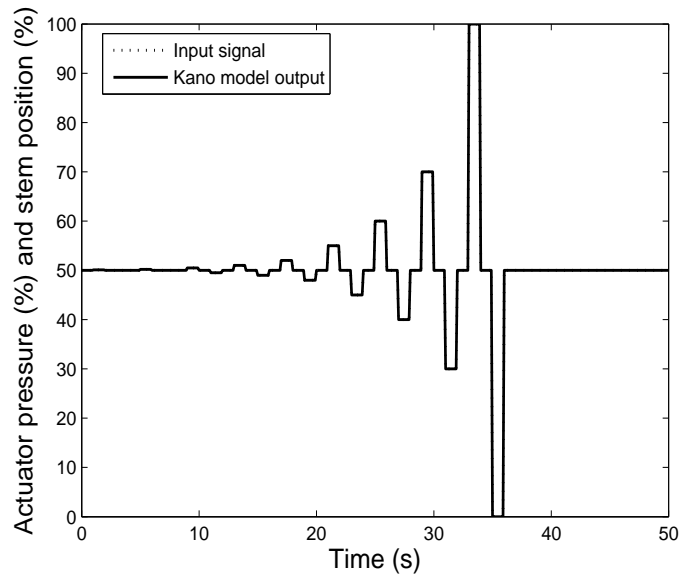


Figure 3.46: Response Time Test on Kano Model (No Stiction).
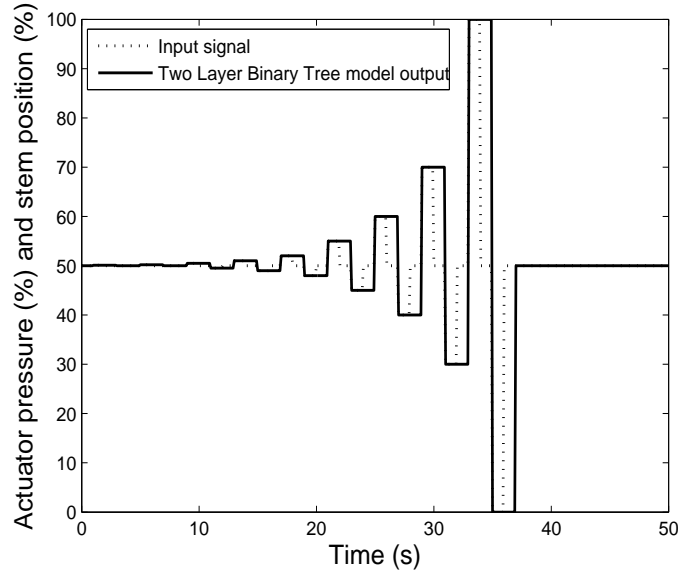
Figure 3.47: Response Time Test on Two Layer Binary Tree Model (No Stiction).

to stiction detection and quantification in several papers.

The Stenman model is used in Stenman et al. (2003) for stiction detection. In Kano et al. (2004) the authors propose an algorithm for valve stiction detection. In Rossi and Scali (2005) and Singhal and Salsbury (2005) the Choudhury model is used to analyze the proposed valve stiction detection method. In He et al. (2007) the authors consider the He model to detect stiction. The Two Layer Binary Tree model is extended work based on He model. Concerning quantification of control valve stiction, the papers Garcia (2007) and Romano and Garcia (2007, 2008) focus on techniques to estimate the parameters of the Karnopp model (m, k, Fv, Fc and Fs). The idea of "Detection and quantification of control valve stiction" is to detect if the control valve presents stiction and to find out the friction parameters. In Srinivasan, Rengaswamy, Narasimhan, and Miller (2005) the goal is to find the parameter $d$ of the Stenman model. In Choudhury, Shah, Thornhill, and Shook (2006), and Choudhury, Shah,

and Thornhill (2004) and Hagglund (2007) the idea is to estimate the parameter S, whereas in Choudhury, Jain and Shah (2008), Choudhury, Jain et al. (2006), Jain et al. (2006) and Schoene and Qin (2005) the concern is with J and S. These parameters are related to the Choudhury and Kano models. Papers on "Friction compensation for control valves" are concerned with developing friction compensators to deal with the control valves that are affected by this problem. The authors Kayihan and Doyle (2000) use the Classical model to develop their compensator. The compensator in Srinivasan and Rengaswamy (2005, 2006, 2008) employs the Stenman model.

None of the existing compensation techniques are based on rigorous control design theory. Compensation technique has been proposed around single parameter stiction models followed by linear dynamic plants. Extensive research is required to improve control loop performance of the loops suffering from valve stiction. Investigation of stiction models, proposed definitions of stiction phenomena, and practical loop data with sticky valves points in the direction of new models based on fuzzy adaptive rules or Hammerstein Wiener models. The good things about the fuzzy based model and Hammerstein Wiener based model is to bring them into identification and control frameworks.

## 3.7    Hammerstein-Wiener Model of Valve Stiction

Hammerstein model has been used to represent valve stiction with plant dynamics in several papers [22] [24] [29] [41]. All the published approaches did not use the mathematical formulation of Hammerstein Model, instead they used Hammerstein Model to

define the structure of the plant with valve stiction nonlinearity. The stiction phenomena can be defined as a combination of two nonlinearities surrounding the dynamics of the valve. For that, Hammerstein Wiener model is considered better to represent the stiction phenomena in a valve.

Hammerstein-Wiener model can be considered as the system where two static nonlinear elements $N_1$ and $N_2$ surround a linear block $L$, as shown in Fig. 3.48. The model
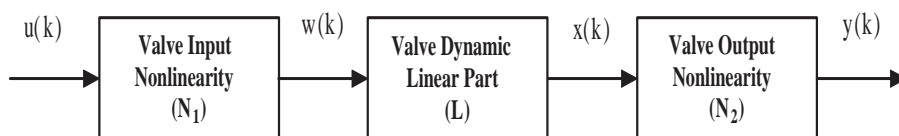


Figure 3.48: The Hammerstein-Wiener model of a valve.

is given as:

$$y(k) = \sum_{j=1}^{q} d_j f^j \left[ \frac{B(q^{-1})}{A(q^{-1})} \sum_{i=1}^{p} c_i g_i [u(k)] \right] \tag{3.8}$$

$$= \sum_{j=1}^{q} d_j f^j \left[ \frac{B(q^{-1})}{A(q^{-1})} N_1(u(k)) \right] \tag{3.9}$$

$$= \sum_{j=1}^{q} d_j f_j [x(k)] \tag{3.10}$$

$$= N_2(x(k)) \tag{3.11}$$

where $g_i(.)(i = 1....p)$ and $f_j(.)(j = 1...q)$ are the nonlinear functions for the nonlinear blocks $N_1$ and $N_2$, respectively. From study and simulation, we are able to say that the first nonlinearity $N_1$ can be defined as deadband and second nonlinearity $N_2$ can be used to model the small stickband and slip jumps. Functions that can make approximation of discontinuities like can be used to represent $N_2$. In the following

66

discussion, we compare the Hammerstein-Wiener with the Hammerstein Model to represent the stiction nonlinearity. It is found that the Hammerstein-Wiener Model is better to represent the stiction phenomena as compared to the Hammerstein Model as described in several research paper e.g., [29] and [36].

The stiction can be defined as a combination of two nonlinearities: sticking and slipping. These two nonlinearities can be interconnected with the linear dynamics of control valve. Following this idea, the Hammerstein-Wiener model is identified and compared with the Hammerstein Model. Figs. 3.49 3.50 3.51 and 3.52 show the comparison of Hammerstein model with the Hamerstein-Wiener model for sinusoidal input. The models are identified using simulated bench data (i.e., open loop data) for different cases of stiction from absence of stiction i.e., when $S = 0, J = 0$ to higher case of stiction e.g., $S = 12, J = 4$. It is found that the Hammerstein-Wiener model approximates the stiction model better than the Hammerstein model when stiction is considerably high.

Thus we figure out that the Hammerstein-Wiener model representation is more appropriate to represent the stiction model in control valve. But, the problem with Hammerstein-Wiener model is that it does not explicitly represent the stiction parameters that can be directly related to friction forces (like static, dynamic and Coulomb friction forces) as we have in data driven models. Hence, although an integrated framework for identification and compensation can be achieved using Hammerstein-Wiener, but this is not suitable for the case when we need to probe the loop problem
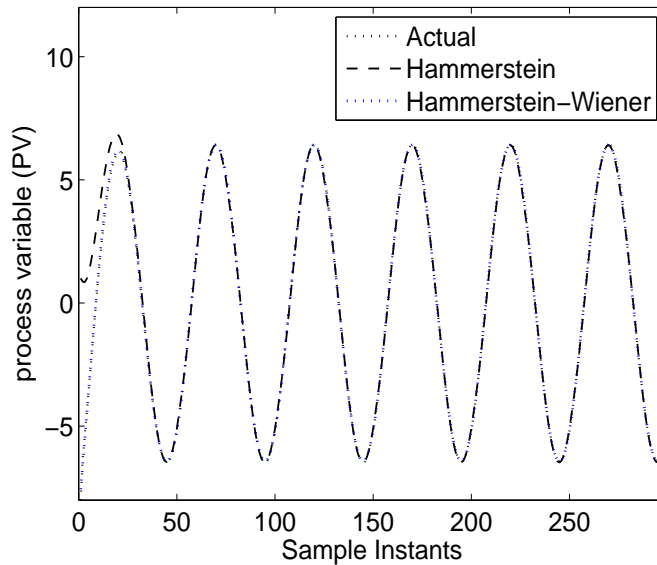
Figure 3.49: Comparison of Hammerstein-Wiener Modeling and Hammerstein Models $(S = 0, J = 0)$.

clearly. Hence, next chapters use data driven model for detection, quantification and compensation purposes.

## 3.8   Summary

Several friction models have been investigated in this chapter emphasizing the valve stiction. Simulation studies confirm the validity of data driven models to be used instead of complex physical models to represent the sticky valves. ISA bench tests are also applied on the data driven models to judge their performance. Although the open loop responses for the data driven models were satisfactory, the ISA recommended tests enable us to judge the better performing data driven models. The model by Choudhury et al. 2005 was unable to pass the Ramp & Pause test and the Response Time tests as shown in Fig. 3.30 and Fig. 3.45. Kano and Two
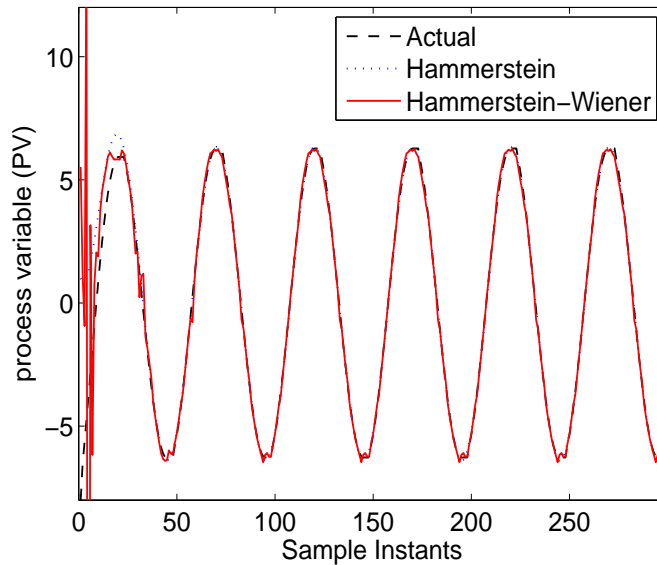
Figure 3.50: Comparison of Hammerstein-Wiener Modeling and Hammerstein Model ($S = 4, J = 2$).

layer Binary Tree models were able to pass all the tests. Stenman also shows good response to all tests but this model is an approximate model for stiction and bears less practical interpretation than Kano and Two Layer Binary Tree models. In the end, Hammerstein-Wiener model is proposed to model the stiction phenomena in control valves. The Hammerstein-Wiener model is better that the Hammerstein model representation of valve stiction specially when stiction is considerably high and complex. But Hammerstein-Wiener model is not good for stiction quantification and compensation since it does not rectify the stiction in terms of explicit parameters. Therefore, work done and presented in next chapters is based on data driven stiction models.
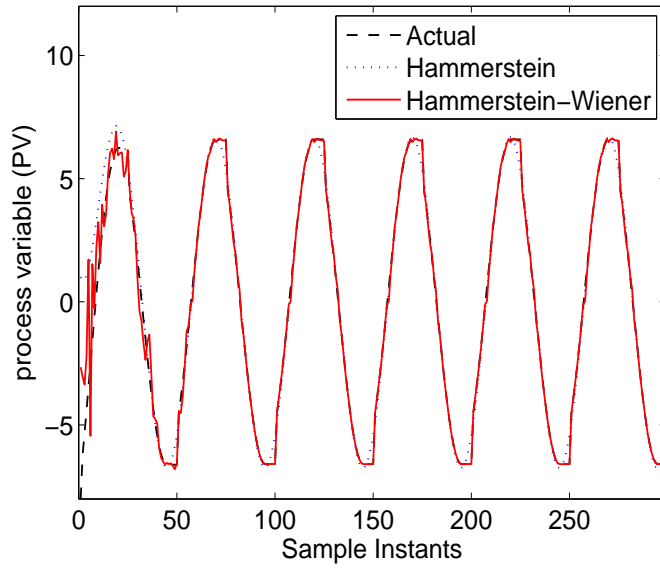
Figure 3.51: Comparison of Hammerstein-Wiener Modeling and Hammerstein Model $(S = 8, J = 10)$.
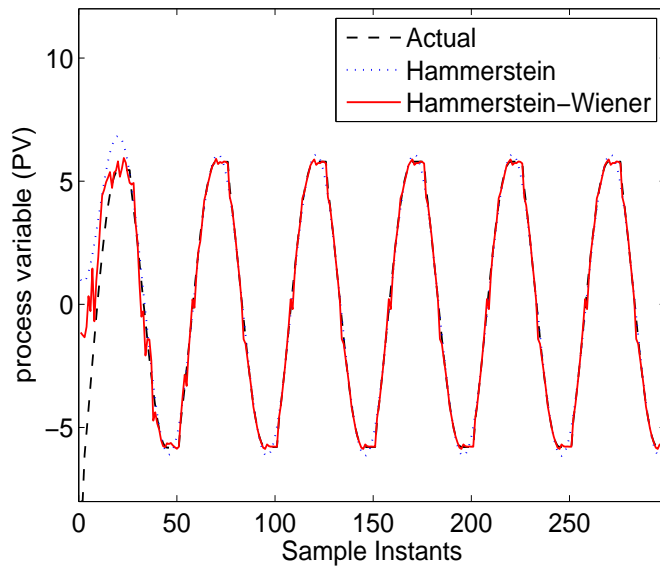


Figure 3.52: Comparison of Hammerstein-Wiener Modeling and Hammerstein Model $(S = 12, J = 4)$.

# CHAPTER 4

# STICTION DETECTION AND

# QUANTIFICATION

## 4.1 Introduction

Nonlinearity can come from process or from valve. Considering the process working at steady state, the process nonlinearity can be neglected (a reasonable assumption) and thus nonlinearity if present is considered due to valve nonlinearity (stiction, backlash, deadband or deadzone). Stiction is the most common problem.

## 4.2 Detection and Quantification Methods: Reviewed

Several techniques for automatic detection of stiction in control loops have been proposed in literature. A brief review of three popular methods will now be given. A

good stiction detection method should manage to identify stiction correctly and not wrongly characterize for instance changes in the set point or disturbances as stiction in the loops. It is desired that the quantifying method has some index that gives a measure of how much stiction is present. Further it is desired that the methods does not have any uncertainty regions. If this is the case they should be well defined and preferably as small as possible.

**Cross-correlation technique** Horch and Isaksson [1] proposed a method based on the cross-correlation between the control signal and the process output. The method by Horch is simple but it often gives wrong indications (see for example Kano et al., [25] and Yamashita [42]). Even with giving wrong indications, it is also regarded as being popular and easy to implement (Rossi and Scali [26]).

The following assumptions are needed to be valid for application of the cross-correlation method:

- The process does not have an integral action.

- The process is controlled by a PI-controller.

- The oscillating loop has been detected as being oscillating with a significant large amplitude.

For a data set with $N$ data points, the cross-correlation function between $u$ and $y$ for lag $\tau$ (where $\tau$ is an integer) is given by Horch [19]:

$$r_{uy}(\tau) = \frac{\Sigma_{k=k_0}^{k_1} u(k)y(k+\tau)}{\Sigma_{k=1}^{N} u(k)y(k)} \qquad (4.1)$$

where

$$k_0 = 1 \text{ for } \tau \geq 0$$

$$k_0 = \tau + 1 \text{ for } \tau < 0$$

$$k_1 = N - \tau \text{ for } \tau \geq 0$$

$$k_1 = N \text{ for } \tau < 0$$

For an external oscillating disturbance, the phase lag in the cross-correlation is $-\pi$, while it is $-\pi/2$ for a loop with valve stiction present.

Using the method, two parameters are calculated. According to the values of these parameters the loop will be regarded as either sticky or subject to sinusoidal perturbations. There is also an uncertainty region where no decision can be taken (Rossi and Scali [26]).

**Bi-coherence method** Choudhury et al. [28] have proposed a method based on Higher Order Statistics. It is observed that the first and second order statics (mean, variance, autocorrelation, power spectrum etc.) are only sufficient to describe linear systems. Non-linear behavior must be detected using higher order statics such as "bi-spectrum" and "bi-coherence".

The bi-spectrum is defined as

$$B(f_1, f_2) = E[X(f_1)X(f_2)X^*(f_1 + f_2)], \qquad (4.2)$$

where $B(f_1, f_2)$ is the bi-spectrum in the bi-frequency $(f_1, f_2)$, $X(f)$ is the discrete Fourier transform of time series $x(k)$ and $'*'$ denotes complex conjugate.

**Example of Bispectrum and Bicoherence:**

Following example is used to illustrate the estimation of bispectrum of a quadratically phase-coupled signal (QPC). Let a QPC signal be constructed as follows:

$$y(t) = sin(2\pi f_1 t + \phi_1) + sin(2\pi f_2 t + \phi_2) + 0.1 sin(2\pi f_3 t + \phi_3) + d(t) \qquad (4.3)$$

where the values of $f_1$, $f_2$ and $f_3$ are 0.12, 0.18 and 0.30, respectively; the values of $\phi_1$, $\phi_2$ and $\phi_3$ are $\pi/3$, $\pi/12$ and $5\pi/12$, respectively; $d(t)$ is a zero-mean white noise signal and $t$ corresponds to discrete sample instants from 1 to 4096 s. The signal $y(t)$, as shown in Fig. 4.1, is a quadratic phase-coupled signal because its frequencies have the relation $f_1 + f_2 = f_3$ and its phases have the relation $\phi_1 + \phi_2 = \phi_3$. Therefore, the phase coupling at bifrequency (0.12,0.18) appears in the bispectrum plot as shown in Fig. 4.2.

The bi-spectrum in Eq. 4.2 is dependent on the signal energy. This dependance can
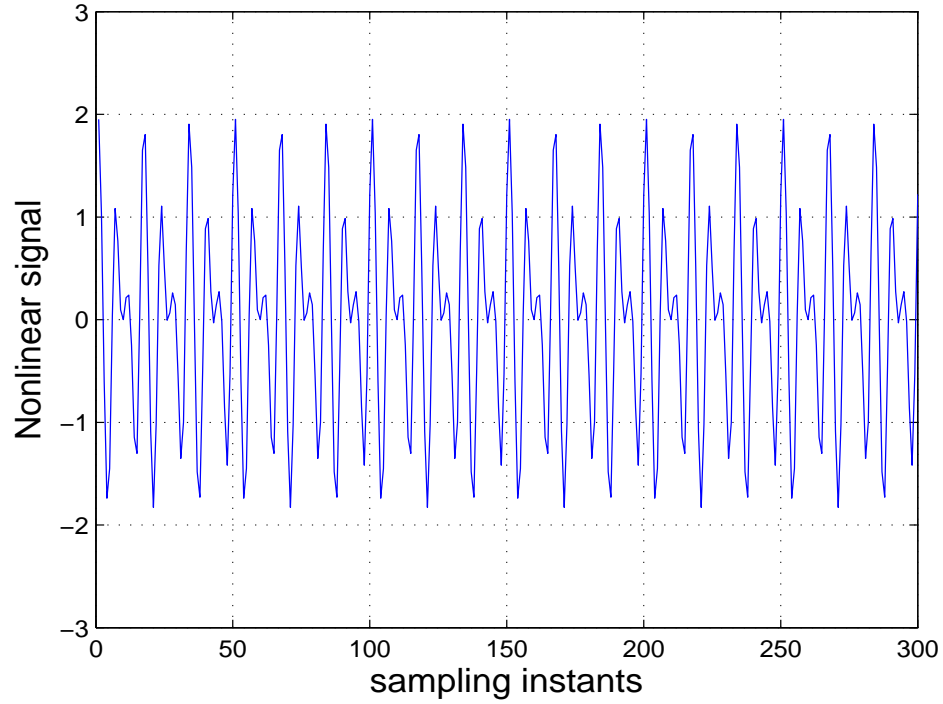
Figure 4.1: Example of a nonlinear signal.

be removed by doing the following normalization, defining the bi-coherence function:

$$bic^2(f_1, f_2) = \frac{|B(f_1, f_2)|^2}{E[|X(f_1)X(f_2)|^2]E[|X(f_1, f_2)|^2]} \tag{4.4}$$

where "*bic*" is known as the bi-coherence method. This is bounded between 0 and 1. The phase coupling at bifrequency (0.12,0.18) appears as a single peak in the bicoherence plot as shown in Fig. 4.3.

Using the bi-coherence function two indices can be calculated, a non-Gaussian index and a non-linear index. For a loop to be regarded as sticky both indices needs to be higher than a given threshold.
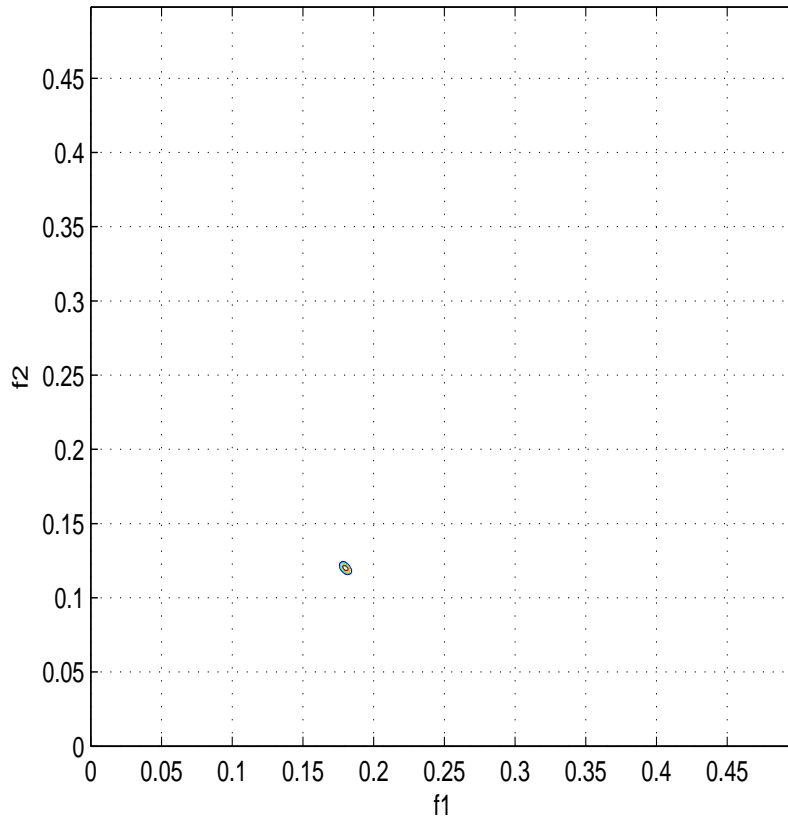
Figure 4.2: Bispectrum estimation of the phase-coupled signal.

**Relay technique curve fitting** This method, proposed by Rossi and Scali [26], is based on curve fitting of the recorded signals. Every significant half cycle of the recorded oscillation is fitted by using three different models:

- The output response of a first order plus delay model under relay control.

- A triangular wave.

- A sine wave.

Some error norm is evaluated between the plant data and the fitted model. The model with the smallest norm is said to describe the recorded signal. The relay model
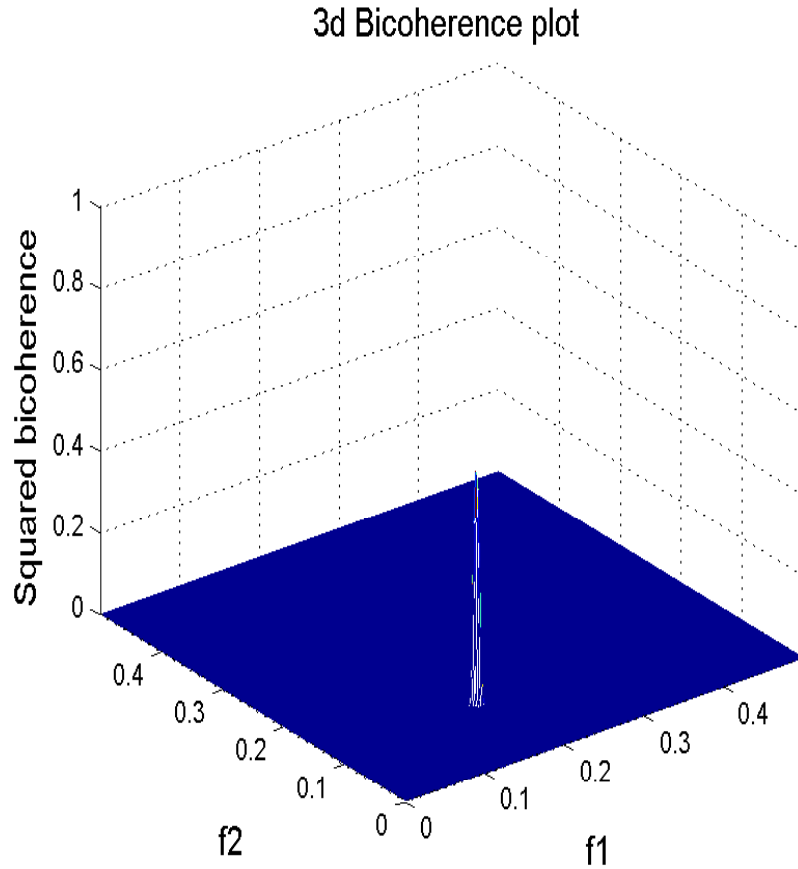
Figure 4.3: Squared bicoherence of the phase-coupled signal.

and the triangular wave are associated with stiction, whereas the sine wave with the presence of external perturbations.

Also this method has an index that characterizes the loop as sticky or subject to other phenomena. This index is rather intuitive and will be included here as an example of a stiction index. Let $E_S$ be the minimum square error obtained by the sinusoidal approximation and $E_{RT}$ the one obtained by the better fit of either the

relay model or the triangular wave. The index $S_I$ is then

$$S_I = \frac{E_S - E_{RT}}{E_S + E_{RT}}, \tag{4.5}$$

$S_I$ is normalized, so $S_I \in [-1, 1]$. Negative values indicate better fit of sinusoids, positive values indicate better fit of the relay model or triangular waves. The uncertainty zone is defined as $|S_I| < 0.21$ ([26]).

Choudhury [11] proposed a method of ellipse fitting to quantify stiction, but it quantifies stiction as "apparent stiction". Rossi and Scali [26] also proposed a method based on the magnitude of the controller output signal when the valve is stuck and normalizes with the span of the output. Stiction quantification is an active research area and published literature shows few attempts of proposed stiction quantification methods.

## 4.3 Example: Control Loop Suffering From Valve Stiction

From the last chapter, it is observed that data driven models are able to represent the stiction phenomena in a control loop. This section defines the control loop having a sticky valve. Fig. shows the simulink block diagram used for generating stiction data (process variable (pv), valve output (mv), and controller output (op)). This data is used to test the stiction detection and quantification methods.
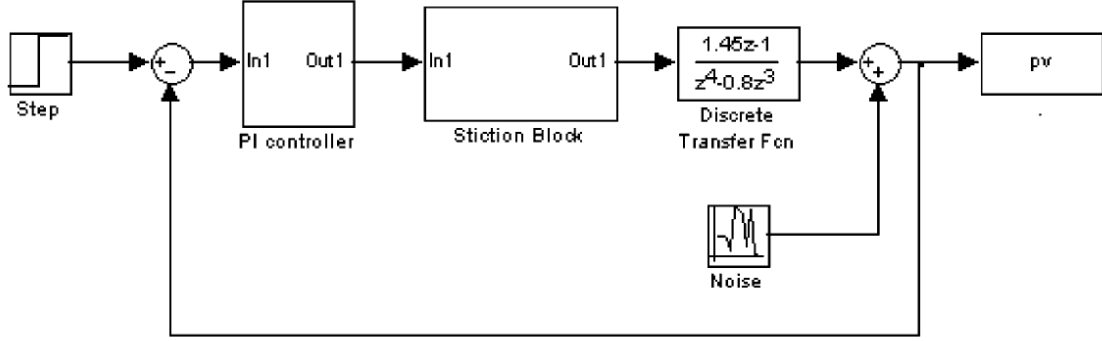
Figure 4.4: Simulink block diagram used for generating stiction data.

The process model given below is taken from [29]:

$$G(z) = \frac{1.45z - 1}{z^4 - 0.8z^3} \qquad (4.6)$$

The PI controller is implemented with reset time, $\tau_I = 1$ and the gain, $K_c = 0.15$ [29]. The sampling time $T_s$ is 1. The data is generated for different cases of S and J. For the simulations, Choudhury and Kano models take the two parameters S and J. Stenman model takes only one parameter $d$, while Two Layer Binary Tree model takes two parameters static friction $(f_s)$ and dynamic friction $(f_d)$. Static friction $(f_s)$ and dynamic friction $(f_d)$ are related to S and J in Chouchury and Kano models by the relations: $S = f_s + f_d$ and $S = f_s - f_d$ [39].

Here we consider data for different cases of S and J. Data is generated for different cases as shown in Table 4.1 and 4.2. Data is also generated with noise disturbance and no stiction to verify the robustness of detection method. We considered noise variance of 0, 0.05, 0.1, 0.2, 0.4 and 0.5 with no stiction.

Note that the stiction detection and diagnosis methods are applied on the steady

state data. This is general practice to consider healthy data portions for the analysis of problems in control loops.

Table 4.1: Data generated for different cases of S and J without noise.

| S | J |
|---|---|
| 1 | 0 |
| 1 | 1 |
| 4 | 2 |
| 6 | 4 |
| 8 | 8 |
| 8 | 10 |
| 10 | 2 |
| 10 | 5 |
| 10 | 8 |
| 12 | 4 |

Table 4.2: Different cases of noise are generated for fixed S and (S=6, J=4).

| SNR | Noise Variance |
|---|---|
| 100 | 0.05 |
| 50 | 0.1 |
| 25 | 0.2 |
| 12.5 | 0.4 |
| 10 | 0.5 |

## 4.4 Stiction detection method

Several techniques for automatic detection of stiction in control loops have been presented in literature. In the beginning of this chapter, we briefly discussed few methods for detection and diagnosis of stiction. This section discusses the promising stiction detection method by Yamashita [42] in detail. This method is based on qualitative description (Yamashita [42]). The method is implemented and investigation results are shown on the example control loop discussed above.

### 4.4.1 Yamashita Method [42]

Yamashita method [42] formulates the qualitative description of input-output characteristics of a valve into a stiction detection algorithm. Main idea is to use sequence of symbolic values to represent the qualitative trends of a time series (signal). The three basic symbols used are: Increasing (I), decreasing (D), and steady (S) as shown in Figure 4.5. These three symbols are sometimes called plus (+), zero (0) and minus (-). They correspond to the signs of their respective derivatives.
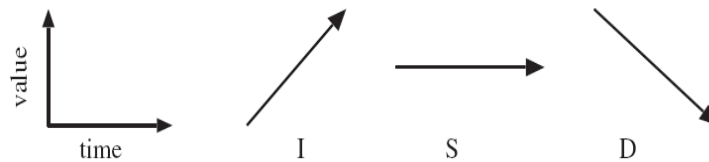
Figure 4.5: Symbolic representations of a time series (Increasing (I), Steady (S), and Decreasing (D)).

For analysis of time series it is often useful to consider two variables simultaneously in x-y plot, such as x and y. The time series is not shown explicitly in that plane, but it corresponds to the movement of the plots. To represent qualitative movement in an x-y plane, a combination of the three qualitative primitives for each variable is introduced here. As shown in Table 4.3, nine symbols can be defined to represent qualitative movement. The qualitative description of above movements in an x-y plot

Table 4.3: Symbolic representation of behavior of a time series in x-y plots

| x/y | D | S | I |
|-----|-----|-----|-----|
| I | ID | IS | II |
| S | SD | SS | SI |
| D | DD | DS | DI |

is shown in Fig. 4.6, where each arrow starts from the center and shows the direction

of movement. The symbol SS does not move in this plane and represents the center
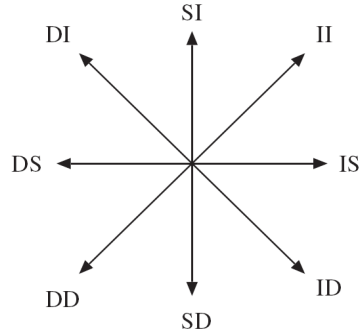


Figure 4.6: Qualitative movements in x-y plots.

point of the figure. Movements in the x-y plane can be represented qualitatively using these nine symbols. A sequence of these symbols represents a movement pattern in the plane. For example, (IS SD DS SI) = [increase-steady steady-decrease decrease-steady steady-increase] represents a clockwise rectangular movement. In the sequence of movements, similar movements are combined to form episodes. For example, (IS IS SI SI SI) is equivalent to (IS2 SI3). Before analysis, all SS patterns are deleted from the sequence of the symbols, because SS patterns have no meaning in the x-y plane. For example (IS3 SS2 IS2 II3) is converted to (IS5 II3).

## Algorithm:

**Stuck index:** This simple idea is to count the periods of sticky movement by finding IS and DS patterns in the input-output plots of the valve. Based on this idea, an index $\rho_1$ to detect the loop with stiction can be defined in an appropriate time window:

$$\rho_1 = (\tau_{IS} + \tau_{DS})/(\tau_{total} - \tau_{SS}) \tag{4.7}$$

where $\tau_{total}$ is the width of the time window, and $\tau_{IS}$ and $\tau_{DS}$ are time periods for patterns IS and DS, respectively. This index will become large if the valve has severe stiction ($0 \leq \rho_1 \leq 1$). As an extreme case, the index $\rho_1$ becomes unity if the valve does not move at all for changes of controller output. If the signals are random, the value of $\rho_1$ is likely to become 0.25 because $\rho_1$ represents two out of eight patterns. Therefore, one can infer that the loop is likely to have valve stiction if the index value is greater then 0.25. These two patterns can occur by various causes other then stiction: disturbances, time delay, and noise. Improvement of the accuracy of detection is attainable by reducing these irrelevant causes in the movement sequence.

**Matched stiction index:**: A fragment of the movement sequence can be represented by a sequence of two successive patterns. For example, if pattern II (increase-increase) follows the pattern IS (increase-steady), the movement is represented as (IS, II). Using this representation, typical movement for the valve stiction can be represented as four segments (IS II), (DS DD), (IS SI), and (DS SD) as shown in Fig. 4.7. All sticky
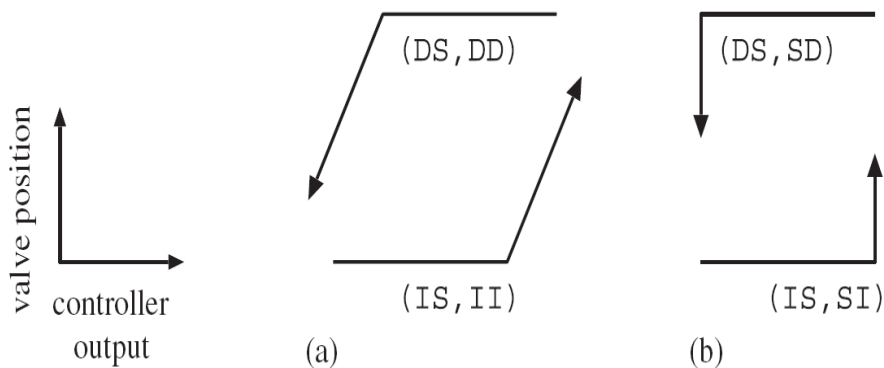


Figure 4.7: Qualitative shapes found in typical sticky valves.

motions of valve stiction, IS and DS, should be a part of these patterns. The degree

of stiction can be evaluated by counting the time period of IS and DS in these four fragments of patterns. Subsequently, an improved index $\rho_2$ can be defined as Eq. 4.8 below:

$$\rho_2 = (\tau_{ISII} + \tau_{ISSI} + \tau_{DSDD} + \tau_{DSSD})/(\tau_{total} - \tau_{SS}) \qquad (4.8)$$

where $\tau_{ISII}$ is the total number of IS samples in all of the found (IS, II) movements in the observation window, $\tau_{DSDD}$ is the number of DS samples in the found (DS, DD) movements, and so on. This index includes only the sticky movements matched with the four typical fragment of a sequence of movement patterns. If the entire pattern is a typical stiction pattern, the value of $\rho_2$ should be identical to $\rho_1$. One may consider that a loop has stiction if $\rho_2$ is greater than 0.25, which is the same criterion for $\rho_1$. Table 4.3 shows eight symbols for qualitative patterns. In general, to represent a sequence of two successive symbols, seven symbols can be used followed by the symbol, except for the symbol used in the first segment. Typical patterns for stiction are shown in Fig. 4.7(a) and (b); they each include two patterns. Therefore, patterns that have nothing to do with stiction can be represented by one of five possible symbols following the symbol IS or DS. By removing these five patterns each from the index $\rho_1$, a new index $\rho_3$, can be defined as

$$\rho_3 = \rho_1 - (\tau_{ISDD} + \tau_{ISDI} + \tau_{ISSD} + \tau_{ISID} + \tau_{ISDS} + \tau_{DSDI} + \tau_{DSSI} + \tau_{DSID} + \tau_{DSII} + \tau_{DSIS})/(\tau_{total} - \tau_{SS})$$

$$(4.9)$$

The second term of Eq. 4.9 and the right-hand side of Eq. 4.8 contains all the sticky movement used in Eq. 4.7. Therefore, except for the special case described

above, the value of $\rho_3$ is identical to the value of $\rho_2$. The detection procedure can be summarized as follows:

- Obtain a time series of the controller output and valve position (or corresponding flow rate).

- Calculate the time difference for each measurement variable.

- Normalize the difference values using the mean and standard deviation.

- Quantize each variable in three symbols.

- Describe qualitative movements in x-y plots by combining symbolic values of each variable.

- Skip SS patterns from the symbol sequence.

- Evaluate the index by $\rho_1$ counting IS and DS periods in the patterns found.

- specific patterns and count stuck periods. Then evaluate the index $\rho_3$.

First, both the time differences of valve input and the flowrate in the given data are normalized to have zero mean and unit standard deviation. Second, each variable is converted to a sequence of three qualitative primitive. In this conversion, the standard deviation of differential values for each variable is used as the quantization threshold. Then, primitives of valve-input and the flowrate are combined to produce qualitative symbols to represent qualitative movements. By summarizing these symbols, they are converted to a sequence of qualitative trends.

This is a diagnosis method for valve stiction based on typical patterns observed from

the valve-input and output in the process control loop. For implementation of the algorithm, the description of qualitative movement in the phase plant is formulated by extending the qualitative shape analysis formalism. The method is claimed to diagnose stiction in the loops where the autocorrelation between controller output and loop output fails. The method is able to distinguish stiction from poor controller tuning and external disturbances.

**Application of Yamashita Method:**

Stiction detection method is applied on the data from Example discussed in section 4.3 for different cases. Table 4.4 shows the results of the stiction detection method [42] for 2500 data points. The method is found to have a lower limit on the data samples to give correct answer. For 500 data samples, the method was found incorrect for 1 case (no stiction and no noise) out of 21 different cases. So, the at least 2000 samples are required to get correct results for the Yamashita method [42].

## 4.5 Stiction quantification methods

### 4.5.1 Ellipse Fitting Method

Ellipse fitting method [27] uses the process variable (pv), controller output (op) and the set point (sp) of a control loop to diagnose the value of stiction. The method gives an apparent value (approximate) for the stiction present in control valve. It does not

Table 4.4: Stiction detection indices for Scenario A Data

| S.No. | SNR | S | J | $\rho_1$ | $\rho_3$ | Is stiction present? | Results |
|---|---|---|---|---|---|---|---|
| 1 | 100 | 6 | 4 | 0.5607 | 0.5607 | *Yes* | *Correct* |
| 2 | 50 | 6 | 4 | 0.5446 | 0.5446 | *Yes* | *Correct* |
| 3 | 25 | 6 | 4 | 0.5258 | 0.5221 | *Yes* | *Correct* |
| 4 | 12.5 | 6 | 4 | 0.5064 | 0.4968 | *Yes* | *Correct* |
| 5 | 10 | 6 | 4 | 0.5 | 0.4887 | *Yes* | *Correct* |
| 6 | 100 | 0 | 0 | 0.3755 | 0.1536 | *No* | *Correct* |
| 7 | 50 | 0 | 0 | 0.3755 | 0.1536 | *No* | *Correct* |
| 8 | 25 | 0 | 0 | 0.3755 | 0.1536 | *No* | *Correct* |
| 9 | 12.5 | 0 | 0 | 0.3755 | 0.1536 | *No* | *Correct* |
| 10 | 10 | 0 | 0 | 0.3755 | 0.1536 | *No* | *Correct* |
| 11 | *NoNoise* | 0 | 0 | 0.2147 | 0.2147 | *No* | *Correct* |
| 12 | *NoNoise* | 10 | 2 | 0.899 | 0.6983 | *Yes* | *Correct* |
| 13 | *NoNoise* | 10 | 5 | 0.5292 | 0.5292 | *Yes* | *Correct* |
| 14 | *NoNoise* | 10 | 8 | 0.7352 | 0.7352 | *Yes* | *Correct* |
| 15 | *NoNoise* | 12 | 4 | 0.4833 | 0.4833 | *Yes* | *Correct* |
| 16 | *NoNoise* | 1 | 0 | 0.4415 | 0.4415 | *Yes* | *Correct* |
| 17 | *NoNoise* | 1 | 1 | 0.896 | 0.7146 | *Yes* | *Correct* |
| 18 | *NoNoise* | 4 | 2 | 0.5288 | 0.5288 | *Yes* | *Correct* |
| 19 | *NoNoise* | 6 | 4 | 0.6034 | 0.6034 | *Yes* | *Correct* |
| 20 | *NoNoise* | 8 | 10 | 0.899 | 0.6983 | *Yes* | *Correct* |
| 21 | *NoNoise* | 8 | 8 | 0.8967 | 0.7153 | *Yes* | *Correct* |

require the valve position (mv) which is not available in most cases [27]. The method given in Choudhury et al., [27] can be summarized as follows:

- **Step 1: Detection of Nonlinearity**. Calculate NGI and NLI for the control error signal (sp-pv). If both of the indices are greater than the threshold values (this is 0 in Choudhury [11]), the loop is detected as nonlinear. Go to the following step; otherwise STOP and send message "Nonlinearity is not a problem". The problem may be tightly tuned controller or external disturbances.

- **Step 2: Filtering pv and op data**. After nonlinearity is detected, obtain the frequencies f1 and f2 corresponding to the maximum bicoherence peak in step 1. All frequencies are normalized such that the sampling frequency is 1.

Take $f_1 = min(f_1, f_2)$ and $f_2 = max(f_1, f_2)$ The boundaries of Wiener filter are $w_L = max(0.004, f_1' - 0.05)$, $w_H = min(0.5, f_2' + 0.05)$. Here, 0.05 is subtracted or added from the frequencies in order to ensure that the exact location of significant peak does not fall on the filter boundaries. The min possible value for the lower boundary is 0.004 or 250 samples/cycle. Any oscillation longer than this is extended and a method to deal with longer oscillation is described in implementation section. Filter pv and op data using the Wiener filter to obtain pvf and opf.

- **Step 3: Obtain the segment of data with most regular oscillations**.

  - (a) Choose a segment length L, (e.g., L = 1000)

  - (b) Divide the $op_f$ data into segments of length L. Here $op_f$ is chosen because it is less noisy than pv signal.

  - (c) Calculate $r$ and $T_p$ for each segment of $op_f$ data

$$r = \frac{1}{3}\frac{T_p}{\sigma_{T_p}} \tag{4.10}$$

  where, $T_p$ is the mean value of the period of oscillation, and $\sigma_{T_p}$ is the standard deviation of the period of oscillation.

  - (d) Obtain $r_{max} = max(r)$

  - (e) Obtain $T_{ps}$, which is equal to $T_p$ of the segment of op with $r_{max}$

  - (f) If $L > 4 * T_{ps}$, then choose $L = 4 * T_{ps}$ and go to step (b)

– (g) Now, $op_{fs}$ is the segment of the $op_f$ data that corresponds to the $r_{max}$ and $pv_{fs}$ is the part of the $pv_f$ data that corresponds to $op_{fs}$.

- **Step 4: Fitting an ellipse**. Fit a conic to the mapping of $pv_{fs}$ and $op_{fs}$. In case of stiction present in the control valve, the $pv_f$ vs. $op_f$ plot can be fitted by an ellipse [27];

- **Step 5: Quantifying stiction**. Quantify stiction using stiction formula (Eq. 4.11).

$$ApparentStiction = \frac{2mn}{\sqrt{(m^2 sin^2\alpha + n^2 cos^2\alpha)}} \tag{4.11}$$

where, $m$ and $n$ are the length of the major and minor axes of the fitted ellipse, respectively, and $\alpha$ is the angle of rotation of the ellipse.
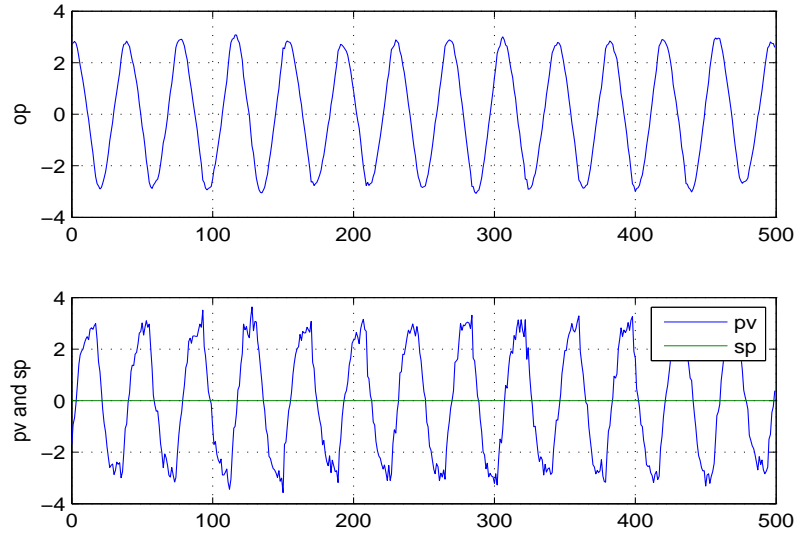


Figure 4.8: Time trends of process variables for $S = 6$, $J = 4$ and $SNR = 100$.

## 4.5.2 Clustering Technique

Clustering is a method for dividing scattered groups of data into several groups. Since the pv-op plot for a control loop with a sticky valve exhibits elliptic patterns, the data corresponding to a **narrow strip along the mean of pv and parallel to the op axis** can be collected and used for quantifying stiction any clustering technique (like c-means clustering [11]). The amount of stiction can be estimated from the absolute value of the difference between the x coordinates of the centers of the two clusters. If the final centers of the clusters are $(op_1, pv_1)$ and $(op_2, pv_2)$, then the amount of stiction is determined using the following expression:

$$ApparentStiction = |op_1 - op_2| \qquad (4.12)$$

In c-means clustering, data are partitioned into C number of initial clusters. Then



Figure 4.9: Phase plot of pv and op for $S = 6$, $J = 4$ and $SNR = 100$.
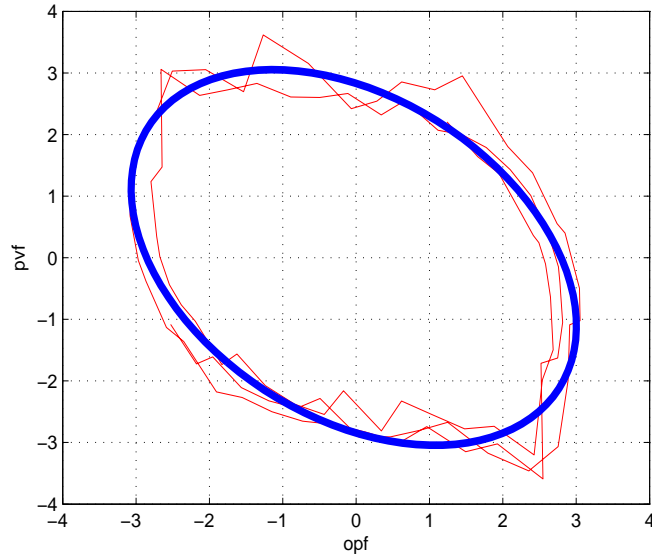
Figure 4.10: Ellipse Fitting for $S = 6$, $J = 4$ and $SNR = 100$.

proceeding through all data points, each point is assigned to the nearest cluster (in terms of Euclidean distance). The centroids for the cluster receiving the new item and for the cluster losing the item are recalculated. This procedure is repeated until no more reassignments take place. This method requires the initialization of the centers of the clusters.

In our case, there are only two clusters and the centers can be specified as [min(opf), mean(pvf)] and [max(opf), mean(pvf)] calculated from the data obtained along the strip in the pvf-opf plot. Eq 4.12 is used to calculate the apparent stiction as a percent of input signal span.

## Limitation of Ellipse fitting method

Since, in ellipse fitting method, the controller output (op) and process variable (pv) are used, there is a shortcoming of this method. The slip jump pattern, which is

characterized by J, is destroyed by the dynamics between valve output (mv) and process variable (pv). Therefore, only the S parameter can be quantified in this method. Following, results are also shown with the effect of different J and noise levels on the quantified value of S.
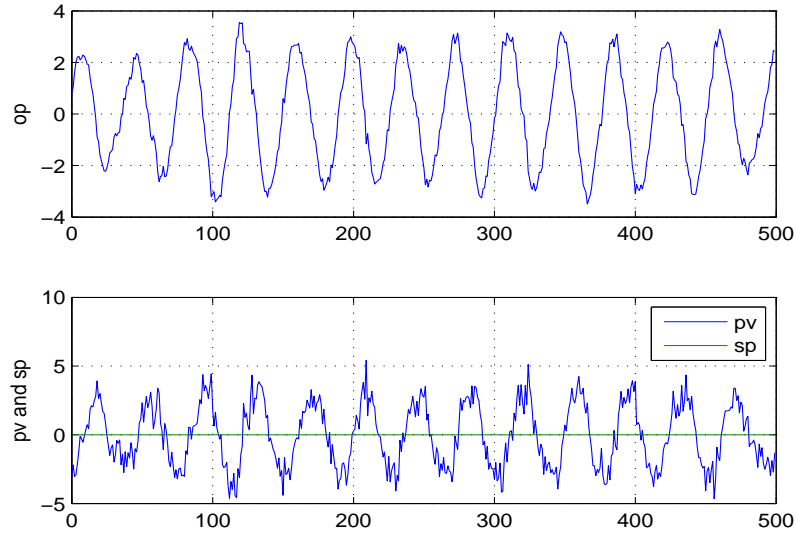


Figure 4.11: Time trends of process variables for $S = 6$, $J = 4$ and $SNR = 10$.

## Effect of SNR on Ellipse Fitting Method

Ellipse fitting method is able to quantify only the S parameter of the two parameter model which consists of parameters S and J. The ellipse fitting method is investigated for different cases of Signal to Noise Ratio (SNR) keeping $S = 6$ and $J = 4$. The results are shown in Table 4.5.

Table 4.5: Estimating Stiction for Noisy Data when $S = 6$, $J = 4$

| S.No. | SNR | S (Ellipse Fitting) | S (Clustering) | Average |
|-------|-----|--------------------|----------------|---------|
| 1 | 100 | 5.65 | 6.13 | 5.89 |
| 2 | 50 | 5.81 | 6.45 | 6.12 |
| 3 | 25 | 5.36 | 6.08 | 5.72 |
| 4 | 12.5 | 3.93 | 3.93 | 4.86 |
| 5 | 10 | 5.60 | 6.24 | 5.92 |

## Simulations

Fig. 4.8 shows the graphs for the time trends of the process variable (pv), controller output (op) and set point (sp) for the example 4.4. Results for two different cases of Signal to Noise ratio (SNR) are shown here. In first case, the ellipse fitting is shown when $S = 6$, $J = 4$ and $SNR = 100$, while in the other case $S = 6$, $J = 4$ and $SNR = 10$. The phase plot of process variable (pv) and controller output (op) for the case of $SNR = 100$ is shown in Fig. 4.9. Fitted ellipse for $SNR = 100$ is shown in Fig. 4.10. While Fig. 4.11, Fig. 4.12 and Fig. 4.13 illustrate the results for the case
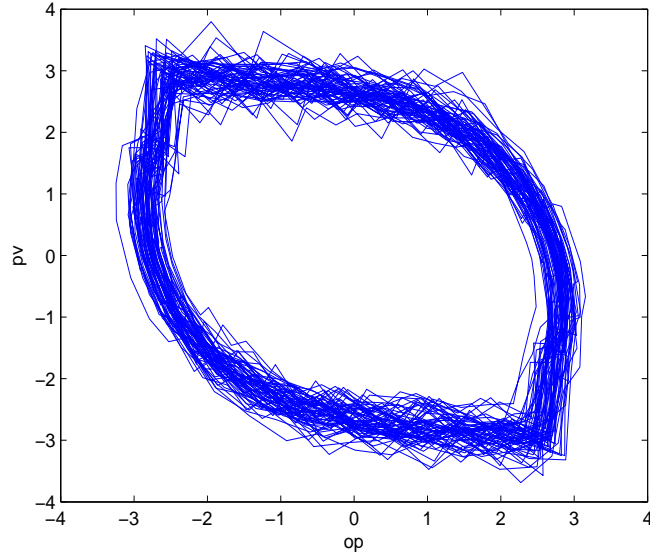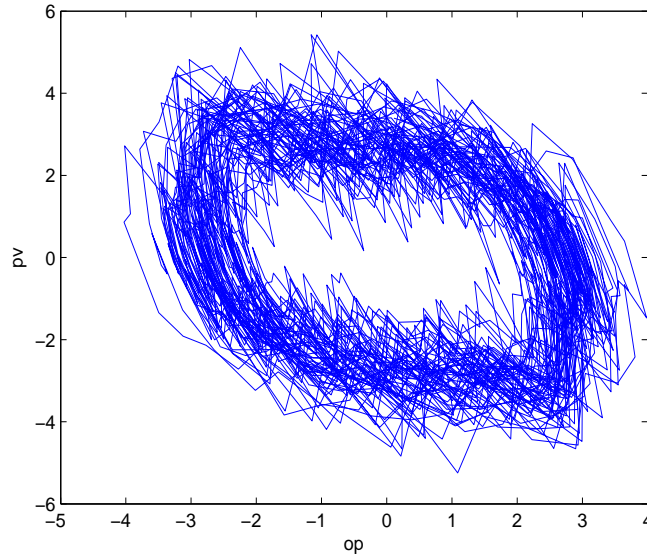


Figure 4.12: Phase plot of pv and op for $S = 6$, $J = 4$ and $SNR = 10$.
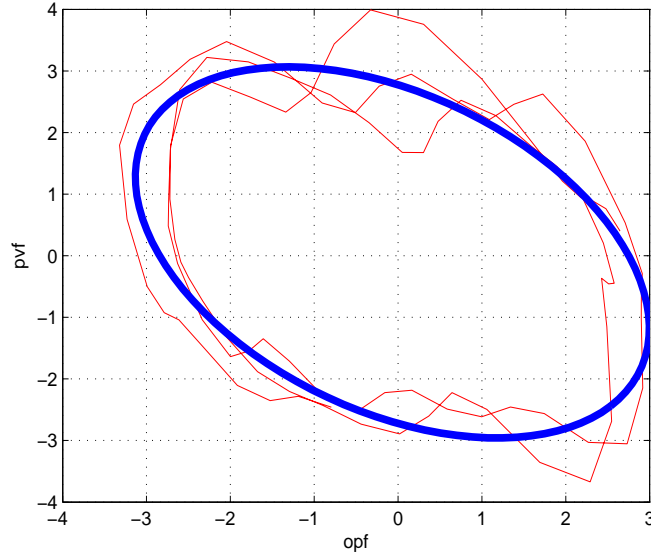
Figure 4.13: Ellipse Fitting for $S = 6$, $J = 4$, and $SNR = 10$.

Table 4.6: Estimating Stiction for different cases of S and J.

| S.No. | Actual S | Actual J | S (Ellipse Fitting) | S (Clustering) | Average |
|-------|----------|----------|---------------------|----------------|---------|
| 1 | 10 | 5 | 9.75 | 10.02 | 9.88 |
| 2 | 10 | 8 | 8.98 | 9.35 | 9.16 |
| 3 | 12 | 4 | 12.51 | 12.81 | 12.66 |
| 4 | 1 | 1 | 0.89 | 0.95 | 0.92 |
| 5 | 8 | 8 | 7.07 | 7.62 | 7.35 |

of $SNR = 10$.

## 4.6    Summary

A brief discussion on existing detection and quantification method is presented. For

simulations, two methods are selected and implemented on the data of a control

loop simulated example for several cases of stiction and noise. The method was able

to distinguish the oscillations caused by external disturbance and due to the valve

stiction. To quantify the stiction, ellipse fitting method was also implemented. It

94

is found that the ellipse fitting method along with a simple clustering technique can refine the quantified stiction value.

<center>CHAPTER 5</center>

# STICTION COMPENSATION

## 5.1 Introduction

This chapter presents the proposed idea of stiction compensation by introducing inverse of nonlinearity in the control loop. The adaptive inverse compensation takes two different routes here. The first approach uses ellipse fitting method to quantify the stiction value and then an approximated inverse is used in the control loop after the controller to compensate the stiction. In second approach, the inverse model of the nonlinearity is made using the adaptive inverse modeling approach presented by Widrow et al., in [9]. These approaches are compared with the knocker based approach highlighting the advantages and disadvantages of these methods.

## 5.2 Existing Compensation Techniques

There is no well accepted method in industry to compensate for valve stiction unless the valves are completely removed or maintenance is carried out as scheduled proce-
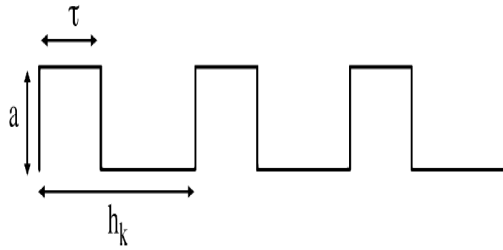
Figure 5.1: Knocker pulse.

dure. Gerry from ExperTune Inc. and Ruel from TOP Control in [21] proposed steps
to measure and re-tune the controller to combat valve stiction, which require highly
skilled operator and is carried out in manual mode. The knocker based approach by
Hagglund [17] introduced in 2002 is considered best method to compensate for stiction
[37].

In the following sections, adaptive inverse based approaches to compensate stiction
are presented. These innovative approaches are compared with the knocker based
approach.

### 5.2.1 Industry's Way To Combat Valve Stiction On-Line [21]

**Manual method to measure stiction on-line:**

To measure stiction-line, following are the steps:

- Put the controller in manual with the output near the normal operating range.

- Start recording data using a strip chart recorder or computer system

- Change the controller output by 5 to 10% to overcome the hysteresis on the
  loop. If the process variable does not move from this change, repeat it until the

97

process variable moves.

- Wait for the process variable to settle

- Make a small change in the controller output - about 0.2% in the same direction as the last step. Wait for the same amount of time as the previous step to see if the process variable moves

- Repeat the last step until the process variable moves

The stiction in the loop is the total amount of controller output change required to make the process variable move.

**Combating Stiction**

The best solution for increasing performance in a control loop containing stiction is to repair the valve or positioner to eliminate the stiction. In many cases, however, this is not possible because of the economics of keeping production running. In these cases, methods for combating the stiction to reduce the effects are beneficial. The negative effects of stiction cannot be totally eliminated without repairing the valve. However, there are techniques for reducing the effects of stiction on control loop performance.

**Conditions when the valve cannot be repaired**

Sometimes the valve cannot be feasibly repaired. This condition may occur for these reasons:

- economically not feasible to stop production,

- valve/actuator type is the problem and it is necessary to use this type of valve/actuator for fail safe considerations

- replacing the valve actuator could be too expensive

- the process imposes this type of valve where a lot of friction is present, e.g., Gate valve

**Techniques for combating stiction on-line**

These tuning techniques can be used to keep the plant running:

1. Tune the positioner using a large proportional gain, and no Integral action. If Derivative action is available, use some to make the valve continuously move. With integral action in the positioner, the positioner may wind up, causing the valve to seemingly have a mind of its own. After some period of time, the stem will jump, after the positioner has wound up enough. By removing integral action from the positioner, this windup problem is eliminated.

2. If a smart positioner is used, adjust the parameters. Some positioners do not use PID but special algorithms to send a burst of pressure each time a new position is requested. The positioner action is to stop the valve at the requested position.

3. Use a PID controller (for the control loop) where the Integral action has a variable strength. If absolute error is smaller than some value then take out the integral action otherwise use it: For $error < some\,threshold\,value$ $K_i = 0$ (or $T_i = infinite$); if not $K_i = normal\,value$. Using this method, when the valve is within the stiction band, the integral action is missing from the controller, the controller output will not integrate, having the end effect of removing the stiction cycle from the loop.

4. Use a PID with gap; if the absolute error is smaller than x, the controller output
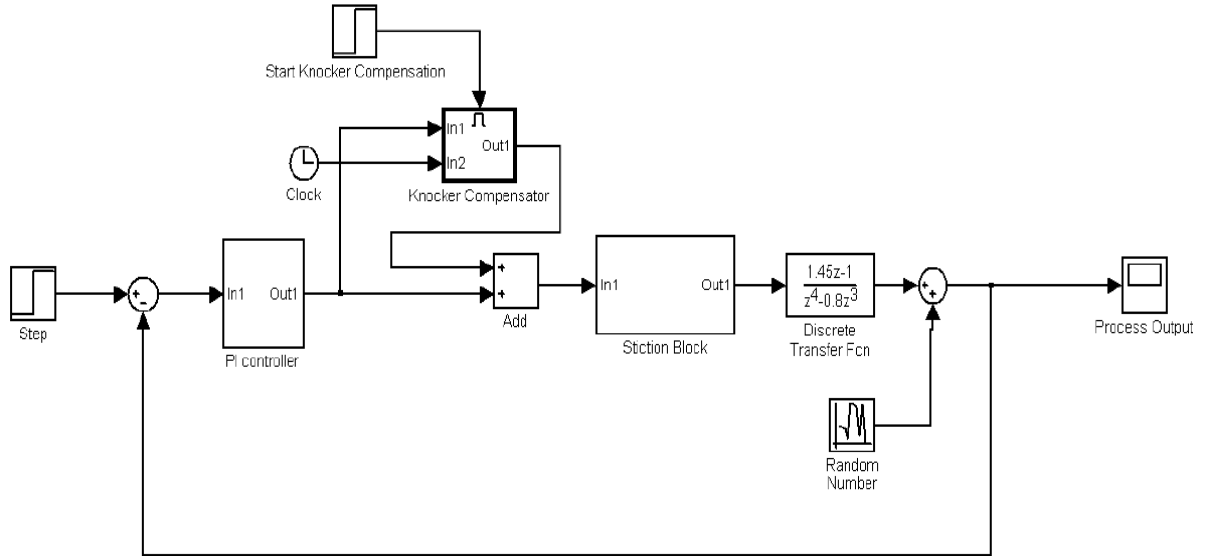   is frozen; if not, the amount of error from the gap is used as the controller input.



Figure 5.2: Block diagram of Knocker based stiction compensation.
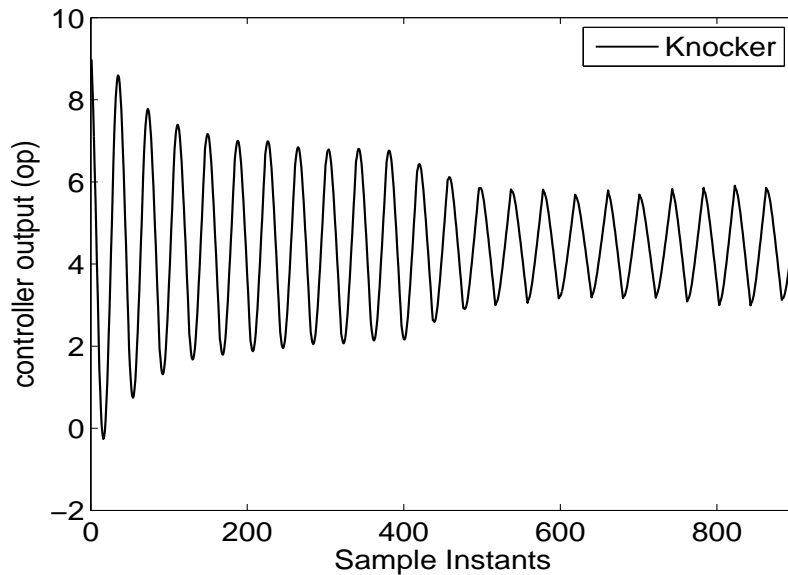


Figure 5.3: Knocker compensation ($S = 5$, $J = 3$): controller output (op).

## 5.2.2  Knocker method (Hagglund 2002)

In the technique proposed by Hagglund [17], short pulses, termed as 'knocker', see Fig. 5.1, are added to the control signal in the direction of the rate of change of the control signal. However, there is a need to tune three parameters that characterize the short pulses: amplitude (a), pulse width ($\tau$) and time between each pulse ($h_k$). Knocker pulses are used to compensate for Stiction. Following are the results with nominal values of the parameters. The parameters should be tuned with optimization algorithm integrated with stiction quantification [17].
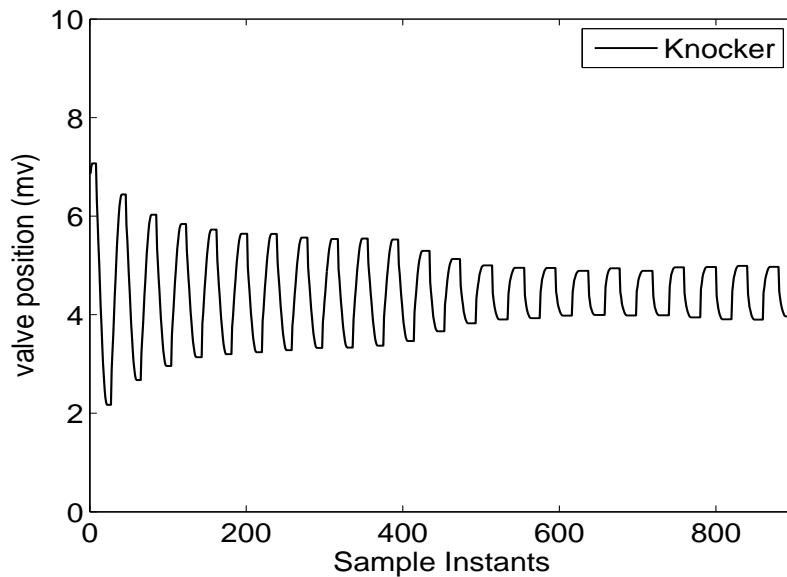


Figure 5.4: Knocker compensation ($S = 5$, $J = 3$): valve position (mv).

Figure 5.2 shows the knocker based stiction compensation approach. For current simulation, we considered pulse amplitude of 0.25, time constant of 2 seconds and period of 5 second. The stiction parameter for this case are $S = 5$ and $J = 3$. The simulation results are given in Figures 5.3, 5.4 and 5.5.
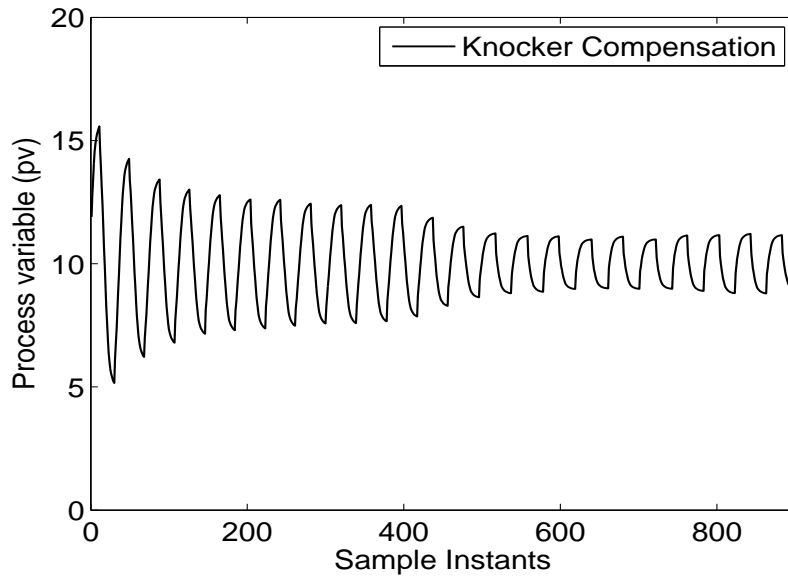
Figure 5.5: Knocker compensation ($S = 5$, $J = 3$): process variable (pv).

## 5.2.3 Drawbacks with Knocker compensation

This technique requires three parameters to be set by the operator. Hagglund [17] in his work mentions that there is no reason to have an adjustable pulse amplitude $a$ but that $a$ can be fixed once and for all. We found that choosing a correct $a$ is extremely important for the knocker technique to work. Following settings are recommended in [17] for Knocker parameters:

- the pulse amplitude ($a$) may be chosen in the range of 1-5% (default is 2%)

- pulse width ($\tau$) can be fixed to one or a few sampling times (default $\tau = h$

- the time between each pulse ($h_k$) is chosen between 2 and 5 sampling times (default $h_k = 2h$)

102

## 5.3 Proposed Approximated Inverse Model Based Compensation

An approximated inverse of Stiction (i.e., the backlash inverse) is used to compensate for stiction severity. The inverse approximates the S term and the results are giving below (Table 5.1). Clearly, variance is reduced more in case of smaller value of J. Stiction can be represented as composed of other nonlinearities like deadband and backlash. With simulations, it is figured out that the backlash is the dominating nonlinearity in the stiction phenomenon. Therefore, it is inferred to use inverse of backlash as approximate inverse in case inverse of stiction is not available.

The idea here is to compensate for stiction using an approximate inverse model of stiction (i.e., backlash inverse) to reduce the oscillations caused by stiction.

Consider the Figure 5.6 for the input output behavior of a valve in case of stiction.
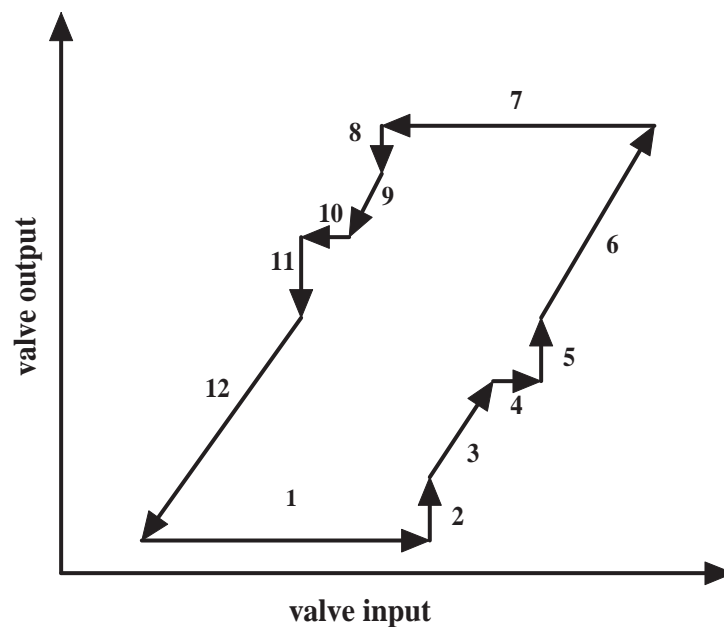
Figure 5.6: Valve input-output pattern in case of stiction.
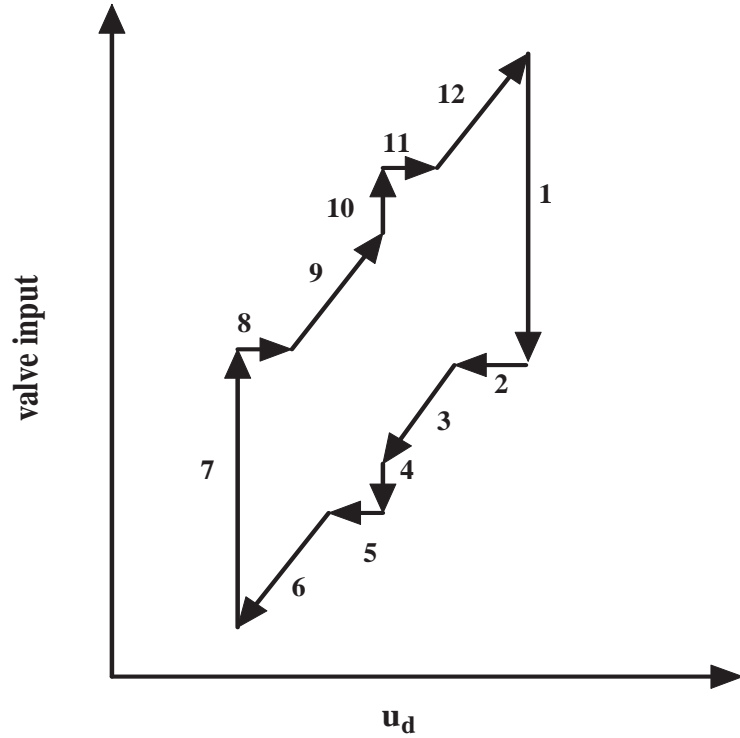
Figure 5.7: Inverse pattern of valve stiction.

Following inverse finding techniques discussed in Gang et al., [15], we can directly infer the inverse pattern of Figure 5.6 as Figure 5.7. In Figure 5.6, sections 2, 4, 5 8, 10 and 11 represent slip jump (J) as defined in Choudhury and Kano Stiction models [30] and [25], while sections 1 and 7 represent the deadband+stickband (S). If S is considered as prominent term and J is small, the inverse pattern of stiction as given in Figure 5.7 resembles the inverse of backlash. The inverse of backlash is defined in Gang et al., [15].

## 5.3.1 Approximated Stiction Inverse

Valve nonlinearities like deadband, hysteresis and backlash can be defined in parametric form and their inverses exists [15]. Literature on inverse modeling and control

104

does not contain any inverse model of stiction.

Here we propose a new way to resolve this issue of inverse. The input-output behavior of a valve with stiction is shown in Figure 5.6. The sections are labeled with numbers to represent various moving paths in this input-output map. The inverse can be made of each individual move. The inverse pattern of these individual moves is shown in Figure 5.7. From [15], the inverse pattern of stiction is shown in Figure 5.8.



Figure 5.8: Approximated stiction inverse.

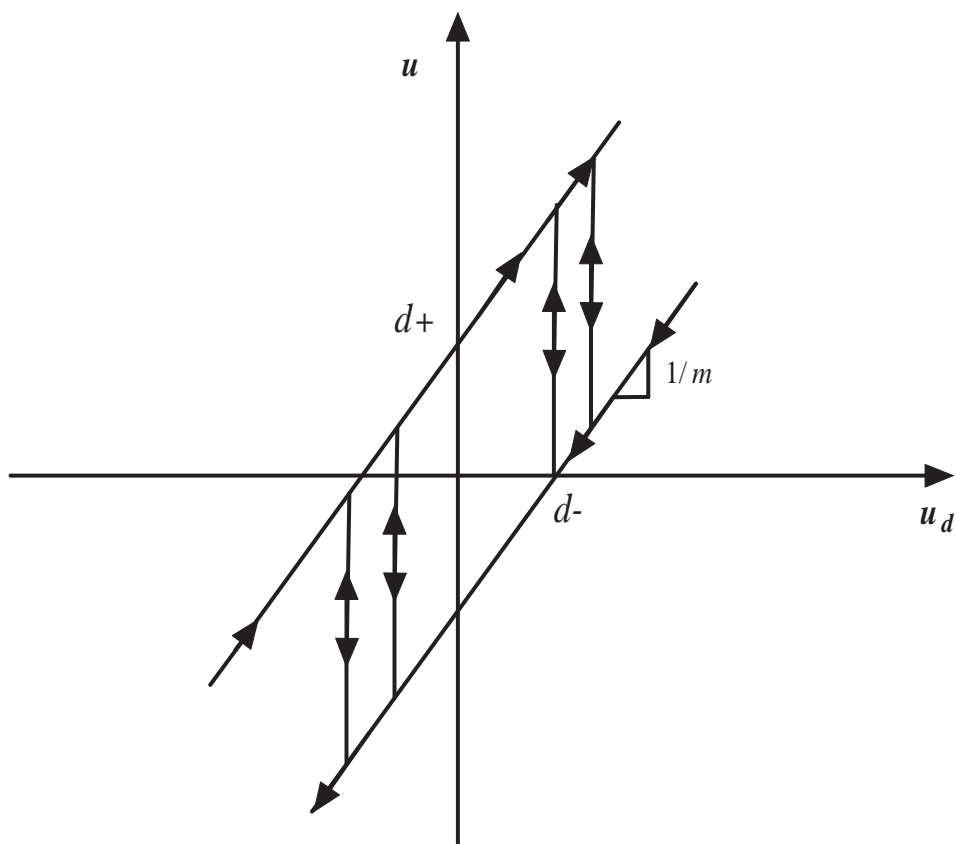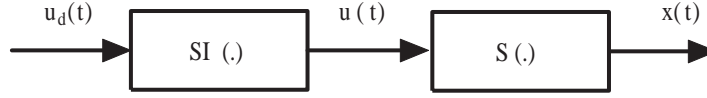Figure 5.9: Block diagram of stiction and stiction inverse.

The backlash inverse is

$$u_t = \begin{cases} u(t-1) & if\ u_d(t) = u(t-1) \\ \frac{u(t)}{m} + d_- & if\ u_d(t) < u(t-1) \\ \frac{u(t)}{m} + d_+ & if\ u_d(t) > u(t-1). \end{cases} \tag{5.1}$$

where $1/m$ is the slope of the parallel lines, $d_-$ and $d_+$ are the crossings on the vertical axis. Here $d_+ = S/2$ and $d_- = -S/2$, where $S$ is the $stickband + deadband$. Stiction nonlinearity with inverse is represented in a block diagram as shown in Figure 5.9. Assume $S(.)$ is the nonlinear function representing stiction nonlinearity and $SI(.)$ represents the inverse of stiction. Then the stiction nonlinearity can be represented as $x(t) = S(u(t))$ and the stiction inverse can be written as $u(t) = SI(u_d(t))$.

$$u_t = SI(u_d(t)) \tag{5.2}$$

Figure 5.10 shows the inverse compensation approach using approximate model. The approximate inverse model is derived from backlash inverse and is fixed for this discussion. By integrating the inverse with the stiction quantification method, this model can be made adaptive.

Control valve suffering with stiction values of $S = 12$ and $J = 5$ are considered to demonstrate the inverse compensation technique. The idea is to use an approximate

106

| Process Variable | Var (No Compensation) | Var (Compensation) |
|:---:|:---:|:---:|
| $OP$ | 2.72 | 0.15 |
| $PV$ | 4.11 | 1.39 |
| $MV$ | 1.13 | 0.63 |

Table 5.1: Compensation results for $S = 5$ and $J = 7$.

inverse model of stiction. It is found that the backlash inverse can represent inverse

model of stiction approximately.

The actual stiction present in the valve is $S = 12$ and $J = 5$. The inverse compensation

starts from $t = 1000$. Inverse parameter used in the backlash inverse approximating

stiction inverse is fixed at 6 for this case.

For Ts=1, following results are obtained for the process variable (pv), controller output

(op), valve position (mv) and the modified input to the control valve.
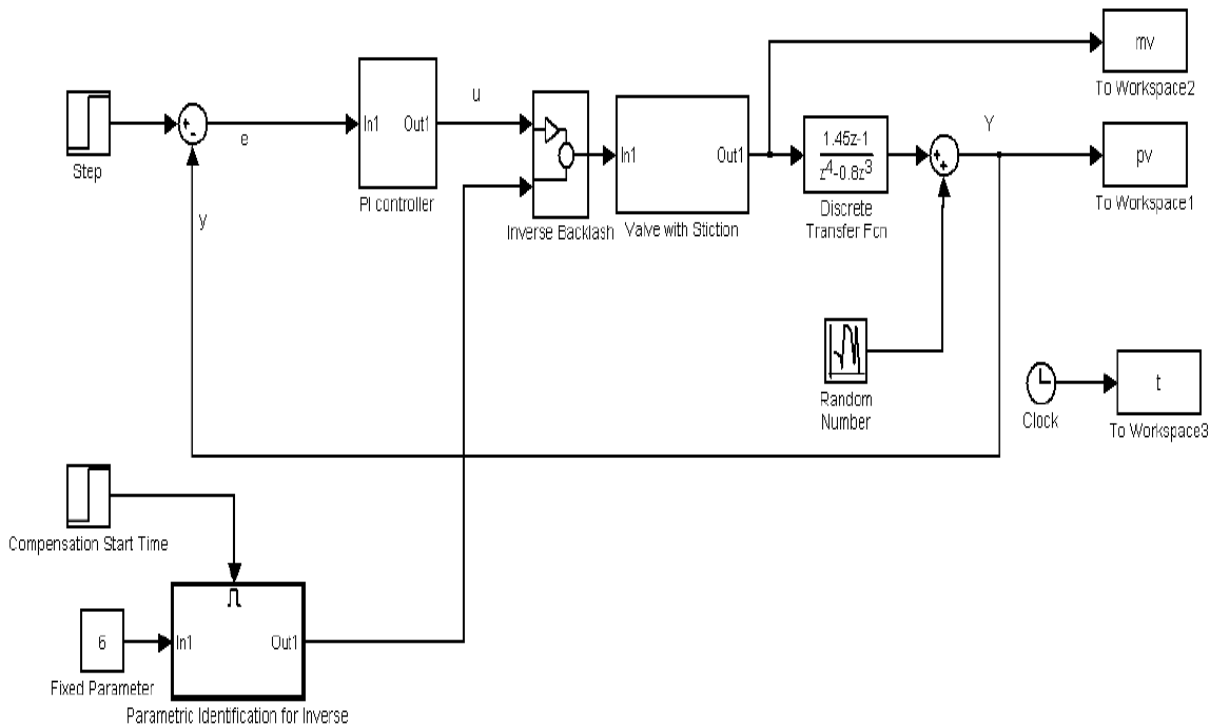


Figure 5.10: Block diagram of the Approximate Inverse Compensation.
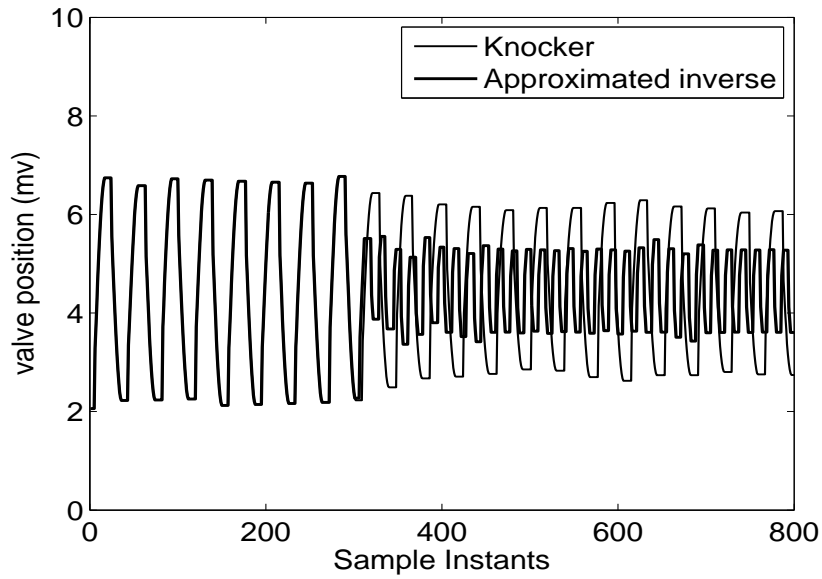
Figure 5.11: Valve position (mv) for $S = 10, J = 7$.

## 5.4   Proposed Adaptive Inverse Compensation

In this section adaptive filtering theory is used to propose the adaptive inverse model of control valve nonlinearity. An introduction to adaptive technique and the Least
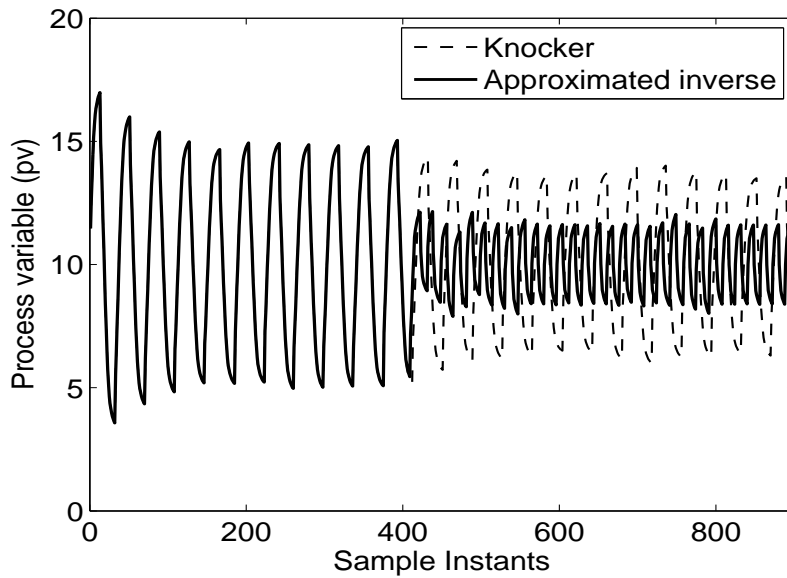


Figure 5.12: Process variable (pv) for $S = 10, J = 7$
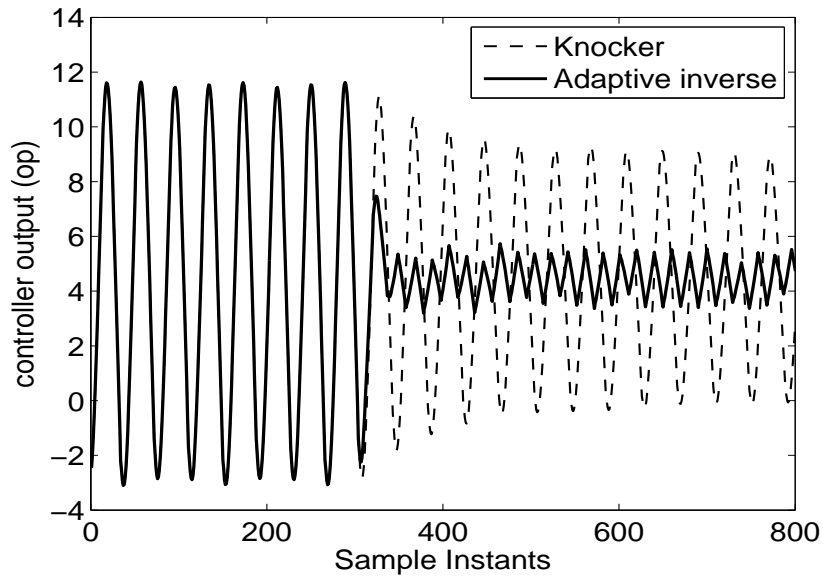
Figure 5.13: Approx. Inverse Compensation: Controller output (op) when $S = 12, J = 5$.
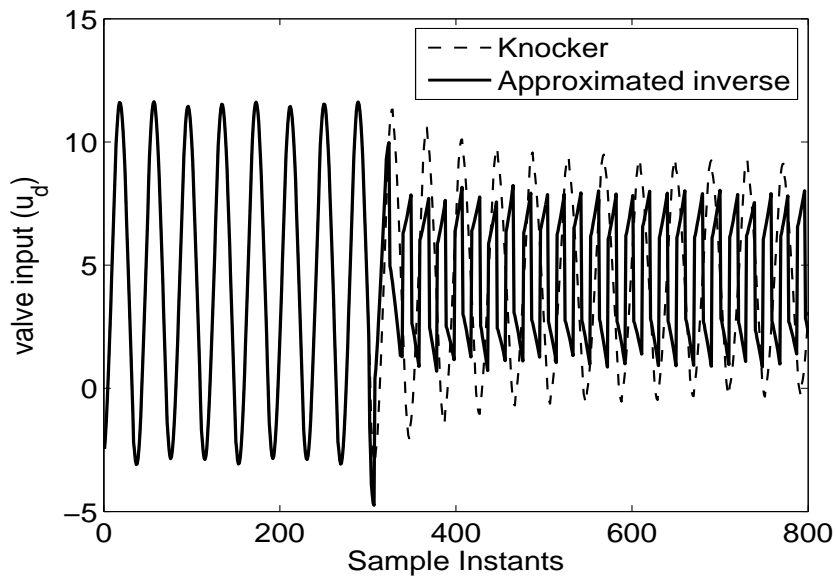


Figure 5.14: Approx. Inverse Compensation: Modified Valve input when $S = 12, J = 5$.

Mean Square adaptive algorithm is given. Then an adaptive inverse scheme is given to model inverse of the valve nonlinearity.
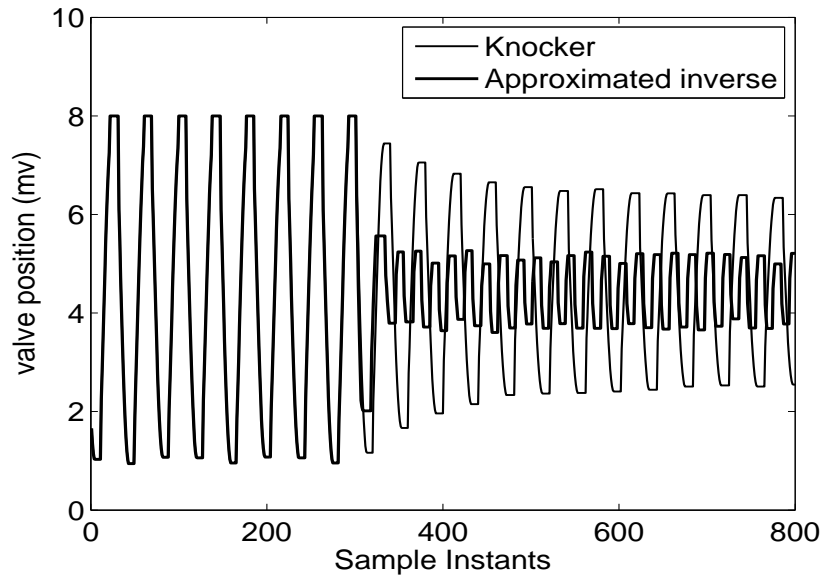
Figure 5.15: Approx. Inverse Compensation: Valve position / valve output (mv) when $S = 12, J = 5$.

## 5.4.1 Adaptive inverse model using adaptive filtering

Filter is a primary subsystem in any signal processing system. Filters are employed

to remove undesirable signal components from the desired signal. In adaptive filters,
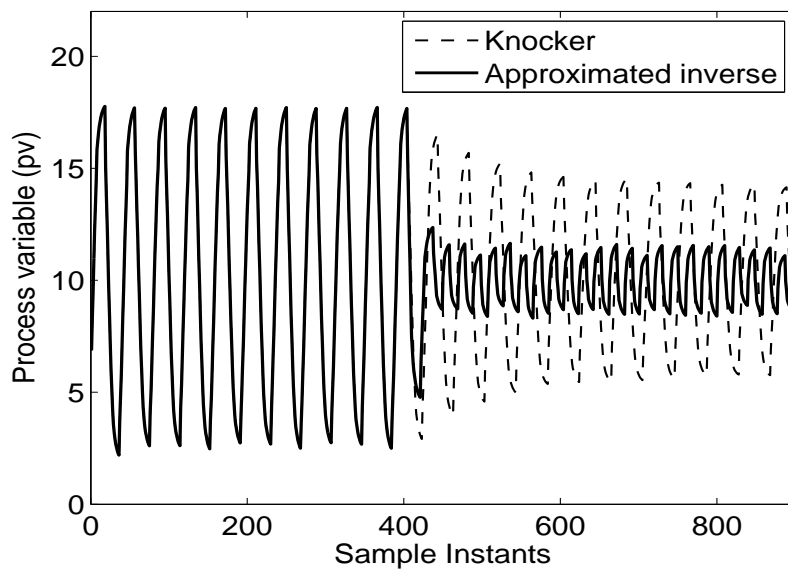


Figure 5.16: Approx. Inverse Compensation: Process variable (pv) when $S = 12, J = 5$.
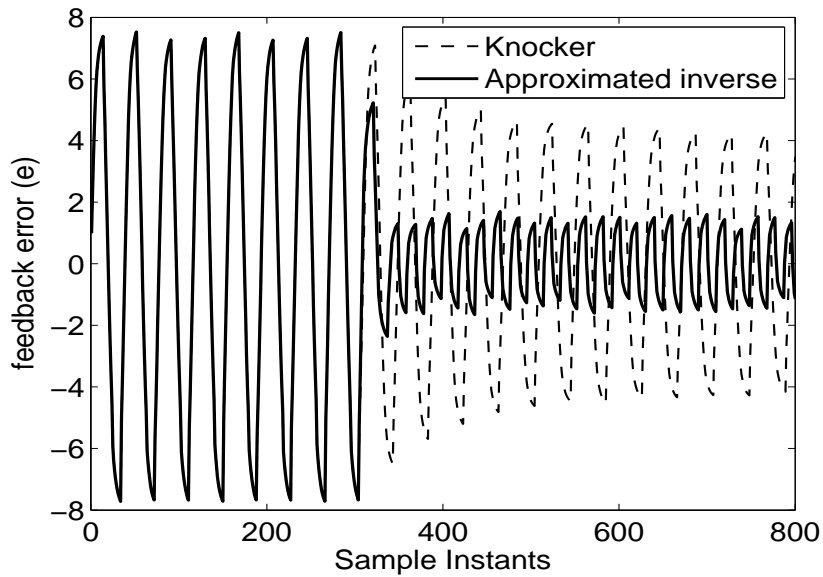
Figure 5.17: Approx. Inverse Compensation: Error between sp and pv when $S = 12, J = 5$.

the coefficient can be changed from time to time depending on the situation. Here the filter updates its coefficients from the knowledge of the past input and the present error. The error is generated from the reference input and actual output. The update
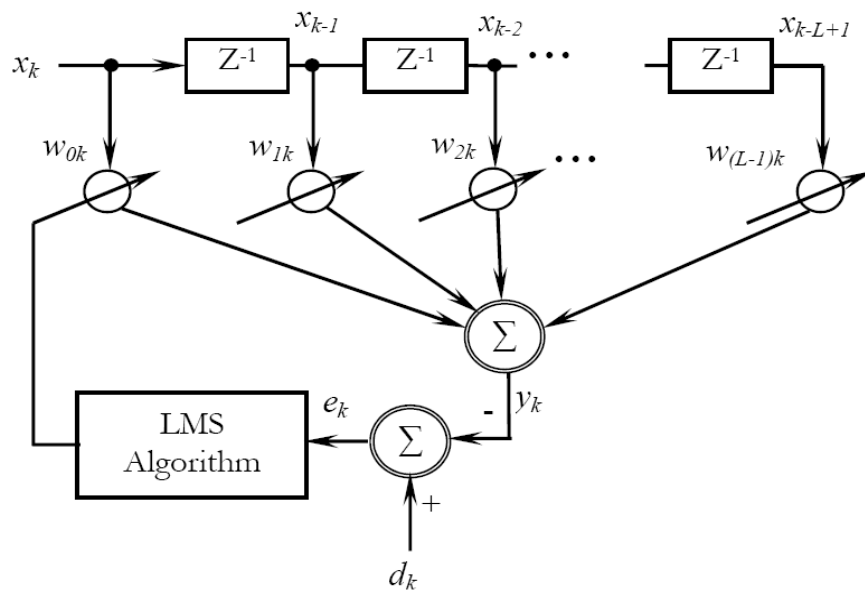


Figure 5.18: Adaptive filter using LMS algorithm.

111

procedure depends upon the different algorithms used.

**Least Mean Square (LMS) Algorithm:** The general architecture of the LMS
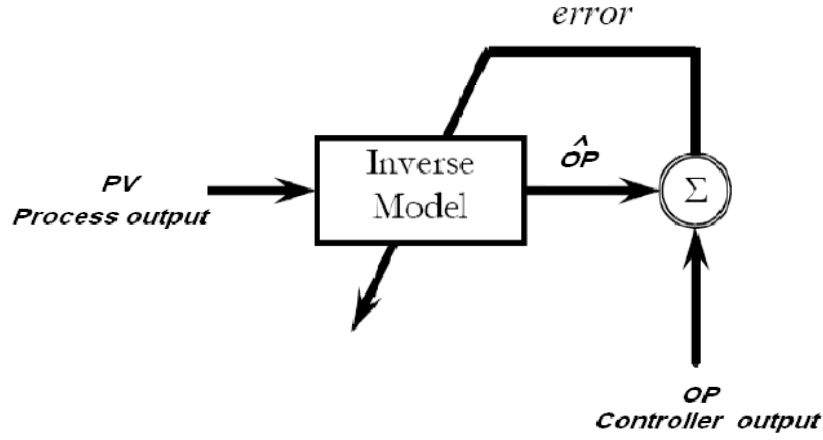


Figure 5.19: Adaptive inverse model scheme.

based adaptive filter is depicted in Figure 5.18. The $X$ is $N^{th}$ input pattern having one

unit delay in each instant. This process is called as adaptive linear combiner [Widrow

et al., [8]]. Let $X_k = [x_k x_{k-1} x_{k-L+1}]^T$ form of the L-by-1 tap input vector. Where L-1

is the number of delay elements; these input span a multidimensional space denoted

by $N_k$. Correspondingly, the tap weights $W_k = [w_{0k} w_{1k} w_{(L-1)k}]^T$ form the elements of

the L-by-1 tap weight vector. The output is represented as,

$$y_k = \sum_{l=0}^{L-1} w_{lk} x_{x-l} \tag{5.3}$$

The output can be represented in vector notation as

$$y_k = X_k^T W_k = W_k^T X_k \tag{5.4}$$

Generally for the adaptive linear combiner the other data include a "desired response" or "training signal", $d_k$. This is accomplished by comparing the output with the desired response to obtain an "error signal" $e_k$ and then adjusting the weight vector to minimize this signal. This error signal is,

$$e_k = d_k - y_k \qquad (5.5)$$

The weights associated with the network are then updated using the LMS algorithm [8]. The weight updates equation for $n^{th}$ instant is given by:

$$w_k(n+1) = w_k(n) + \triangle w_k(n) \qquad (5.6)$$

It can be further derived as:

$$w_k(n+1) = w_k(n) + 2.\eta.e_k(n).X_k^T \qquad (5.7)$$

where $\eta$ is the learning rate parameter ($0 \leq \eta \leq 1$). This procedure is repeated till the Mean Square Error (MSE) of the network approaches a minimum value. The MSE at the time index k may be defined as, $\xi = E[e_k^2]$, where $E[.]$ is the expectation value or average of the signal.

## 5.4.2  Inverse model using adaptive filtering

Scheme to find the adaptive inverse model of the control valve is given in Figure 5.19. Since valve position MV is not available in most cases, the input to the adaptive inverse model is the process variable PV. The adaptive filter is adjusted with respect to the error between filter output and the controller output OP. The learning error for the adaptive filter is $error = \hat{OP} - OP$. An LMS based inverse model is employed for the nonlinearity compensation of the control valve. The scheme shown in Figure 5.19 is implemented in MATLAB-SIMULINK utilizing the Signal Processing Toolbox. The LMS filter parameters are: normalized LMS algorithm, filter length of 4, step size ($\mu$) is 0.1 with a leakage factor of 1. Due to the nonlinearity of the stiction behavior, a delayed scheme for adaptive inverse modeling as shown in Figure 5.20 [8] is used here.
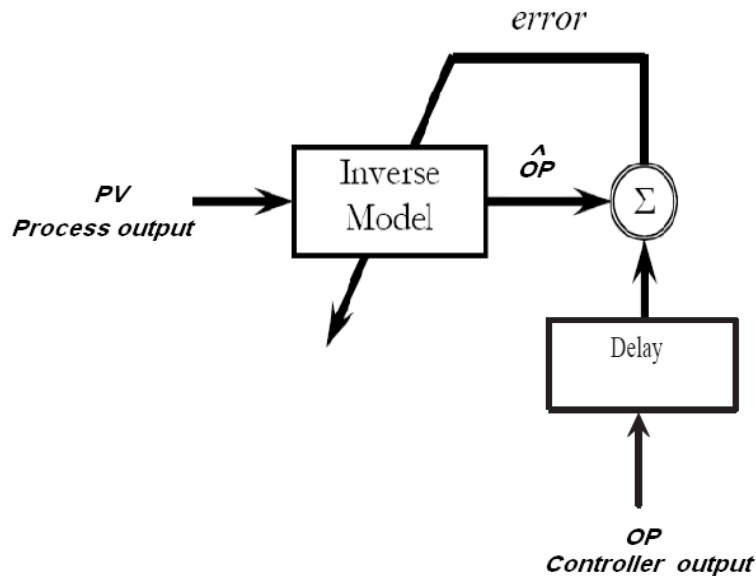


Figure 5.20: Adaptive inverse model scheme delayed.

114

### Compensation using adaptive inverse model

Following are the simulation results with the adaptive inverse based stiction compensation. Figures 5.21, 5.22, 5.23, 5.24 and 5.25 show the better performance of adaptive inverse compensation as compared to the approximated model compensation.
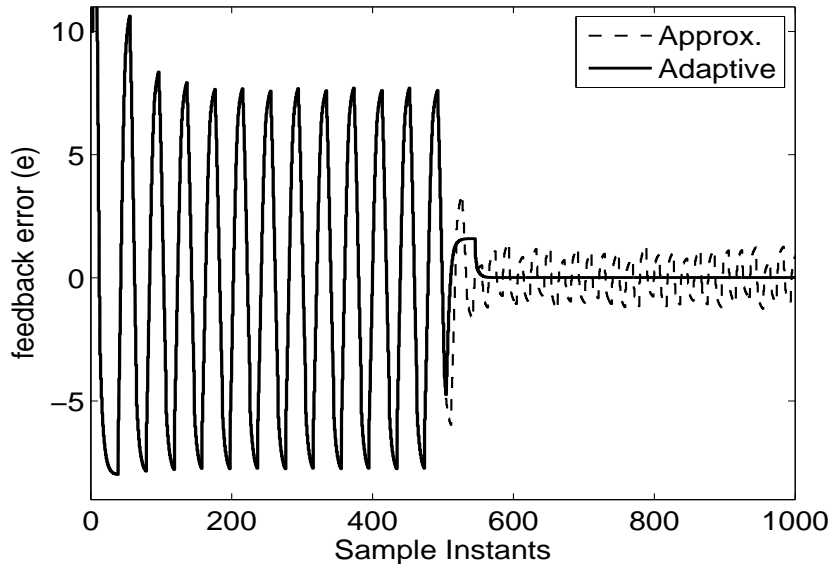


Figure 5.21: Adaptive Inverse Compensation: Error (sp-pv) when $S = 12, J = 3$.

## 5.5   Comparison of Knocker and Inverse Model Based Compensation Methods

A simulation study is carried out to compare performance of Knocker and Inverse Compensation methods. Note that the values for the Knocker pulse parameters and inverse model parameters are taken as typical. A better comparison can be made by coupling these parameters to an optimization algorithm.

The stiction parameters are $S = 10$ and $J = 7$ while same configurations are used for

Knocker and Inverse methods as discussed in previous sections for these methods.

## Knocker parameters

The three parameters of Knocker pulses are set according to the default values mentioned in Hagglund [17].

- Pulse amplitude is 2%,

- Pulse width ($\tau$) is taken as the sampling time of system, which is 1

- Time between each pulse ($h_k$) is taken as $h_k = 2h$

## Approximated Inverse parameter

Approximated inverse needs only one parameter which is directly coupled with the stiction quantified. An ellipse fitting method can be used to get the value of esti-
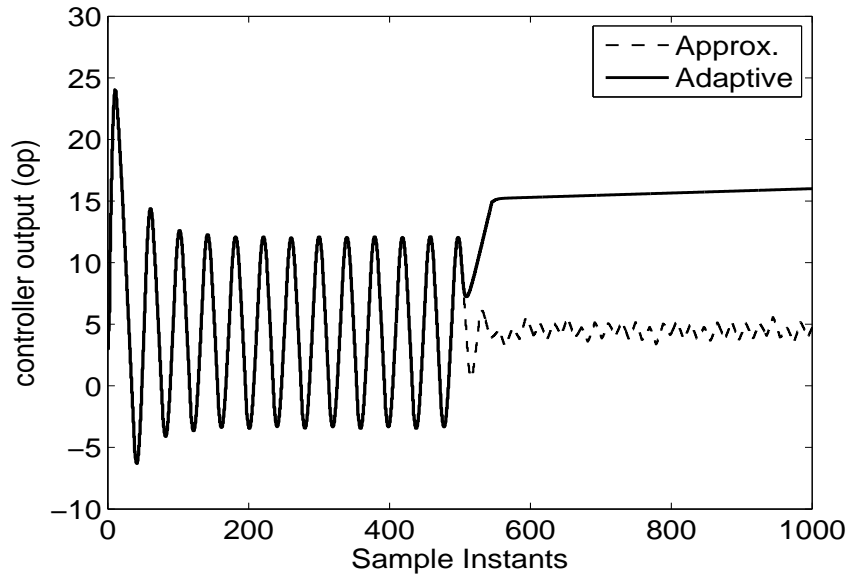


Figure 5.22: Adaptive Inverse Compensation: Controller output when $S = 12, J = 3$.
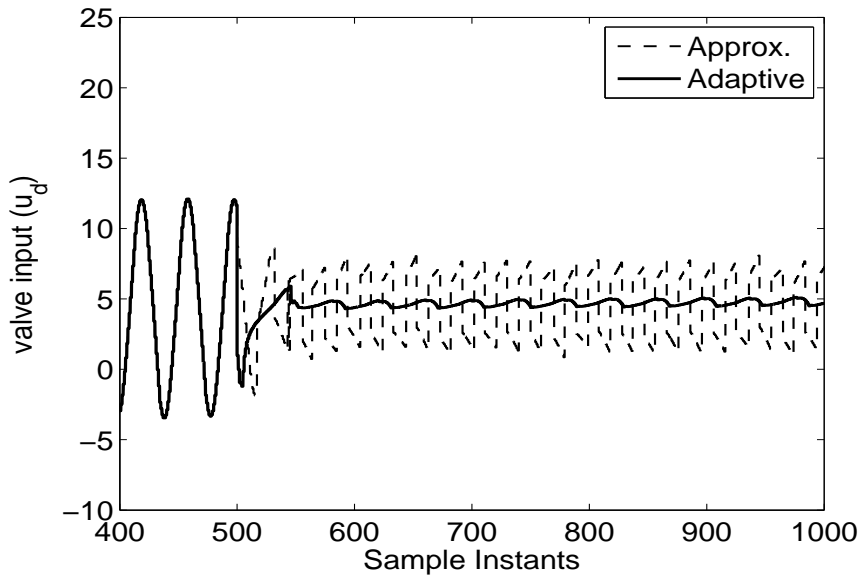
Figure 5.23: Adaptive Inverse Compensation: Valve input when $S = 12, J = 3$.

mated stiction. This value is passed to the approximated inverse model without any

human interpretation or other computations needed. Figures 5.11 and 5.12 show the

comparison of the Knocker based compensation and Approximated Inverse based com-
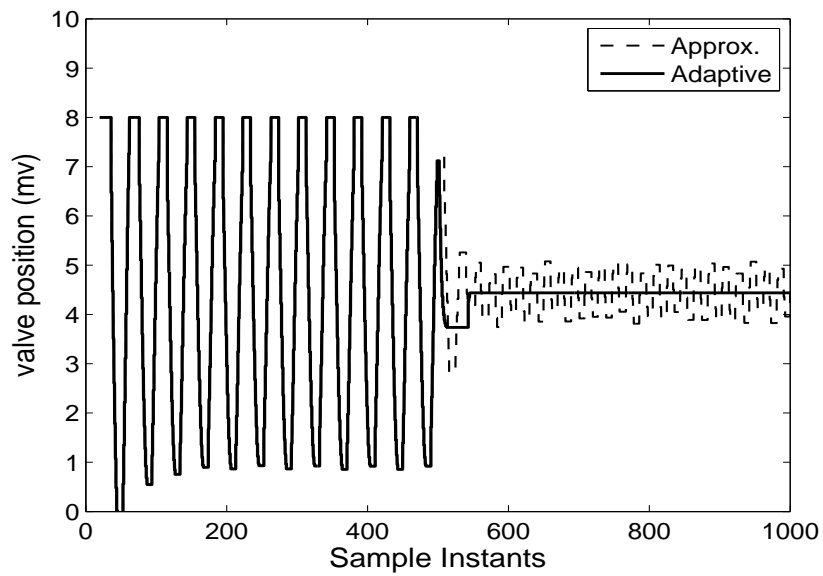


Figure 5.24: Adaptive Inverse Compensation: Valve output when $S = 12, J = 3$.
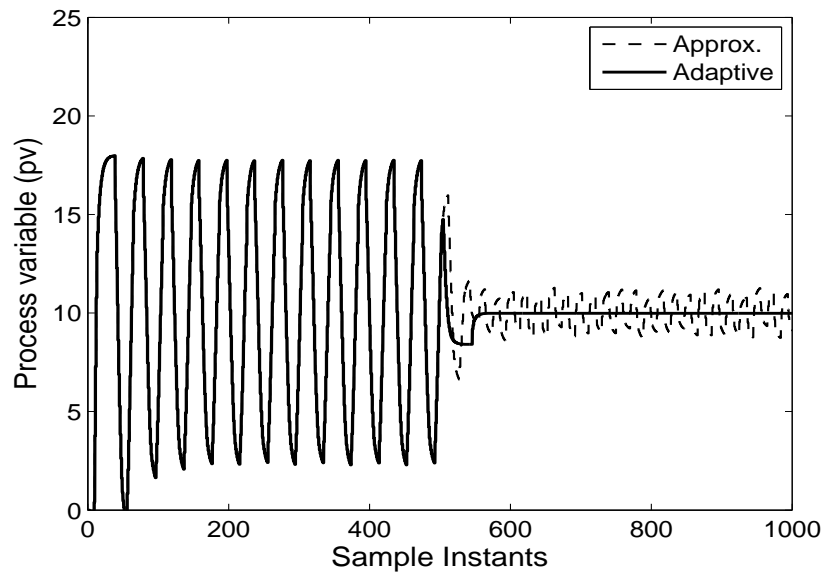
Figure 5.25: Adaptive Inverse Compensation: Controller output when $S = 12, J = 3$.

pensation. The results show better performance of the approximated inverse method over the Knocker based method.

## Advantages of Approximated Inverse Model Approach:

- This compensation approach requires one parameter only while knocker based method requires to tune three parameters.

- The single required parameter is directly related to the quantified valve of stiction while knocker parameters are not.

- The method requires only controller output (op) and process variable (pv) to find the inverse parameter.

- This method does not alter the controller, instead it reduces the computational load on the controller. The overall reduction in variability in controller effort is

found more than reduction in other process variables.

## Disadvantage:

- The only disadvantage observed is that the efficiency of approximated inverse compensation is sensitive to the quantified value of stiction.

## Adaptive Inverse Model

The adaptive inverse method uses the inverse modeling approach discussed in section 5.4.2. The method uses delayed controller output (op) as reference signal and input to the inverse model is the valve position (mv).

## Advantages of Adaptive Inverse Model Approach:

- This compensation approach does not require an explicit stiction quantification method (like ellipse fitting method) to work.

- This method uses adaptive algorithm to adapt the inverse model directly from the control loop variables.

## Disadvantage:

- The method reduces the effects of valve-stiction without making a clear indication of the severity of stiction. This may be troublesome from performance monitoring view point since the exact health condition of valve is hidden in this

method. A solution to this problem may be to use another stiction quantifica-
tion method using adaptive inverse model in the reference model to reconstruct
the nonlinearity behavior present in the control loop.

- This method requires controller output (op) and valve output (mv). The valve
  output (mv) may not be available in most of the cases. In such cases, the method
  based on approximated inverse model can be used.

## 5.6 Stability Analysis of Inverse Model Based Compensation

In this section, stability analysis for the inverse model based compensation is pre-
sented. Consider the simple block diagram of a feedback control loop with an actuator
nonlinearity and the inverse model of the nonlinearity as shown in Fig. 5.26. Let the
stiction nonlinearity is represented by $NL$ and the inverse is represented by $\hat{NL}$.
Conceptually, the nonlinearity inverse should cancel the nonlinearity resulting in a
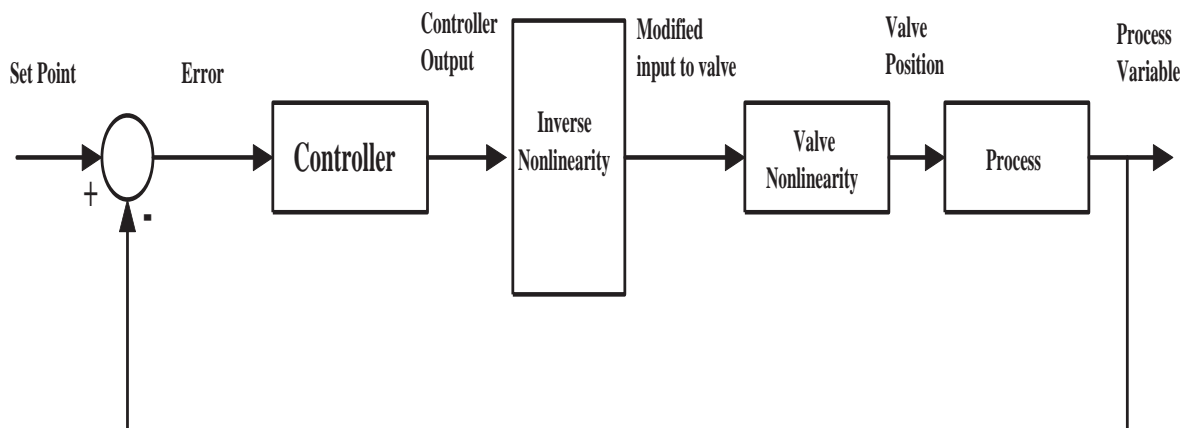


Figure 5.26: Control loop with inverse model of nonlinearity.

gain of unity as given in Eq.

$$(\hat{NL})(NL) = 1 \tag{5.8}$$

Unfortunately, explicit inverse of valve stiction is not available due to the discontinuities. Such discontinuities occur because of the unique stick-slip mechanism of stiction nonlinearity in control valves. Therefore, the relation between $NL$ and $\hat{NL}$ can be written as:

$$(\hat{NL})(NL) \neq 1 \tag{5.9}$$

Due to this reason, the inverse $(\hat{NL})$ is called as approximate inverse. Assuming the mismatch factor is $\Delta NL$. With the approximated inverse, the control loop is shown in Fig. 5.27.
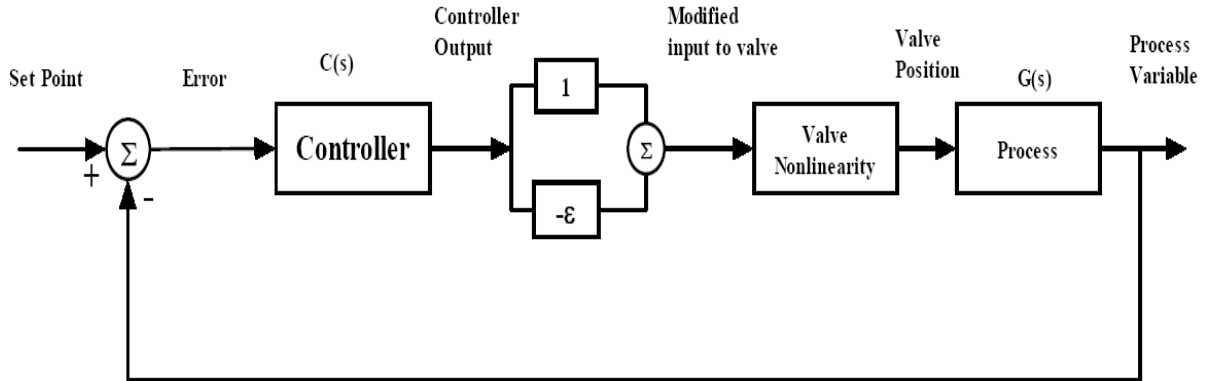


Figure 5.27: Control loop with approximated inverse model.

The approximated inverse $(\hat{NL})$ can be written as:

$$(\hat{NL}) = [NL + \Delta NL]^{-1} \tag{5.10}$$

121

$$(\hat{NL}) = \frac{1}{NL + \Delta NL} \tag{5.11}$$

$$(\hat{NL}) = (\frac{1}{NL})\frac{1}{1 + (\frac{\Delta NL}{NL})} \tag{5.12}$$

Let $\varepsilon = \frac{\Delta NL}{NL}$, where $\varepsilon$ is very small, the above expression becomes:

$$(\hat{NL}) = \frac{1}{NL}[\frac{1}{1 + \varepsilon}] \tag{5.13}$$

By Tayler series expansion, $\frac{1}{1+\varepsilon}$ can be written as:

$$\frac{1}{1 + \varepsilon} \approx 1 - \varepsilon + \varepsilon^2 - \varepsilon^3... \tag{5.14}$$

Since $\varepsilon$ is small, terms containing higher powers of $\varepsilon$ can be neglected and $\frac{1}{1+\varepsilon}$ can be approximated as:

$$\frac{1}{1 + \varepsilon} \approx 1 - \varepsilon \tag{5.15}$$

Hence, the inverse can be represented approximately as:

$$(\hat{NL}) = \frac{1}{NL}(1 - \varepsilon) \tag{5.16}$$

The closed loop transfer function becomes:

$$Y(s)/R(s) = \frac{G(s)C(s)}{\frac{1}{1-\varepsilon} + G(s)C(s)} \tag{5.17}$$

The characteristic equation of this control loop becomes:

$$1 - \varepsilon \frac{G(s)C(s)}{1 + G(s)C(s)} \tag{5.18}$$

Assuming $G(s) = 1/s$ and $C(s) = 0.2(\frac{10s+1}{10s})$ The root locus according to Eq. 5.18 is shown in Fig. 5.28. The root locus shows that the system is locally stable for the proposed inverse model approach.
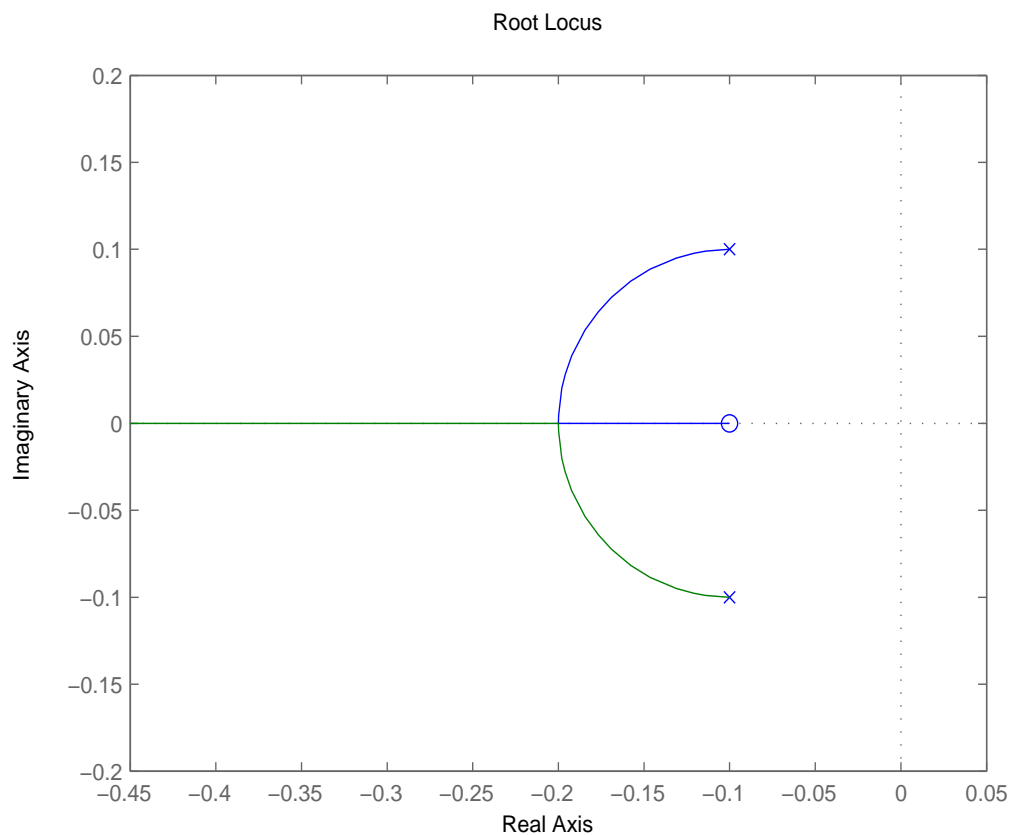


Figure 5.28: Root locus w.r.t $\varepsilon$.

## 5.7　Summary

Inverse control approach is quite simpler to implement than the knocker based compensation. Knocker based method requires three pulse parameters to be defined properly. The main problem with setting knocker parameters is that there is no design law and rules that can directly map the setting of these parameters with the severity of stiction quantified. One way can be to use the optimization algorithm to achieve good set of the three parameters for each loop. These optimized parameters needs to be evaluated when performance deviates again.

On the other hand, the approximated inverse based compensation is directly coupled with the stiction value quantified. This approximated inverse being proposed in this work takes one parameter only which is directly related to the stiction value quantified.

Another advantage of the approximated inverse is that it reduces load on the controller. It is found that the approximated inverse greatly reduces the variability in the controller output signal. The approximated inverse of the stiction nonlinearity is taking care of the stiction nonlinearity, in effect reducing total nonlinearity effects on the control loop and specifically for the controller.

Note that the proposed method is applied on two parameter stiction model simulating both deadband+stick-band and slip-jump (i.e., S and J), while existing compensation techniques are proposed and tested for the one parameter model (Stenman model).

# CHAPTER 6

# SUMMARY, CONCLUSION AND FUTURE WORK

## 6.1 Summary

1. Physical model of valve and four data driven models are implemented in MATLAB-SIMULINK environment. These models are investigated in open loop and closed loop. The models are tested for the ISA bench tests. The data driven models are found capable to represent the stiction phenomena and are used to generate the simulated data for several cases of stiction. The simulated data is further used in the detection and quantification methods.

2. Yamashita method for detection & Ellipse fitting method for quantification are implemented on the simulated data.

3. Knocker based stiction compensation method is implemented on a control loop suffering from stiction.

4. **Contributions:**

   (a) Hammerstein-Wiener model is proposed to model stiction in control valves. Hammerstein-Wiener is better than the Hammerstein model when stiction is significant.

   (b) Approximated inverse model of stiction is proposed. It is found that the inverse pattern of stiction-suffering valve is quite similar to the inverse of backlash. When slip-jump is considered small relative to the $stickband + deadband$, inverse of backlash can be used as stiction inverse.

   (c) A technique is proposed to find the adaptive inverse model of stiction. The proposed adaptive inverse model is based on the adaptive learning and is tested with Least Mean Squares (LMS) and Recursive Least Squares (RLS) algorithms. As expected, RLS performs better than the LMS.

   (d) Stiction compensation scheme based on the approximated inverse model and ellipse fitting method is proposed. The stiction valve quantified from ellipse fitting method is used to set the inverse parameter of the approximated inverse model. This compensation scheme performs better than the knocker based compensation.

   (e) Adaptive compensation based on the adaptive inverse model is proposed. In this approach, stiction explicit stiction quantification is not required. The inverse model is adaptive and updates the inverse parameters from the learning algorithm of LMS or RLS algorithms. It is important to note that both of the above compensation techniques does not change the controller

and other settings of the control loop. In both approaches, the idea is to tackle the valve nonlinearity from its approximated inverse.

## 6.2  Conclusion

Several tasks around the topic of valve stiction is carried out in this research work from modeling, detection, quantification and compensation view point. The data driven models were investigated in addition ISA tests for valve were carried out for validation of their responses. The models are implemented in MATLAB-SIMULINK environment and can be used for further research study in this field. The investigation of models help understand the stiction posed problem and consequently the quantification and compensation of stiction posed oscillations in process variables. Detection and quantification methods from recent literature were tested on the simulated data of a control loop suffering from sticky valve. Several cases of such disturbances are studied. Two approaches to combat valve stiction are proposed based on simple but innovative idea of inverse model of the nonlinearity. Since inverse of the stiction nonlinearity is not possible, approximated inverse is used. The proposed inverse model based compensations does not alter any setting of the controller and are able to reduce the oscillations caused by stiction in valve. The proposed methods keep the control loop stable and also reduce the controller effort.

## 6.3   Future Work

We end this chapter and the thesis with the following as the possible future work.

Current work used the linear adaptive filter to reduce the oscillations. It is recommended to use nonlinear adaptive filter to remove the oscillations completely.

Quantification and compensation of valve stiction can be explored for the case of nonlinear process models, since this work considered linear plant dynamics.

# REFERENCES

[1] A.J. Isaksson A. Horch. A simple method for detection of stiction in control valves. *Control Engineering Practice*, 7:1221–1231, 1999.

[2] F. J. Doyle III A. Kayihan. Friction compensation for a process control valve. *Control Engineering Practice*, 8:799–812, 2000.

[3] T.I. Salsbury A. Singhal. A simple method for detecting valve stiction in oscillating control loops. *Journal of Process Control*, 15:371–382, 2005.

[4] K. Forsman A. Stenman, F. Gustafsson. A segmentation-based method for detection of stiction in control valves. *International Journal on Adaptive Control and Signal Processing*, 17:625–634, 2003.

[5] Standard ANSI/ISA-75.25.01-2000. Test procedures for control valve response measurement from step inputs. 2000.

[6] Standard ANSI/ISA-75.26.01-2006. Control valve diagnostic data acquisition and reporting. 2006.

[7] De Wit Armstrong-Helouvry, B. Dupont. A survey of models, analysis tools and compensation methods for the control of machines with friction. *Automatica*, 30:1083–1138, 1994.

[8] E. Walach B. Widrow. *Adaptive inverse control.*

[9] G. L. Plett B. Widrow. Adaptive inverse control based on linear and non-linear adaptive filtering.

[10] C. Ghelardoni C. Scali. An improved qualitative shape analysis technique for automatic detection of valve stiction in flow control loops. *Control Engineering Practice*, 16:1501–1508, 2008.

[11] M.A.A.S. Choudhury. Detection and diagnosis of control loop nonlinearities, valve stiction and data compression. *Ph.D. Dissertation, Department of Chemical and Materials Engineering, University of Alberta*, 2005.

[12] EnTech. Entech control valve dynamic specification. *version 3.0*, 1998.

[13] Lahoucine Ettaleb. Diagnostic for poorly tuned control loops. 2006.

[14] R.K.Pearson F.J.Doyle, B.A.Ogunnaike. Nonlinear model-based control using second-order volterra models. *Automatica*, 31(5):697–714, 1995.

[15] Peter V. Kokotovic Gang Tao. *Adaptive control of systems with actuator and sensor nonlinearities.*

[16] C. Garcia. Comparison of friction models applied to a control valve. *Control Engineering Practice*, 16:1231–1243, October 2008.

[17] T. Hagglund. A friction compensator for pneumatic control valves. *Journal of Process Control*, 12:897–904, 2002.

[18] T.J. Harris. Assessment of control loop performance. *The Canadian Journal of Chemical Engineering*, 67:856–861, 1989.

[19] A. Horch. Condition monitoring of control loops. *Ph.D. Dissertation, Dept. of Signal, Sensors and System., Royal Institute of Technology, Stockholm, Sweden*, 2000.

[20] Alexander Horch. Oscillation diagnosis in control loops: stiction and other causes. *Proceedings of the 2006 American Control Conference, Minneapolis, Minnesota, USA*, pages 1221–1231, June 2006.

[21] M. Ruel J. Gerry. How to measure and combat valve stiction online. *Houston, USA:ISA*, 2001.

[22] M. Jelali. Estimation of valve stiction in control loops using separable least-squares and global search algorithms. *Journal of Process Control*, 18:632–642, 2008.

[23] R. Miller L. Desborough. Increasing customer value of industrial control performance monitoring - honeywell's experience.

[24] S. Lakshminarayanan Lee Zhi Xiang Ivan. A new unified approach to valve stiction quantification and compensation.

[25] H. Kugemoto K. Shimizu M. Kano, H. Maruta. Practical model and detection algorithm for valve stiction. *Proceedings of the IFAC Symposim DYCOPS, Cambridge, USA*, 2004.

[26] C. Scali M. Rossi. A comparison of techniques for automatic detection of stiction: simulation and application to industrial data. *Journal of Process Control*, 15:505–514, 2005.

[27] S.L. Shah David S. Shook M.A.A. Shoukat Choudhury, N.F. Thornhill. Automatic detection and quantification of stiction in control valves. *Control Engineering Practice*, 2006.

[28] N.F. Thornhill M.A.A.S. Choudhury, S.L. Shah. Diagnosis of poor control-loop performance using higher-order statistics. *Automatica*, 40:1719–1728, 2004.

[29] S.L. Shah M.A.A.S. Choudhury, M. Jain. Stiction - definition, modelling, detection and quantification. *Journal of Process Control*, 18 (3-4):232–243, 2008.

[30] S.L. Shah M.A.A.S. Choudhury, N.F. Thornhill. A data-driven model for valve stiction. *IFAC Symposium on Advanced Control of Chemical Processes (AD-CHEM), Hong-Kong*, Jan. 11-14 2004.

[31] S.L. Shah M.A.A.S. Choudhury, N.F. Thornhill. Modelling valve stiction. *Control Engineering Practice*, 13:641–658, 2005.

[32] R. Rengaswamy N. Ulaganathan. Blind identification of stiction in nonlinear process control loops. *2008 American Control Conference*, pages 3380–3384, 2008.

[33] M.S. Davies O. Taha, G.A. Dumont. Detection and diagnosis of oscillations in control loops. *Proceedings of the 35th Conference on Decision and Control, Kobe, Japan*, pages 2432–2437, 1996.

[34] Henrik Olsson. Control systems with friction. *Lund Institute of Technology, University of Lund*, 1996.

[35] M. Pottmann S.Joe Qin Q.P. He, J. Wang. A curve fitting method for detecting valve stiction in oscillating control loops. *Industrial and Engineering Chemistry Research*, 46:4549–4560, 2007.

[36] Raghunathan Rengaswamy Ranganathan Srinivasan. Stiction compensation in process control loops: A framework for integrating stiction measure and compensation. *Industrial Engineering Chemical Research*, 44:9164–9174, 2005.

[37] Raghunathan Rengaswamy Ranganathan Srinivasan. Approaches for efficient stiction compensation in process control valves. *Computers and Chemical Engineering*, 32:218–229, 2008.

[38] M. Ruel. Stiction: The hidden menace. *Control Magazine, http://www.expertune.com/articles/RuelNov2000/stiction.html*, 2000.

[39] Sunan Huang Si-Lu Chen, Kok Kiong Tan. Two-layer binary tree data-driven model for valve stiction. *Ind. Eng. Chemical Research*, 47:2842–2848, 2008.

[40] ISA Subcommittee SP75.05. Process instrumentation terminology. *Technical Report ANSI/ISA-S51.1-1979, Instrument Society of America*, 1979.

[41] R. Srinivasan. Control loop performance monitoring: Modeling, diagnosis and compensating stiction phenomenon in process control valves. *Ph.D. Dissertation, Department of Chemical, Clarkson University*, 2005.

[42] Yoshiyuki Yamashita. An automatic method for detection of valve stiction in process control loops. *Control Engineering Practice*, 2006.

# VITAE

- *Name:* **Muhammad Sabih son of Muhammad Shafi**.

- *Nationality:* Pakistani.

- *Date of Birth:* 11-February-1977, Karachi, Pakistan.

- *Present Address:* Room-417, Building 9903, Graduate Housing, KFUPM, Dhahran, Saudi Arabia.
  *Permanent Address:* House No. R-1504, Block-14, Federal "B" Area, Naseer Abad, Karachi, Pakistan.

- *Bachelor of Engineering (BE):* Industrial Electronics, Institute of Industrial Electronics Engineering (IIEE), NED University, Karachi, Pakistan, November 2000.

- *Master of Science (MS):* Systems Engineering, Automation & Controls, June 2009.

- *Lecturer:* Hamdard University, Karachi, Pakistan, March 2001 to March 2004.

- *Assistant Manager (R&D):* National Engineering and Scientific Commission

(NESCOM), Pakistan, April 2004 to February 2007.

- *Research Assistant:* Systems Engineering Department, King Fahd University of Petroleum & Minerals (KFUPM), February 2007 to November 2009.

- *Research Interests:* Industrial Instrumentation, Automation & Controls, Optimization & Intelligent Control, Performance Optimization of Process Control.

Muhammad Sabih can be contacted at `muhammad.sabih@gmail.com`.